

DISSERTATION

ACCURATE DIMENSION REDUCTION BASED POLYNOMIAL CHAOS APPROACH
FOR UNCERTAINTY QUANTIFICATION OF HIGH SPEED NETWORKS

Submitted by

Aditi Krishna Prasad

Department of Electrical and Computer Engineering

In partial fulfillment of the requirements

For the Degree of Doctor of Philosophy

Colorado State University

Fort Collins, Colorado

Spring 2018

Doctoral Committee:

Advisor: Sourajeet Roy

Ali Pezeshki

Branislav Notaros

Charles Anderson

Copyright by Aditi Krishna Prasad 2018

All Rights Reserved

ABSTRACT

ACCURATE DIMENSION REDUCTION BASED POLYNOMIAL CHAOS APPROACH FOR UNCERTAINTY QUANTIFICATION OF HIGH SPEED NETWORKS

With the continued miniaturization of VLSI technology to sub-45 nm levels, uncertainty in nanoscale manufacturing processes and operating conditions have been found to translate into unpredictable system-level behavior of integrated circuits. As a result, there is a need for contemporary circuit simulation tools/solvers to model the forward propagation of device level uncertainty to the network response. Recently, techniques based on the robust generalized polynomial chaos (PC) theory have been reported for the uncertainty quantification of high-speed circuit, electromagnetic, and electronic packaging problems. The major bottleneck in all PC approaches is that the computational effort required to generate the metamodel scales in a polynomial fashion with the number of random input dimensions.

In order to mitigate this poor scalability of conventional PC approaches, in this dissertation, a reduced dimensional PC approach is proposed. This PC approach is based on using a high dimensional model representation (HDMR) to quantify the relative impact of each dimension on the variance of the network response. The reduced dimensional PC approach is further extended to problems with mixed aleatory and epistemic uncertainties. In this mixed PC approach, a parameterized formulation of analysis of variance (ANOVA) is used to identify the statistically significant dimensions and subsequently perform dimension reduction. Mixed problems are however characterized by far greater number of dimensions than purely epistemic or aleatory problems, thus exacerbating the poor scalability of PC expansions. To address this

issue, in this dissertation, a novel dimension fusion approach is proposed. This approach fuses the epistemic and aleatory dimensions within the same model parameter into a mixed dimension. The accuracy and efficiency of the proposed approaches are validated through multiple numerical examples.

ACKNOWLEDGEMENTS

I would first of all like to thank my advisor, Dr. Sourajeet Roy for being the finest mentor. His advice and guidance at every stage has been extremely valuable and this work would not have been possible without him. Next, I thank Dr. Ali Pezeshki, Dr. Branislav Notaros and Dr. Charles Anderson for accepting to be part of my thesis committee and shaping my research. I also would like to thank Dr. Xinfeng Gao for her guidance and for enabling this work to be applied in other disciplines of engineering.

I thank my colleagues Majid Ahadi and Ishan Kapse for their contributions in my publications. I also thank my friends at CSU for making this journey a memorable one.

I also express my gratitude to my parents - Mrs. Geeta Krishna Prasad and Mr. S. Krishna Prasad and other family members for providing constant support and encouragement. I thank my husband Vijay for providing invaluable inputs from his experience as a Ph.D student and for the unconditional love and motivation. I finally thank our baby girl Prakriti, who came into this world on September 17th, 2017 and brought us immeasurable joy.

TABLE OF CONTENTS

ABSTRACT.....	ii
ACKNOWLEDGEMENTS.....	iv
CHAPTER 1: INTRODUCTION	1
1.1 Problem statement.....	1
1.2 Scope of the thesis	3
1.3 Organization of the text	5
CHAPTER 2: RELATED WORK.....	7
2.1 Monte Carlo	7
2.2 Quasi Monte Carlo.....	8
2.3 Latin Hypercube Sampling	8
2.4 Generalized Polynomial Chaos (gPC) Theory.....	10
2.4.1 One-dimensional orthonormal polynomials.....	11
2.4.2 Multidimensional orthonormal polynomials.....	13
2.4.3 Derivation of statistics	14
2.5 Intrusive and non-intrusive methods.....	16
2.5.1 Intrusive methods.....	16
2.5.2 Non-intrusive methods.....	17
2.5.2.1 Pseudo-spectral collocation.....	17
2.5.2.2 Conventional Linear Regression approach	19
2.5.2.3 Non-intrusive formulation of Stochastic Testing.....	20
2.6 Sparse Polynomial Chaos Techniques	21
2.6.1 Sensitivity Indices using ANOVA-HDMR.....	22
2.6.2 Hierarchical Sparse PC Approach.....	23
2.6.3 Anisotropic Sparse PC Approach	25
2.6.4 Hyperbolic PC Expansion.....	26
CHAPTER 3: APPROACHES TO ACCELERATE THE CLASSICAL FEDOROV SEARCH ALGORITHM.....	29
3.1 PC expansion using Linear Regression.....	29
3.2 Advantages over intrusive approaches.....	31
3.3 Proposed D-Optimal Linear Regression Approach.....	31

3.3.1 D-optimal Criterion.....	31
3.3.2 Greedy Search Algorithm to Identify DoE	32
3.3.3 Computational cost of the search algorithm.....	34
3.4 Expediting the Search Algorithm for High-Dimensional Random Spaces.....	36
3.4.1 Substituting K worst DoE	36
3.4.2 Implicit Matrix Inversion	37
3.5 Numerical Efficiency of the Modified Search Algorithm.....	38
3.6 Comparative Analysis of Overall CPU Costs	40
3.6.1 Proposed Linear Regression Approach.....	40
3.6.2 Stochastic Testing Approach	41
3.6.3 Stochastic Collocation Approach.....	41
3.6.4 Other Approaches	42
3.7 Numerical Examples.....	43
3.7.1 Example 1: CMOS Low Noise Amplifier (LNA).....	44
3.7.2 Example 2: Transmission Line Network.....	46
3.7.3 Example 3: BJT Low Noise Amplifier (LNA)	49
CHAPTER 4: DEVELOPMENT OF THE REDUCED DIMENSIONAL POLYNOMIAL CHAOS APPROACH	56
4.1 Development of Proposed Reduced Dimensional PC Approach.....	57
4.1.1 Evaluating Sensitivity Indices.....	57
4.1.2 Recovering the Reduced Dimensional PC Expansion via Linear Regression	61
4.1.3 Sensitivity Analysis for Multiple Network Responses	63
4.1.4 Contraction of PC due to Dimension Reduction.....	63
4.1.5 Comparing Performance of Proposed Approach with Respect to Existing Sparse PC Approaches	65
4.2 Numerical Examples.....	67
4.2.1 Example 1	67
4.2.2 Example 2	70
4.2.3 Example 3	72
CHAPTER 5: EXTENDING THE REDUCED DIMENSIONAL POLYNOMIAL CHAOS APPROACH FOR MIXED EPISTEMIC-ALEATORY PROBLEMS	77
5.1 Overview of Mixed Uncertainty Problems and Unified Polynomial Chaos.....	80
5.2 Development of Proposed Mixed Dimension Reduction Approach.....	83
5.2.1 Constructing a Crude Representation of the Response	83

5.2.2 Sensitivity Sweeping Algorithm for Aleatory Dimensions.....	85
5.2.3 Modified Sensitivity Sweeping Algorithm for Epistemic Dimensions.....	88
5.2.4 Constructing the Reduced Dimensional PC Expansion	90
5.3 Numerical Examples	90
5.3.1 Example 1	90
5.3.2 Example 2	94
5.3.3 Example 3	96
CHAPTER 6: A NOVEL DIMENSION FUSION BASED POLYNOMIAL CHAOS APPROACH FOR MIXED ALEATORY-EPISTEMIC UNCERTAINTY QUANTIFICATION.....	100
6.1 Proposed Dimension Fusion Based PC Approach.....	102
6.1.1 Model Parameters with Mixed Uncertainty	102
6.1.2 Dimension Fusion	103
6.1.3 Orthonormal Basis Construction for Mixed Dimensions.....	104
6.2 Dimension Reduction Using Sensitivity Sweeping Approach for Mixed Parameters.....	106
6.2.1 Sensitivity Sweeping for Aleatory Part of the Mixed Parameters	107
6.2.2 Sensitivity Sweeping for Epistemic Part of Mixed Parameters	109
6.2.3 Constructing the Reduced Dimensional PC Expansion	110
6.2.4 Evaluating max/min bounds of statistical moments.....	111
6.3 Numerical Examples	112
6.3.1 Example 1	112
6.3.2 Example 2	114
6.3.2 Example 3	117
CHAPTER 7: CONCLUSION.....	120
REFERENCES	122
APPENDIX A: LIST OF PUBLICATIONS	134

CHAPTER 1: INTRODUCTION

1.1 Problem statement

With the scaling of VLSI technology to sub-45 nm levels, uncertainty in the nanoscale manufacturing processes and operating conditions have been found to result in unpredictable behavior of high speed circuits. As a result, contemporary computer aided design (CAD) tools need to be flexible enough to be able to predict the impact of parametric uncertainty on general circuit responses. Traditionally, uncertainty quantification of circuit networks has been performed using the brute-force Monte Carlo approach [1]-[6]. Despite the simplicity of this approach, its slow convergence translates to a prohibitively large number of deterministic simulations of the original network model in order to achieve accurate statistical results. This makes the Monte Carlo approach computationally infeasible for analyzing large networks [7].

Recently, more robust uncertainty quantification techniques based on the generalized polynomial chaos (PC) theory have been reported for various high-speed circuit, electromagnetic (EM) and electronic packaging problems [7]-[41]. These techniques attempt to model the uncertainty in the network response as an expansion of predefined orthogonal polynomial basis functions of the input random variables. The coefficients of the expansion form the new unknowns of the system and are evaluated via intrusive or non-intrusive approaches [42].

The existing literature in circuit and EM simulation has been dominated by the highly accurate but intrusive stochastic Galerkin (SG) approach [7]-[22]. This approach requires the solution of a single but augmented coupled deterministic network model to

determine the PC coefficients. Overall, the simulation costs of such large models scale in a near-exponential manner with the number of random dimensions. While recent works such as the decoupled PC algorithm [17] and the stochastic testing method [37], can mitigate the time and memory costs of the standard SG approach, both these approaches require the development of intrusive codes that preclude the direct exploitation of SPICE-like legacy circuit simulators. These bottlenecks have limited the applicability of the SG approach to problems featuring only low-dimensional random spaces [42], [43].

On the other hand, non-intrusive PC approaches such as the stochastic collocation (SC) approach, pseudo-spectral collocation approach and linear regression approach, among others, have recently been explored for circuit and EM problems as well [23]-[36]. The advantage of these non-intrusive approaches over the intrusive SG approach lies in their ability to compute the PC coefficients of the network responses by simply probing the original model at a sparse set of nodes located within the random space [43]. The deterministic simulation of the network at each node can be performed by a direct invocation of SPICE without the need for any intrusive coding. In addition, the relevant deterministic simulations can be parallelized unlike the conventional SG approach where the augmented network is always coupled.

Irrespective of the approach used to evaluate the coefficients, the major bottleneck in all PC approaches is that the number of unknown coefficients scales in a polynomial fashion with the number of random dimension [42], [43]. Thus, conventional PC approaches are often too computationally expensive for high-dimensional random spaces.

1.2 Scope of the thesis

Among non-intrusive approaches, the linear regression approach has been found to be highly popular [24], [25], [43]. This approach probes the PC expansion of the network responses at an oversampled set of multidimensional nodes located within the random space, thereby leading to the formulation of an overdetermined set of linear algebraic equations. These equations can be solved in a least-square sense to directly evaluate the PC coefficients of the network responses [43]. Typically, the multidimensional regression nodes are chosen from the tensor product grid of one dimensional (1D) quadrature nodes [24], [25]. Since the number of nodes in the tensor product grid increases exponentially with the number of random dimensions, realistically only a sparse subset of the nodes, also referred to as design of experiments (DoE), can be chosen. In the work of [36], it was demonstrated that blindly choosing the DoE can lead to inaccurate evaluation of the PC coefficients. However, the contemporary literature on linear regression based PC analysis of EM and circuit problems have not identified any specific formal criterion for choosing the best set of DoE [24], [25]. Recently, the stochastic testing approach has developed a reliable technique to select possible DoE where the number of DoE is equal to the number of unknown PC coefficients [37], [38]. However, this technique does not choose the DoE using any optimal criterion and hence does not guarantee the maximum possible accuracy of results.

In order to address the above issues, this dissertation presents a new linear regression methodology based on the alternative D-optimal criterion for choosing the DoE. This criterion stipulates that for the most accurate evaluation of the PC coefficients, the corresponding DoE have to be so chosen such that the determinant of the information matrix in the linear regression

problem is maximized [46]. Moreover, this dissertation proposes a greedy search algorithm in order to identify the D-optimal DoE from multidimensional random spaces. The proposed search algorithm begins with an arbitrary set of DoE chosen from the tensor product grid of 1D quadrature nodes and then sequentially replaces each DoE in that initial set with the best possible substitute selected from the remaining set of quadrature nodes. The best possible substitute DoE is chosen to be the one that increases the current determinant of the information matrix by the largest amount. This step-by-step refinement of the starting set of DoE continues till all of them have been replaced at which point the new set forms the D-optimal DoE [36]. Finally, novel numerical strategies to expedite the search of the substitute DoE for problems involving high-dimensional random spaces have also been developed.

In order to mitigate the poor scalability of conventional PC approaches, in this dissertation, an alternative reduced dimensional PC approach is presented that is applicable for mutually uncorrelated random dimensions as commonly encountered in many microwave/RF networks. This approach uses the HDMR formulation only once to directly quantify the impact of each random dimension on the network responses when acting alone [54]. This information is modeled as unidimensional (1D) PC expansions. These 1D expansions are then used in an analysis of variance (ANOVA) formulation to identify the least important random dimensions, which are then removed from the original random space [55], [56]. Now performing a PC expansion in the resultant low-dimensional random subspace leads to the recovery of a very sparse set of coefficients with negligible loss of accuracy. This reduced dimensional PC approach is further extended to model the impact of both aleatory (random) and epistemic (ignorance based) uncertainty on the performance of high speed networks. The key feature of this approach is the development of a parameterized analysis of variance (ANOVA) strategy to

identify which of the aleatory random dimensions have minimal impact on the response surface of the network. By removing the statistically insignificant dimensions, a highly compact PC representation of the response surface can be developed. This PC representation will serve as a metamodel capturing the impact of the purely epistemic, purely aleatory, and mixed epistemic-aleatory effects.

Mixed problems are characterized by far greater number of dimensions than purely epistemic or aleatory problems. Thus, the poor scalability of PC expansions is even more prominent for mixed problems. This issue is further compounded by the fact that traditional sparse PC methods use statistical measures to decide which PC bases can be removed or retained [41], [57]. However, for mixed problems, the presence of epistemic uncertainty makes it impossible to define unique statistical moments. Therefore, sparse PC representations are not available for mixed problems. In this dissertation, a novel dimension fusion approach to address the above scalability issue of mixed problems is proposed. As the name suggests, this approach fuses the epistemic and aleatory dimensions within the same model parameter into a mixed dimension which allows the information contained within a large dimensional mixed uncertainty space to be compressed into a low dimensional space.

1.3 Organization of the text

In this dissertation, most of the state of the art PC approaches are reviewed. Exploited techniques are explained in details, and novel ideas are supported with extensive numerical examples and discussions. The rest of text is organized as follows: Chapter 2 provides a review of basics of the generalized PC theory and the most common nonintrusive uncertainty quantification approaches including stochastic collocation and the

linear regression approach, and finally concludes with an overview of sparse polynomial chaos techniques. Moreover, the major advantages and disadvantages of these approaches are provided in this chapter. Chapter 3 mainly deals with improvements to the linear regression approach. This chapter starts with a review of the D-optimal criterion and the Fedorov search algorithm for the linear regression approach. Next, two novel numerical strategies to expedite the search algorithm for high-dimensional problems, are presented. The chapter then concludes with a comparative analysis of CPU costs of the proposed D-optimal linear regression approach against other non-intrusive approaches. Chapter 4 uses a high dimensional model representation (HDMR) to formulate sensitivity indices which enable the truncation of a high dimensional PC model to a reduced model. Novel strategies to reuse PC bases and SPICE simulations are discussed. The same HDMR formulation is then used to further extend the reduced dimensional PC method to mixed problems which contain both aleatory (random) and epistemic (ignorance based) uncertainty. In Chapter 5, parameterized sensitivity indices are developed to enable truncation of high dimensional mixed problems. Chapter 6 uses a dimension fusion strategy whereby the aleatory and epistemic uncertainty in a model parameter is collectively represented using a single mixed variable. In all the chapters, every proposed method is validated using multiple numerical examples.

CHAPTER 2: RELATED WORK

In this chapter, a comprehensive review of existing uncertainty quantification techniques is discussed. First, a brief review brute force techniques like Monte Carlo and its variants are presented. Their drawbacks are discussed, leading to the requirement of more robust uncertainty quantification techniques. Next, an overview of the generalized polynomial chaos (gPC) approach is presented and intrusive/non-intrusive approaches to quantify uncertainty using gPC are discussed. The intrusive approaches discussed are Stochastic Galerkin (SG) [7]-[22] and Stochastic Testing [37]. The non-intrusive approaches discussed are Pseudo Spectral Stochastic Collocation [26], classical linear regression [48], [49], Stochastic Collocation [29], [30], [42], [43], Stroud cubature rules [23], [31], [33], [35] and the non-intrusive formulation of stochastic testing [34]. Since the main focus of this thesis is the development of methodologies to sparsify the gPC expansion, other sparse PC techniques such as the anisotropic PC [73], Hyperbolic Polynomial Chaos Expansion (HPCE) [59] and the hierarchical sparse PC approaches [40], [41] are discussed. The merits and demerits of using each technique with respect to other techniques are finally discussed.

2.1 Monte Carlo

Traditionally, brute-force Monte Carlo techniques were used to quantify uncertainty for high-speed circuit networks. In this approach, a large number of pseudo-random multidimensional samples are collected based on the PDF of the input parameters [1]. The network is simulated at each of these samples and the ensemble of the output response is obtained. Any desired statistical moment can be computed from this ensemble of responses.

If N observations of a quantity X represented by $\{x_1, x_2, \dots, x_N\}$ are obtained, the Monte Carlo approach estimates the mean value of X as the expected value of the set $\{x_i\}_{i=1}^N$

$$\mu_x = \frac{1}{N} \sum_{i=1}^N x_i \quad (2.1)$$

The variance of X is given by

$$\text{Var}_x = \frac{1}{N} \sum_{i=1}^N (x_i - \mu_x)^2 \quad (2.2)$$

The main drawback of Monte Carlo is that a large number of simulations are required for convergence $\sim O(\frac{1}{\sqrt{N}})$. The computational cost especially becomes prohibitive if the time taken for each simulation of the network is large.

2.2 Quasi Monte Carlo

Quasi Monte Carlo technique differs from Monte Carlo in the way that the input samples are generated. Monte Carlo uses pseudo-random samples whereas quasi Monte-Carlo uses a low discrepancy sequence like Sobol's sequence. This difference is illustrated in Fig. 2.1.

The main advantage of using a low discrepancy sequence is that a faster rate of convergence is obtained. Quasi Monte Carlo has a rate of convergence which is $O(1/N)$.

2.3 Latin Hypercube Sampling

Latin Hypercube Sampling, like Quasi Monte Carlo attempts to generate points that are evenly distributed over the entire random space of the input parameters.

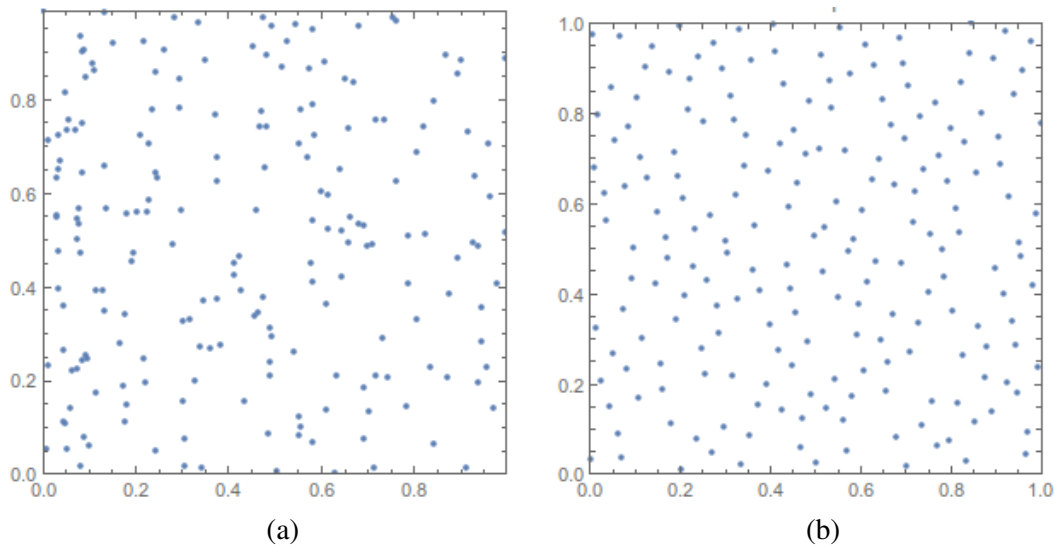


Fig. 2.1: Difference between a low discrepancy sequence and pseudo-random sequence. (a) Pseudo random sequence (b) Sobol's sequence

This is achieved by partitioning the input distribution into multiple intervals of equal probability and selecting one sample from each interval. Doing so prevents clustering of points that could happen when pseudo-random sequences are used. LHS sampling is illustrated in Fig. 2.2. Like Quasi Monte Carlo, LHS sampling has a better convergence than Monte Carlo which is $O(1/N)$.

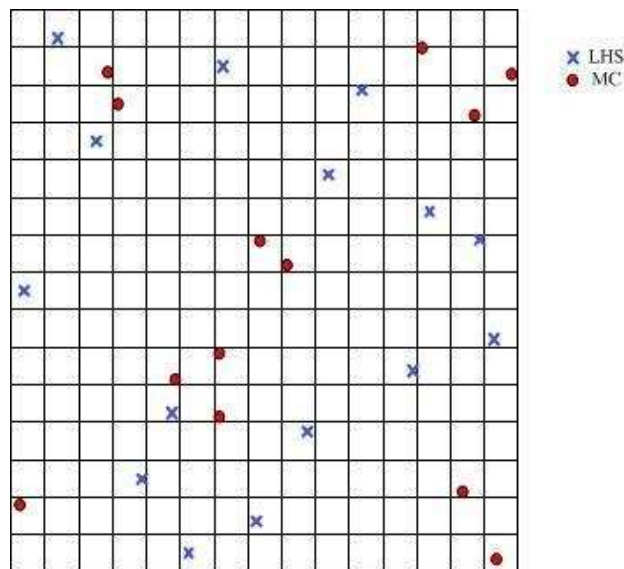


Fig. 2.2: Latin hypercube sampling

2.4 Generalized Polynomial Chaos (gPC) Theory

The concept of orthogonal polynomials has existed for a long time [44]. Polynomial Chaos Theory was first introduced only for Hermite orthogonal polynomials and was called ‘Hermite-Chaos’. However, due to the need to solving differential equations in the presence of uncertainty for a large number of engineering disciplines, the polynomial chaos technique was extended to include other orthogonal polynomials and was renamed as the generalized Polynomial Chaos (gPC) theory.

Consider a network where the input uncertainty is represented by one random variable, λ occupying the random space Ω . Provided the variables have finite second order moments, the uncertainty in the network response $X(t, \lambda)$ is modeled using gPC theory and is represented as an expansion of orthogonal polynomials and their coefficients.

$$X(t, \lambda) = \sum_{k=0}^{\infty} c_k(t) \varphi_k(\lambda) \quad (2.3)$$

where $c_k(t)$ represents the coefficient as a function of time and $\varphi_k(\lambda)$ is a unidimensional orthogonal polynomial basis with respect to the probability distribution function (PDF) of the input random variable. The expansion in 2.3 is truncated to

$$X(t, \lambda) = \sum_{k=0}^m c_k(t) \varphi_k(\lambda) \quad (2.4)$$

where m represents the order of expansion of the polynomial and there are $m+ 1$ terms in the expansion. The polynomials $\varphi_k(\lambda)$ are orthogonal with respect to the PDF of the random input parameter λ .

$$\langle \phi_i(\lambda) \phi_j(\lambda) \rangle = \int_{\Omega} \phi_i(\lambda) \phi_j(\lambda) \rho(\lambda) d\lambda = \alpha_i^2 \delta_{ij} \quad (2.5)$$

Table 2.1: Polynomials and their corresponding distributions

Distribution of λ	Orthogonal Polynomials	Support
Gaussian	Hermite	$(-\infty, \infty)$
Uniform	Legendre	$[-1, 1]$
Beta	Jacobi	$[-1, 1]$
Gamma	Laguerre	$[0, \infty)$

where \langle, \rangle represents the inner product operation, ρ represents the PDF of λ , α_i^2 is a constant and δ_{ij} is the Kronecker delta function. The constant term α_i^2 is used as a normalizing factor to generate orthonormal polynomials. It is important to note that polynomials need to be chosen based on the Wiener-Askey scheme [44], which states that there is a one-one correspondence between the distribution of the polynomials and the kind of orthogonal polynomial used in the expansion. This guarantees the fastest rate of convergence for the PC expansion which is exponential. The corresponding class of orthogonal polynomials with respect to standard distributions can be found in Table 2.1

2.4.1 One-dimensional orthonormal polynomials

Consider the standard normal distribution $N(0,1)$ where the PDF $\rho(\lambda)$ is represented as

$$\rho(\lambda) = \frac{1}{\sqrt{2\pi}} e^{-\frac{\lambda^2}{2}} \quad (2.6)$$

According to Table 2.1, the Hermite polynomials are the appropriate orthogonal polynomials to the normal distribution. These polynomials can either be generated in an analytic manner [44]

$$H_k(\lambda) = (-1)^k e^{\frac{\lambda^2}{2}} \frac{d^k}{d\lambda^k} e^{-\frac{\lambda^2}{2}} \quad (2.7)$$

or using a three-term recurrence relation

$$H_{k+1}(\lambda) = \lambda H_k(\lambda) - kH_{k-1}(\lambda) \quad (2.8)$$

From 2.7, it can be observed that $H_0 = 1$ and $H_1 = \lambda$. The normalizing factor for Hermite polynomials can be obtained as

$$\langle H_k(\lambda), H_k(\lambda) \rangle = k! \quad (2.9)$$

Similarly, considering the standard uniform distribution $U(-1,1)$, the PDF $\rho(\lambda)$ is represented as

$$\rho(\lambda) = \begin{cases} \frac{1}{2} & -1 \leq \lambda \leq 1 \\ 0 & \text{otherwise} \end{cases} \quad (2.10)$$

According to Table 2.1, the Legendre polynomials are the appropriate orthogonal polynomials to the uniform distribution. These polynomials too can either be generated in an analytic manner [44]

$$P_k(\lambda) = \frac{1}{2^k k!} \frac{d^k}{d\lambda^k} (\lambda^2 - 1)^k \quad (2.11)$$

or using the three-term recurrence relation

$$P_{k+1}(\lambda) = \frac{2k+1}{k+1} \lambda P_k(\lambda) - \frac{k}{k+1} P_{k-1}(\lambda) \quad (2.12)$$

From 2.11, it can be observed that $P_0 = 1$ and $P_1 = \lambda$. The normalizing factor for Hermite polynomials can be obtained as

$$\langle P_k(\lambda), P_k(\lambda) \rangle = \frac{1}{2k+1} \quad (2.13)$$

For ease of understanding, the first six univariate orthonormal Hermite and Legendre polynomials are listed in Table 2.2

Table 2.2: Univariate orthonormal Hermite and Legendre polynomials

Index k	Orthonormal Hermite polynomial $H_k(\lambda)$	Orthonormal Legendre polynomial $P_k(\lambda)$
0	1	1
1	λ	$\sqrt{3}\lambda$
2	$(\lambda^2 - 1)/\sqrt{2}$	$\sqrt{5}(\frac{3}{2}\lambda^2 - \frac{1}{2})$
3	$(\lambda^3 - 3\lambda)/\sqrt{6}$	$\sqrt{7}(\frac{5}{2}\lambda^3 - \frac{3}{2}\lambda)$
4	$(\lambda^4 - 6\lambda^2 + 3)/2\sqrt{6}$	$3(\frac{35}{8}\lambda^4 - \frac{30}{8}\lambda^2 + \frac{3}{8})$
5	$(\lambda^5 - 10\lambda^3 + 15\lambda)/2\sqrt{30}$	$\sqrt{11}(\frac{63}{8}\lambda^5 - \frac{70}{8}\lambda^3 + \frac{15}{8})$

2.4.2 Multidimensional orthonormal polynomials

Most practical applications deal with uncertainty quantification in the presence of multiple random variables. In this subsection, generation of multidimensional orthonormal polynomials using univariate orthonormal polynomials is discussed. Consider a general network where the input uncertainty is represented by n mutually uncorrelated random variables $\boldsymbol{\lambda} = [\lambda_1, \lambda_2, \dots, \lambda_n]$. The PC approach approximates the uncertainty in the response $\mathbf{X}(t, \boldsymbol{\lambda})$ as

$$\mathbf{X}(t, \boldsymbol{\lambda}) = \sum_{k=0}^{P+1} c_k(t) \phi_k(\boldsymbol{\lambda}) \quad (2.14)$$

The expansion is truncated to $P+1$ terms which is given by

$$P+1 = \frac{(m+n)!}{m!n!} \quad (2.15)$$

The multivariate polynomials $\phi_k(\boldsymbol{\lambda})$ are now orthonormal to the joint probability distribution function (PDF) of the input random variables. Since the variables are independent, their joint PDF can be expressed as the product of their individual PDF's.

$$\langle \phi_i(\boldsymbol{\lambda})\phi_j(\boldsymbol{\lambda}) \rangle = \int_{\Omega} \phi_i(\boldsymbol{\lambda})\phi_j(\boldsymbol{\lambda})\rho(\boldsymbol{\lambda})d\boldsymbol{\lambda} = \alpha_i^2\delta_{ij} \quad (2.16)$$

The multivariate polynomial basis can be obtained as the product of the univariate polynomial basis across each dimension

$$\phi_k(\boldsymbol{\lambda}) = \prod_{i=1}^n \phi_{k_i}(\lambda_i) \quad \sum_{i=1}^n k_i \leq m \quad (2.17)$$

From 2.16 and 2.17, it is evident that the inner product in 2.16 equals α_i^2 only when both multidimensional polynomials are the same and 0 otherwise.

For illustration purposes, the generation of two-dimensional basis is shown below.

$$\begin{aligned} & \phi_0(\lambda_1)\phi_0(\lambda_2) \\ & \phi_1(\lambda_1)\phi_0(\lambda_2) \quad \phi_0(\lambda_1)\phi_1(\lambda_2) \\ & \phi_2(\lambda_1)\phi_0(\lambda_2) \quad \phi_1(\lambda_1)\phi_1(\lambda_2) \quad \phi_0(\lambda_1)\phi_2(\lambda_2) \\ & \phi_3(\lambda_1)\phi_0(\lambda_2) \quad \phi_2(\lambda_1)\phi_1(\lambda_2) \quad \phi_1(\lambda_1)\phi_2(\lambda_2) \quad \phi_0(\lambda_1)\phi_3(\lambda_2) \\ & \phi_4(\lambda_1)\phi_0(\lambda_2) \quad \phi_3(\lambda_1)\phi_1(\lambda_2) \quad \phi_2(\lambda_1)\phi_2(\lambda_2) \quad \phi_1(\lambda_1)\phi_3(\lambda_2) \quad \phi_0(\lambda_1)\phi_4(\lambda_2) \end{aligned}$$

Fig 2.3: Generation of bivariate basis for $m=4$

It is noted that the total degree across both dimensions remains constant in each row and is incremented row by row [44].

2.4.3 Derivation of statistics

The major benefit of using the gPC approach to model the uncertainty in any system is that all the statistical information of the response is contained in the PC coefficients. The mean and variance of the output can be obtained as a function of the coefficients by integrating over the random space Ω_n . To obtain the PDF and other higher order statistical moments, the PC

metamodel is probed at a large number of Monte Carlo samples. In this subsection, derivation of the statistical information is explained. The temporal dependence of the terms in the expansion is removed for convenience.

The expected value or the mean of the response $X(\lambda)$ is represented as

$$E(X(\lambda)) = \int_{\Omega_n} X(\lambda) \rho(\lambda) d\lambda = \sum_{k=0}^P c_k \int_{\Omega_n} \phi_0(\lambda) \phi_k(\lambda) \rho(\lambda) d\lambda \quad (2.18)$$

It is noted that the first $\phi_0(\lambda)$ is always equal to 1 for all orthonormal polynomials.

$$E(X(\lambda)) = \sum_{k=0}^P c_k \langle \phi_0(\lambda) \phi_k(\lambda) \rangle = c_0 \quad (2.19)$$

Therefore, the mean or expected value of the response is just the first coefficient in the expansion.

The variance of the response $X(\lambda)$ is represented as

$$\begin{aligned} Var(X(\lambda)) &= E(X(\lambda) - E(X(\lambda)))^2 \\ &= \int_{\Omega_n} \left(\sum_{k=0}^P c_k \phi_k(\lambda) - c_0 \phi_0(\lambda) \right)^2 \rho(\lambda) d\lambda \\ &= \sum_{k=0}^P \sum_{j=0}^P c_k c_j \int_{\Omega_n} \phi_k(\lambda) \phi_j(\lambda) \rho(\lambda) d\lambda - c_0^2 \\ &= \sum_{k=0}^P c_k^2 - c_0^2 = \sum_{k=1}^P c_k^2 \end{aligned} \quad (2.20)$$

The variance is the sum of squares of all coefficients except the first.

Any general M^{th} higher order moment can be expressed as

$$\begin{aligned} \mu_m &= E(X(\lambda) - E(X(\lambda)))^M \\ &= \int_{\Omega_n} (X(\lambda) - E(X(\lambda)))^M \rho(\lambda) d\lambda \end{aligned} \quad (2.21)$$

Any higher order moment can be computed by generating a large number of Monte Carlo samples based on the input distribution. Since the PC metamodel is already known, it is not required to simulate the network at all the sample points. The PC metamodel is probed at all the samples and the values of the response $X(\lambda)$ is substituted in 2.21 to easily obtain any higher order statistical moment.

2.5 Intrusive and non-intrusive methods

In this section, approaches to determine the unknown coefficients of 2.3 are discussed. These unknown coefficients are obtained either using intrusive or non-intrusive techniques.

2.5.1 Intrusive methods

Intrusive methods are one of the ways in which the unknown coefficients of the PC metamodel are computed. Intrusive methods like Stochastic Galerkin (SG) are highly accurate and require the construction of an augmented and coupled deterministic network [7]-[22]. The unknown PC coefficients are then determined by a single run of this augmented deterministic network. The main disadvantage of the SG approach is that this augmented and coupled deterministic network is cumbersome to develop. Since the augmentation is $P+1$ times, the CPU time and memory costs scale in a near exponential manner with respect to the number of random dimensions. Since a separate solver is required for the SG approach, it cannot make use of existing deterministic SPICE solvers for the given network. Furthermore, for non-linear circuits, the SG approach uses lumped dependent sources which further augment the network [15]. Due to these reasons, the SG approach is favorable for simple circuits with small number of random parameters.

The intrusive formulation of the Stochastic Testing (ST) approach was developed to address the inefficiencies of the SG approach [37]. The ST approach solves the coupled system of equations of the augmented circuit, but in a decoupled manner at each time point. Like non-intrusive methods, the coupled equations are solved at $P+1$ sampling points which are obtained using a node selection algorithm [37]. Unlike the SG approach, the ST approach can be parallelized since the equations are solved in a decoupled manner. The main disadvantage of the ST approach is that the node selection algorithm does not guarantee the best selection of simulation nodes. For more details of the ST approach, readers are encouraged to read [34], [37].

2.5.2 Non-intrusive methods

Non-intrusive approaches to determine the unknown gPC coefficients are attractive because they do not require the development of new deterministic network solvers. Existing SPICE solvers can be used to simulate the network at the determined simulation points. Also, since the simulations are independent of each other, they can be parallelized leading to greater speedup when compared to intrusive approaches. Popular intrusive approaches are discussed in this section.

2.5.2.1 Pseudo-spectral collocation

In the pseudo-spectral collocation approach, the output is expanded in a series of orthogonal polynomials using the gPC expansion and numerical integration techniques are used to determine the PC coefficients [26]. Numerical integration with Gaussian quadrature techniques approximate the integral of a function $F(\lambda)$ as a weighted sum of function values computed at predetermined sample points

$$\int_{\Omega_n} F(\boldsymbol{\lambda})\rho(\boldsymbol{\lambda})d\boldsymbol{\lambda} \approx \sum_{i=1}^Q F(\boldsymbol{\lambda}^i)w(\boldsymbol{\lambda}^i) \quad (2.22)$$

where Q is the total number of simulation points given by $Q=(m+1)^n$, $\boldsymbol{\lambda}^i=[\lambda_1^i,\lambda_2^i,\dots,\lambda_n^i]$, $F(\boldsymbol{\lambda}^i)$ is the value of the function F evaluated at $\boldsymbol{\lambda}^i$ and $w(\boldsymbol{\lambda}^i)$ represents the weight corresponding to the node $\boldsymbol{\lambda}^i$. For a one-dimensional problem, λ^i are the roots of the one-dimensional polynomial corresponding to the input distribution according to the Askey scheme. For an n -dimensional problem, Q is given by the tensor product of the one-dimensional polynomial roots taken across all n dimensions.

In order to determine the unknown gPC coefficients c_k , using Gaussian quadrature integration rules, the projection theorem is used, which performs an orthogonal projection on to the polynomial basis as

$$c_k = \frac{\langle X, \phi_k \rangle}{\langle \phi_k, \phi_k \rangle} = \int_{\Omega_n} \frac{X(t, \boldsymbol{\lambda})\phi_k(\boldsymbol{\lambda})\rho(\boldsymbol{\lambda})d\boldsymbol{\lambda}}{\alpha_k^2} = \sum_{i=1}^Q X(t, \boldsymbol{\lambda}^i)\phi_k(\boldsymbol{\lambda}^i)w(\boldsymbol{\lambda}^i) \quad (2.23)$$

The nodes are obtained as the roots of the polynomial. Another way to obtain nodes and their corresponding weights $w(\boldsymbol{\lambda}^i)$ is by solving an eigenvalue problem which is known as the Golub-Welsh algorithm [61].

The main advantage of the pseudo-spectral collocation approach is that for moderate number of random dimensions, the number of simulations required will be far lesser than that required for Monte-Carlo. For higher dimensional problems, since the number of required simulations scales in an exponential manner with respect to the number of random dimensions, the pseudo-spectral collocation approach, when used to find the PC coefficients fails to provide any benefits. In such scenarios, it is beneficial to use Monte-Carlo to compute the problem statistics.

2.5.2.2 Conventional Linear Regression approach

The conventional linear regression approach is another non-intrusive way of finding the gPC coefficients. It takes advantage of the linear least squares technique to find the best fit for the PC coefficients [48]. This approach begins by approximating the uncertainty in the network response as shown in 2.14. The expansion of (2.14) is oversampled at $M = 2(P+1)$ nodes located within the random space Ω in order to achieve the best possible fit of the PC coefficients over the entire n -dimensional random space Ω [48]. This results in the formulation of an overdetermined system of linear algebraic equations [38]

$$\mathbf{A}\tilde{\mathbf{X}} + \boldsymbol{\varepsilon} = \mathbf{E} \quad (2.24)$$

where

$$\mathbf{A} = \begin{bmatrix} \phi_0(\boldsymbol{\lambda}^{(1)})\mathbf{I} & \cdots & \phi_P(\boldsymbol{\lambda}^{(1)})\mathbf{I} \\ \vdots & \ddots & \vdots \\ \phi_0(\boldsymbol{\lambda}^{(M)})\mathbf{I} & \cdots & \phi_P(\boldsymbol{\lambda}^{(M)})\mathbf{I} \end{bmatrix}; \quad \tilde{\mathbf{X}} = \begin{bmatrix} \mathbf{X}_0 \\ \vdots \\ \mathbf{X}_P \end{bmatrix}; \quad (2.25)$$

$$\mathbf{E} = \begin{bmatrix} \mathbf{X}(\boldsymbol{\lambda}^{(1)}) \\ \vdots \\ \mathbf{X}(\boldsymbol{\lambda}^{(M)}) \end{bmatrix}; \quad \boldsymbol{\varepsilon} = \begin{bmatrix} \varepsilon_1 \\ \vdots \\ \varepsilon_M \end{bmatrix}$$

2.24 can now be solved in a least square sense to obtain the PC coefficients as

$$\tilde{\mathbf{X}} = (\mathbf{A}^T \mathbf{A})^{-1} \mathbf{A}^T \mathbf{E} \quad (2.26)$$

A detailed description of the linear regression methodology is provided in Chapter 3. The main benefit of the linear regression methodology compared to pseudo-spectral collocation is that the number of simulations required is $M = 2(P+1)$ which means that it scales in a polynomial fashion with respect to the number of random dimensions as opposed to the exponential scaling. This provides significant savings in CPU costs and makes it an attractive approach for large dimensional problems. The main drawback of using the conventional linear regression approach

is that it uses the Fedorov algorithm based on the D-optimality criteria to select the M nodes which involves a $(P+1) \times (P+1)$ size matrix inversion at each stage in the node selection process. This leads to exorbitant CPU costs for finding the nodes. Novel methodologies to mitigate these costs are discussed in Chapter 3.

2.5.2.3 Non-intrusive formulation of Stochastic Testing

The non-intrusive formulation of the Stochastic Testing approach [34] requires less number of nodes when compared to the conventional linear regression approach. The ST approach samples 2.14 at only $M = (P+1)$ points in the random space. The resultant system of equations can be expressed as

$$\begin{bmatrix} \phi_0(\boldsymbol{\lambda}^{(1)})\mathbf{I} & \cdots & \phi_P(\boldsymbol{\lambda}^{(1)})\mathbf{I} \\ \vdots & \ddots & \vdots \\ \phi_0(\boldsymbol{\lambda}^{(M)})\mathbf{I} & \cdots & \phi_P(\boldsymbol{\lambda}^{(M)})\mathbf{I} \end{bmatrix} \begin{bmatrix} \mathbf{X}_0 \\ \vdots \\ \mathbf{X}_P \end{bmatrix} = \begin{bmatrix} \mathbf{X}(\boldsymbol{\lambda}^{(1)}) \\ \vdots \\ \mathbf{X}(\boldsymbol{\lambda}^{(M)}) \end{bmatrix} \quad (2.27)$$

The methodology to select the M nodes is described below.

The major challenge in the ST approach is determination of testing nodes since poor selection of nodes results in ill-conditioned matrices which in turns makes the solution inaccurate or impossible to obtain. In order to address this issue, the ST approach of [34] starts with $(m+1)^n$ nodes obtained by taking the tensor product of the $(m+1)$ unidimensional roots of the polynomial orthogonal to the joint distribution of input random variables. In order to have accurate results, the algorithm states that all the nodes need to be arranged in the descending order of their weights and the first node $\boldsymbol{\lambda}^{(1)}$ is taken to be the one with the highest weight. The vector \mathbf{V} is defined as

$$\mathbf{V} = \frac{\mathbf{H}(\boldsymbol{\lambda}^{(1)})}{\|\mathbf{H}(\boldsymbol{\lambda}^{(1)})\|} \quad (2.28)$$

where $\mathbf{H}(\boldsymbol{\lambda}^{(k)}) = \{\phi_0(\boldsymbol{\lambda}^{(k)}), \phi_1(\boldsymbol{\lambda}^{(k)}), \dots, \phi_p(\boldsymbol{\lambda}^{(k)})\}^T$. Assume that $r-1$ candidate nodes have already been selected. The vector space that spans these $r-1$ nodes can be represented as

$$\mathbf{V} = \text{span}\{\mathbf{H}(\boldsymbol{\lambda}^{(1)}), \mathbf{H}(\boldsymbol{\lambda}^{(2)}), \dots, \mathbf{H}(\boldsymbol{\lambda}^{(r-1)})\} \quad (2.29)$$

Now any node $\boldsymbol{\lambda}^{(r)}$ is considered to be a candidate node if $\mathbf{H}(\boldsymbol{\lambda}^{(r)})$ has a large enough orthogonal component to \mathbf{V} . This is determined as follows

$$\begin{aligned} v &= \mathbf{H}(\boldsymbol{\lambda}^{(r)}) - \mathbf{V}(\mathbf{V}^T \mathbf{H}(\boldsymbol{\lambda}^{(r)})) \\ \frac{\|v\|}{\|\mathbf{H}(\boldsymbol{\lambda}^{(r)})\|} &> \beta \end{aligned} \quad (2.30)$$

where β is a predefined constant. If the condition in 2.30 is satisfied, $\mathbf{H}(\boldsymbol{\lambda}^{(r)})$ is added to the vector span \mathbf{V} .

The node selection algorithm used in the ST approach is faster than the linear regression approach as there are no matrix inversions involved. It also requires the least number of network simulations, only $P+1$ as compared to $2(P+1)$ required in the linear regression approach. The main drawback here is that the ST algorithm selects the first $P+1$ nodes with a large enough orthogonal component to \mathbf{V} . This does not always guarantee optimal selection of the testing nodes.

2.6 Sparse Polynomial Chaos Techniques

It is common knowledge that the CPU cost to evaluate the unknown gPC coefficients scales in a polynomial fashion with respect to the number of random dimensions. This is the

major bottleneck for most PC approach. To mitigate this, the PC expansion needs to be sparsified. In this subsection, some sparse PC techniques are discussed.

2.6.1 Sensitivity Indices using ANOVA-HDMR

One way to sparsify the PC expansion is to get an understanding of how much of an impact each random input parameter has on the network output and retain only those parameters which have a significant impact on the response. For this purpose, the network response is split into a sum of functions of increasing dimensions known as High Dimensional Model Representation (HDMR). This performs the separation of the effects of the input parameters which are transmitted in the decomposition of the variance [54].

$$x(t, \boldsymbol{\lambda}) = x_0(t) + \sum_{i=1}^n x_i(t, \lambda_i) + \sum_{1 \leq i, j \leq n} x_{ij}(t, \lambda_i, \lambda_j) + \dots + x_{12\dots n}(t, \lambda_1 \dots \lambda_n) \quad (2.31)$$

where x_0 is the nominal value of $x(t, \boldsymbol{\lambda})$, $x_i(t, \lambda_i)$ represents the contribution of λ_i to $x(t, \boldsymbol{\lambda})$ acting alone, $x_{ij}(t, \lambda_i, \lambda_j)$ represents the pairwise contribution of λ_i and λ_j to $x(t, \boldsymbol{\lambda})$ etc. The variance of the response is expressed as

$$\begin{aligned} \sigma_x^2 &= \int_{\boldsymbol{\Omega}_n} (x(t, \boldsymbol{\lambda}) - x_0)^2 d\boldsymbol{\lambda} \\ &= \int_{\boldsymbol{\Omega}_n} \left(\sum_{i=1}^n x_i(t, \lambda_i) + \sum_{1 \leq i, j \leq n} x_{ij}(t, \lambda_i, \lambda_j) + \dots + x_{12\dots n}(t, \lambda_1 \dots \lambda_n) \right) d\boldsymbol{\lambda} \\ &= \sum_{i=1}^N \int_{\boldsymbol{\Omega}_n} x_i^2(t, \lambda_i) d\boldsymbol{\lambda} + \sum_{1 \leq i, j \leq n} \int_{\boldsymbol{\Omega}_n} x_{ij}^2(t, \lambda_i, \lambda_j) + \dots \\ &= \sum_{i=1}^N \sigma_i^2 + \sum_{1 \leq i, j \leq n} \sigma_{ij}^2 + \dots \end{aligned} \quad (2.32)$$

Some properties of HDMR are used in the derivation of terms in 2.32 [55], [56].

Since the impact of each random dimension is studied on the variance of the response, this methodology is called Analysis Of Variance (ANOVA). Sensitivity indices quantify the contribution of each parameter on the output variance. They are expressed as

$$S_{i_1 i_2 \dots i_s} = \frac{\sigma_{i_1 i_2 \dots i_s}^2}{\sigma_x^2} \quad 1 \leq i_1 \leq \dots \leq i_s \leq n \quad (2.33)$$

The total sensitivity index of a parameter λ_i represents the total effect of λ_i on the output variance. It is represented as

$$S_{Ti} = S_i + \sum_{j=1, j \neq i}^n S_{ij} + \dots + S_{1..ijk..n} \quad (2.34)$$

The PC expansion can be used to compute the sensitivity indices of each input dimension by rearranging the terms in the expansion to resemble those in the HDMR expansion. Since all the statistical information in the PC expansion is contained in the coefficients, the sensitivity indices can easily be expressed in terms of the PC coefficients.

The main issue with using this method is that, in order to compute the sensitivity indices, all the PC coefficients need to be computed. Although, the dimensionality of the network can be reduced by only considering dimensions with significant values of the sensitivity index, the CPU costs scale in a polynomial fashion with respect to number of dimensions. In order to mitigate this cost, a novel reduced dimensional PC approach is proposed in Chapter 4.

2.6.2 Hierarchical Sparse PC Approach

The hierarchical sparse PC approach is another technique to develop a sparse PC expansion and mitigate the poor scalability of the gPC approach. This method also uses the

HDMR formulation but in an iterative manner by including only the component functions pertinent to the most important random parameters [40], [41].

Consider the HDMR expansion in 2.31. $|u|$ is defined as the cardinality of a component function. For example, $|u| = 1$ for $x_i(t, \lambda_i)$, $|u|=2$ for $x_{ij}(t, \lambda_i, \lambda_j)$ and so on. The iterative algorithm first computes the weights associated with a component function as

$$\gamma_u = \left| \frac{E(x(t, \boldsymbol{\lambda}))}{x_0} \right| \quad |u| = 1 \quad (2.35)$$

If γ_u exceeds a prescribed tolerance, then the random variable corresponding to the component function is considered to be significant. Next, the second order component functions corresponding to only the significant random dimensions are considered as candidates for constructing the second level HDMR. The associated weights are recomputed as

$$\gamma_u = \frac{|E(x_u(t, \lambda_u))|}{\left| \sum_{|v| < |u|-1} E(x_v(t, \lambda_v)) \right|} \quad |u| \geq 2 \quad (2.36)$$

This process continues in an iterative manner until the HDMR converges. At the third level, only the third level interactions of the important second order component functions are considered.

The hierarchical sparse PC approach uses very few terms in the PC expansion owing to its selection/eliminations. This reduces the computational effort to a large extent. The main drawback of this approach is that the error of the PC expansions representing the lower order interactions gets propagated to the higher levels. More details are given in Section 4.

2.6.3 Anisotropic Sparse PC Approach

The Anisotropic Sparse PC (APC) approach is based on the insight that each random dimension does not have equal impact on the network responses. As a result, the maximum degree of expansion along each dimension can be tuned to different values based on the magnitude of the impact each dimension has on the network response. This is in contrast to existing isotropic sparse PC approaches where the expansion requires the maximum degree of expansion along all dimensions to be equal and set to a common value. Due to the intelligent tuning of the maximum degrees of expansion along each dimension, an anisotropic PC expansion will be substantially sparser than a full-blown PC expansion and hence the associated coefficients can be evaluated far more efficiently.

The APC approach in [73] starts with the HDMR expansion in 2.31. The impact of each random dimension on the response $x(t, \boldsymbol{\lambda})$ acting along is quantified using the concept of cut-HDMR whereby

$$\begin{aligned} x_0(t) &= x(t, \boldsymbol{\lambda}^{(0)}) \\ x_i(t, \lambda_i) &= x(t, \boldsymbol{\lambda})|_{\boldsymbol{\lambda}^{(0)} \setminus \lambda_i} - x_0(t) \end{aligned} \quad (2.37)$$

The notation $\boldsymbol{\lambda}^{(0)} \setminus \lambda_i$ represents the vector where all component of $\boldsymbol{\lambda}$ except λ_i is set to 0. Based on (2.37), these impact terms can be expressed using 1D PC expansions as

$$x(t, \boldsymbol{\lambda})|_{\boldsymbol{\lambda}^{(0)} \setminus \lambda_i} - x_0(t) \approx \sum_{j=1}^{m_i} x_i^{(j)}(t) \phi_j(\lambda_i) \quad (2.38)$$

where $x_i^{(j)}(t)$ represents the j^{th} coefficient and ϕ_j is the corresponding 1D basis chosen from the Weiner-Askey scheme.

An iterative approach is used to determine the value of m_i . Its value is initially set to one and the coefficients of (2.38) are evaluated using the pseudo-spectral method [26]. Once the initial

coefficients are obtained, then the value of m_i is iteratively increased in steps of one and in each iteration the new coefficients of (2.38) are evaluated using the same pseudo-spectral method. After the computation of coefficients, the normalized enrichment in the variance predicted using the 1D expansion arising from the increment in the degree of expansion is evaluated as

$$S_i(t) = \frac{\sum_{j=1}^{r+1} (x_i^{(j,r)})^2 - \sum_{j=1}^r (x_i^{(j,r-1)})^2}{\sum_{j=1}^{r+1} (x_i^{(j,r)})^2} \quad (2.39)$$

where r refers to the current iteration. Once the enrichment falls below a prescribed tolerance ε , the iterations are halted.

Once the degree of expansion along all the random dimensions is known using the above methodology, an anisotropic PC expansion of the network response $x(t, \boldsymbol{\lambda})$ can be formulated as

$$\mathbf{X}(t, \boldsymbol{\lambda}) \approx \sum_{k=0}^Q \mathbf{X}_k(t) \psi_k(\boldsymbol{\lambda}) \quad (2.40)$$

where the multidimensional basis $\psi_k(\boldsymbol{\lambda})$ is a product of 1D basis as

$$\psi_k(\boldsymbol{\lambda}) = \prod_{i=1}^N \psi_{k_i}(\lambda_i) \quad (2.41)$$

with the constraint that

$$k_1 \leq m_1; k_2 \leq m_2; \dots; k_N \leq m_N \quad (2.42)$$

2.6.4 Hyperbolic PC Expansion

The Hyperbolic PC Expansion (HPCE) is another sparse PC technique which uses an alternative hyperbolic truncation scheme instead of the conventional linear truncation scheme.

This choice of the hyperbolic truncation scheme is based on the sparsity of effects principle which claims that the dominant effect on the response uncertainty comes from the impact of each

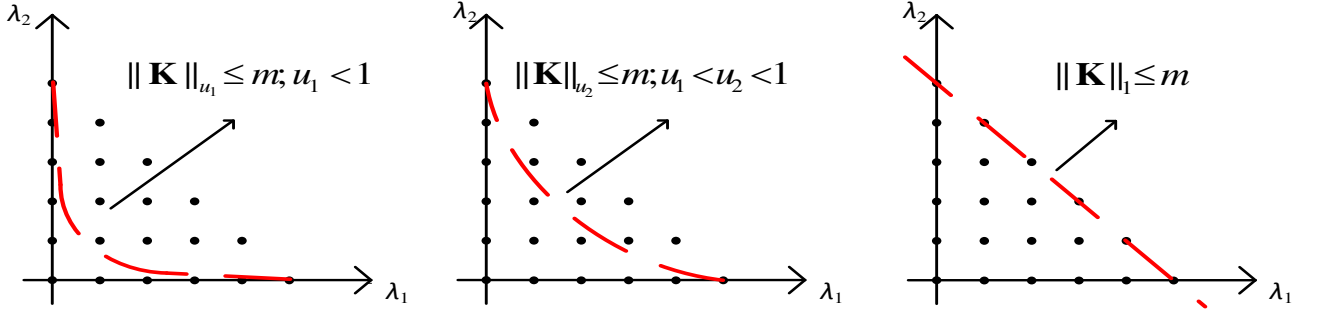


Fig. 2.4: Illustrative example demonstrating the sparsity due to the proposed hyperbolic truncation criterion over the classical linear truncation criterion using a 2D example ($n = 2, m = 5$). The decrease in sparsity with the increase in the hyperbolic factor (u) is shown. At $u = 1$, the proposed HPCE expansion coincides with the full-blown PC expansion.

random variable acting alone and their low-degree interactions. Guided by this principle, the hyperbolic truncation scheme automatically prunes the statistically insignificant high-degree multidimensional bases from a general PC expansion. This hyperbolic truncation scheme results in a substantially sparse PC formulation which is numerically more efficient to construct than the conventional alternatives [59].

Traditionally, for uncorrelated random variables, any arbitrary k^{th} multidimensional basis can be expressed as a product of one dimensional bases as

$$\phi_k(\boldsymbol{\lambda}) = \prod_{i=1}^n \phi_{k_i}(\lambda_i); \quad \sum_{i=1}^n k_i = k \quad (2.43)$$

where $K = [k_1, k_2, \dots, k_n]$ is the vector of the 1D PC degrees. Such a truncation scheme where all relevant PC bases are enclosed between the hyperplane $\|\mathbf{K}\|_1 = m$ and the positive axes representing the random dimensions is referred to as the classical linear truncation scheme. In the

hyperbolic truncation scheme, by pruning the high-degree multidimensional bases from the expansion of (2.14), a sparser PC formulation can be achieved. This hyperbolic truncation scheme is described using the fractional u -th norm of K as

$$\|\mathbf{K}\|_u = \left(\sum_{i=1}^N (k_i)^u \right)^{1/u} \leq m; \quad 0 < u < 1 \quad (2.44)$$

where u is the hyperbolic factor. The hyperbolic truncation scheme of 2.44 ensures that only those multidimensional bases of 2.14 lying under or on the hyperbola $\|\mathbf{K}\|_u = m$, as opposed to a hyper-plane $\|\mathbf{K}\|_1 = m$, are retained in the expansion. In other words, due to the non-zero radius of curvature of the hyperbola $\|\mathbf{K}\|_u = m$, the higher-degree multidimensional bases of 2.14 will be pruned from the expansion. This selective pruning of the PC bases will ensure the best accuracy of the expansion while leading to a sparser formulation than 2.14.

It is noted from Fig. 2.4 that the sparsity achieved by the HPCE depends on the radius of curvature of the truncating hyperbola which in turn depends on the hyperbolic factor u . Therefore, by tuning u it is possible to adapt the HPCE to exhibit the best sparsity-accuracy tradeoff. The main disadvantage of using the HPCE method is that it lacks control over the number of bases pruned because of the hyperbolic factor u takes specific values. So, for large problems, even the penultimate value of u prunes a large number of bases which causes the HPCE method to become inaccurate.

CHAPTER 3: APPROACHES TO ACCELERATE THE CLASSICAL FEDOROV SEARCH ALGORITHM

From the previous chapter, it is evident that among the non-intrusive techniques to evaluate the PC coefficients, the linear regression approach is preferred as it uses only a sparse subset of nodes out of the entire tensor product set of nodes without compromising on the accuracy of the results. However, for large dimensional problems, the traditional search algorithm takes a large amount of time for selecting the DoE nodes. In this dissertation, firstly, the methodology used by the traditional linear regression to select the DoE using the D-optimality criterion and the Fedorov search algorithm is explained. Next, two novel numerical strategies are proposed to expedite the search for the substitute DoE for problems involving high-dimensional random spaces. As the first strategy, instead of substituting all DoE, the proposed algorithm identifies a small fraction of the worst DoE present in the initial selection and replaces only these DoE. As the second strategy, a recursive method to efficiently compute the inverse of the information matrix required for every exchange of DoE is developed. Further, a complexity analysis of the search algorithm in [36] is presented. The accuracy and efficiency of the proposed approaches is illustrated by comparing the results with other PC approaches for microwave/RF networks using multiple numerical examples.

3.1 PC expansion using Linear Regression

Consider a general microwave/RF network where the uncertainty in the physical dimension, circuit elements, and electrical properties of the network is represented by n mutually uncorrelated real valued random variables $\boldsymbol{\lambda} = [\lambda_1, \lambda_2, \dots, \lambda_n]^T$ located within the multidimensional

random space Ω . In order to extract all the statistical information of this network, the variability in the network response is approximated using a PC expansion as

$$\mathbf{X}(t, \boldsymbol{\lambda}) = \sum_{k=0}^P \mathbf{X}_k(t) \phi_k(\boldsymbol{\lambda}) + \boldsymbol{\varepsilon} \quad (3.1)$$

where $\boldsymbol{\varepsilon}$ is the vector of random truncation errors of the PC expansion. The Linear Regression approach begins by oversampling the expansion of (3.1) at $M = 2(P+1)$ nodes located within the random space Ω . The expression of (3.1) is oversampled in order to achieve the best possible fit of the PC coefficients over the entire n -dimensional random space Ω [43]. This results in the formulation of an overdetermined system of linear algebraic equations [43]

$$\mathbf{A}\tilde{\mathbf{X}} + \boldsymbol{\varepsilon} = \mathbf{E} \quad (3.2)$$

where

$$\mathbf{A} = \begin{bmatrix} \phi_0(\boldsymbol{\lambda}^{(1)})\mathbf{I} & \cdots & \phi_P(\boldsymbol{\lambda}^{(1)})\mathbf{I} \\ \vdots & \ddots & \vdots \\ \phi_0(\boldsymbol{\lambda}^{(M)})\mathbf{I} & \cdots & \phi_P(\boldsymbol{\lambda}^{(M)})\mathbf{I} \end{bmatrix}; \quad \tilde{\mathbf{X}} = \begin{bmatrix} \mathbf{X}_0 \\ \vdots \\ \mathbf{X}_P \end{bmatrix}; \quad (3.3)$$

$$\mathbf{E} = \begin{bmatrix} \mathbf{X}(\boldsymbol{\lambda}^{(1)}) \\ \vdots \\ \mathbf{X}(\boldsymbol{\lambda}^{(M)}) \end{bmatrix}; \quad \boldsymbol{\varepsilon} = \begin{bmatrix} \varepsilon_1 \\ \vdots \\ \varepsilon_M \end{bmatrix}$$

and \mathbf{I} represents the identity matrix. The vectors $\boldsymbol{\varepsilon}_j$ of (3.3) are the individual truncation errors at each node. The vector \mathbf{E} consists of the network responses obtained by probing the original stochastic network of (3.1) at the M multidimensional nodes (or DoE) $\boldsymbol{\lambda}^{(j)} = [\lambda_1^{(j)}, \lambda_2^{(j)}, \dots, \lambda_n^{(j)}]$; $1 \leq j \leq M$. Equation (3.3) can now be solved in a least-square sense to evaluate the PC coefficients of the network response. Once the PC coefficients are obtained from (3.3), all statistical moments of the network responses can be obtained from the PC expansion of (3.1).

3.2 Advantages over intrusive approaches

A key benefit of the conventional linear regression approach is that sophisticated deterministic solvers such as SPICE can be directly used to populate the matrix E in (3.3) without any intrusive coding as required in the SG approach and the stochastic testing approach [7]-[22], [37]. More importantly, the M SPICE simulations of (3.3) can be easily parallelized unlike the SG approach.

3.3 Proposed D-Optimal Linear Regression Approach

In order to identify the M nodes satisfying the D-optimal criteria for the regression problem of (3.3), in this dissertation, we propose to utilize the Fedorov search algorithm which has been commonly used in the field of estimation theory and experimental designs [46],[48]. While there are various other exchange algorithms besides the Fedorov algorithm, the work of [46] demonstrates that the Fedorov algorithm reaches successful completion far more frequently than its counterparts. The following subsections explain the rationale behind the choice of the D-optimal criterion, the Fedorov search algorithm to identify the D-optimal nodes and the computational cost associated with the search.

3.3.1 D-optimal Criterion

The importance of the D-optimal criterion to the accuracy of the evaluated PC coefficients of (3.3) is revealed using the following lemma.

Lemma 1: Assuming that the truncation error ϵ_j $1 \leq j \leq M$ at all M DoE of (3.3) are independent of each other and exhibit a normal distribution of zero mean and same variance σ^2 , then in order

to achieve the maximum accuracy of the PC coefficients the DoE must be chosen such that the determinant of the information matrix $\mathbf{A}^t\mathbf{A}$ of (3.2) is maximized.

Proof: Based on the PC expansion of the network responses of (3.1), it is understood that the presence of the random truncation error $\boldsymbol{\varepsilon}$ makes the PC coefficients themselves random variables. The variance of the evaluated PC of (3.3) can be computed as

$$\begin{aligned} \text{Var}(\tilde{\mathbf{X}}) &= \text{Var}((\mathbf{A}^t\mathbf{A})^{-1}\mathbf{A}^t\mathbf{E}) \\ &= (\mathbf{A}^t\mathbf{A})^{-1}\mathbf{A}^t\text{Var}(\mathbf{E})(\mathbf{A}^t\mathbf{A})^{-1}\mathbf{A}^t \end{aligned} \quad (3.4)$$

Knowing that the truncation error for each DoE (i.e., $\boldsymbol{\varepsilon}_j$) is independent and has a constant variance σ^2 , $\text{Var}(\mathbf{E}) = \sigma^2\mathbf{I}$ where \mathbf{I} is the identity matrix. Replacing this in (3.4) the variance of the PC coefficients of (3.4) can be compactly expressed as

$$\text{Var}(\tilde{\mathbf{X}}) = (\mathbf{A}^t\mathbf{A})^{-1}\sigma^2 \quad (3.5)$$

From (3.5) we understand that to ensure the maximum accuracy of the PC coefficients we have to reduce the uncertainty in the solution $\tilde{\mathbf{X}}$ (i.e., the variance of $\tilde{\mathbf{X}}$). Since the variance of $\tilde{\mathbf{X}}$ is inversely proportional to the determinant of the information matrix $\mathbf{A}^t\mathbf{A}$, a simple way to minimize the variance of $\tilde{\mathbf{X}}$ is to maximize the determinant. This criterion is referred to as the D-optimal criterion [46], [47]. It is noted that other optimal criterions besides the D-optimal criterion also exists although the D-optimal criterion has been deemed the most effective and popular till now [46]. In the next subsection, we develop a search algorithm that can efficiently identify the D-optimal nodes from multidimensional random spaces.

3.3.2 Greedy Search Algorithm to Identify DoE

In this subsection, the development of a greedy search algorithm to identify the D-optimal DoE from multidimensional random spaces is described. This greedy search algorithm is

based on the Fedorov algorithm commonly used in the field of estimation theory and data analysis [48], [49]. This algorithm begins by considering a set of $M = 2(P+1)$ starting DoE selected from the tensor product grid of $(m+1)^n$ multidimensional quadrature nodes and creating the corresponding information matrix $\mathbf{A}^t\mathbf{A}$ of (3.3). Thereafter, each DoE in the starting set is replaced by the best possible substitute DoE taken from the remaining $(m+1)^n - M$ quadrature nodes such that the determinant of the information matrix increases by the maximum amount in the process. This step-by-step refinement of the starting DoE continues till all the initial set of nodes has been replaced [36].

As per the above description, at the r^{th} step it is assumed that the first $r-1$ nodes have been replaced by their best possible substitutes. Now if the r^{th} DoE ($\lambda^{(r)}$) of the starting set is removed from \mathbf{A} , then the new determinant of the information matrix can be expressed as

$$\begin{aligned}\det(\mathbf{A}^t\mathbf{A})_{new} &= \det((\mathbf{A}^t\mathbf{A}) - \mathbf{R}(\lambda^{(r)})\mathbf{R}^t(\lambda^{(r)})) \\ &= \det(\mathbf{A}^t\mathbf{A})(1 - \mathbf{R}(\lambda^{(r)})(\mathbf{A}^t\mathbf{A})^{-1}\mathbf{R}^t(\lambda^{(r)}))\end{aligned}\quad (3.6)$$

where $\mathbf{R}(\lambda^{(r)})$ is the row vector contributed by the r th DoE ($\lambda^{(r)}$) in \mathbf{A} . Similarly, if any arbitrary k th DoE ($\lambda^{(k)}$) from the remaining $(m+1)^n - M$ quadrature nodes is included into \mathbf{A} , the new determinant of the information matrix can be expressed as

$$\begin{aligned}\det(\mathbf{A}^t\mathbf{A})_{new} &= \det((\mathbf{A}^t\mathbf{A}) + \mathbf{R}(\lambda^{(k)})\mathbf{R}^t(\lambda^{(k)})) \\ &= \det(\mathbf{A}^t\mathbf{A})(1 + \mathbf{R}(\lambda^{(k)})(\mathbf{A}^t\mathbf{A})^{-1}\mathbf{R}^t(\lambda^{(k)}))\end{aligned}\quad (3.7)$$

Combining the results of (3.6) and (3.7), after exchanging the r^{th} DoE ($\lambda^{(r)}$) of the starting set with any arbitrary k^{th} DoE ($\lambda^{(k)}$) from the remaining $(m+1)^n - M$ quadrature nodes, the new determinant of the new information matrix can be mathematically expressed as the recursive function

$$\begin{aligned} \det(\mathbf{A}^t \mathbf{A})_{new} &= \det(\mathbf{A}^t \mathbf{A})(1 + d_{kk} - d_{rr} + d_{kr}^2 - d_{kk}d_{rr}) \\ d_{kr} &= \mathbf{R}(\boldsymbol{\lambda}^{(k)})\boldsymbol{\Psi}^{(r-1)}\mathbf{R}^t(\boldsymbol{\lambda}^{(r)}) \end{aligned} \quad (3.8)$$

where $\boldsymbol{\Psi}^{(r-1)}$ represents the inverse of the information matrix obtained after the previous (i.e., $r-1^{\text{th}}$) exchange. From (3.8) it is understood that in order to achieve D-optimality, the k^{th} node $\boldsymbol{\lambda}^{(k)}$ needs to be so chosen to satisfy the optimization criterion

$$\max(d_{kk} - d_{rr} + d_{kr}^2 - d_{kk}d_{rr}) \quad (3.9)$$

Once the best possible node $\boldsymbol{\lambda}^{(k)}$ has been found to satisfy (3.9) and the relevant exchange has been made, the new determinant can be directly updated using (3.9) and the substitution process moves on to the $r+1^{\text{th}}$ node. Once all M starting DoE have been replaced the new set of DoE will represent the D-optimal selection. In the next subsection, we derive the computational cost associated with the node selection.

3.3.3 Computational cost of the search algorithm

It is noted that the total computational cost of the search algorithm is due to two main factors. Firstly, identifying the D-optimal DoE requires searching through $(m+1)^n - M$ quadrature nodes for each DoE in the starting set – in other words, a total of $M((m+1)^n - M)$ searches. The associated CPU cost can be expressed as

$$C_a = 2(P+1)((m+1)^n - 2(P+1))C_1 \approx 2(P+1)(m+1)^n C_1 \quad (3.10)$$

where C_1 is the CPU cost of computing the terms in the brackets of (3.9) assuming that the inverse $\boldsymbol{\Psi}^{(r-1)}$ is known. It is noted that based on (3.8) and (3.9) C_1 can be expressed as

$$C_1 = 3k((P+1)^2 + (P+1)) \quad (3.11)$$

where the first term is the cost of the matrix-vector multiplication $\Psi^{(r-1)}\mathbf{R}'(\lambda^{(r)})$, the second term is the cost of the vector-vector multiplication of $\mathbf{R}(\lambda^{(r)})$ with $\Psi^{(r-1)}\mathbf{R}'(\lambda^{(r)})$, and the factor 3 is due to the fact that the above operations needs to be performed for three scalars d_{rr} , d_{kk} , and d_{kr} of (3.8). Also k is assumed to be the cost of each floating point operation. Combining (3.10) and (3.11), it can be concluded that the overall search cost (C_a) scales in an exponential manner with the number of random dimensions (n), quantified as $O((P+1)^3(m+1)^n) \approx O(n^{3m}(m+1)^n)$.

The other source of computational effort arises from the fact that for each substitution, the information matrix changes and the inverse $\Psi^{(r-1)}$ have to be reevaluated. This CPU cost is expressed as

$$C_b = 2(P+1)C_2 \quad (3.12)$$

where C_2 is the CPU cost of each matrix inversion. It is noted that for direct inversion methods C_2 scales as $O((P+1)^3)$ thereby ensuring that the cumulative cost of the matrix inversions (C_b) scales as $O((P+1)^4) \approx O(n^{4m})$ with respect to the number of random dimensions (n). Given that for typical PC problems $2 \leq m \leq 5$, this suggests a near exponential scaling of the associated CPU costs.

The above two features of the search algorithm significantly slow down its performance for high-dimensional problems and may even render it infeasible for some problems. In fact, the cost of implementing the search algorithm can often become a significant fraction of the cost of performing the M deterministic SPICE simulations of (3.3) as will be demonstrated in the numerical examples section. In order to address these computational constraints of the search algorithm, in the next section two novel strategies to expedite the search algorithm for problems involving high-dimensional random spaces is presented.

3.4 Expediting the Search Algorithm for High-Dimensional Random Spaces

In this section, two modifications to the original search algorithm of the previous section are presented.

3.4.1 Substituting K worst DoE

This strategy is based on the rationale that once a reasonably large determinant of the information matrix has been reached, any further enrichment of the determinant will translate to only marginal improvement in the accuracy of the evaluated PC coefficients. Thus, instead of substituting all M DoE (as suggested previously), in this strategy only the K worst DoE in the starting set will be identified and substituted. The substitution of the K worst DoE will result in a sufficiently large increase of the determinant of the information matrix, thereby eliminating the need for exchanging the remaining $M-K$ DoE. Thus, this strategy will reduce the number of searches from $M((m+1)^n - M)$ searches to $K((m+1)^n - M)$ – a reduction of the search cost (C_a) of (3.10) by a factor of M/K .

In this work, K is initially set to $\lceil M/5 \rceil$ where $\lceil \cdot \rceil$ is the ceiling function. Next, from (3.6) it is noted that the depreciation in the value of the determinant caused by removing the r^{th} DoE ($\lambda^{(r)}$) is proportional to the term

$$d_{rr} = \mathbf{R}(\lambda^{(r)}) \Psi^{(0)} \mathbf{R}(\lambda^{(r)})^t \quad (3.13)$$

where $\Psi^{(0)}$ is the inverse of the original information matrix consisting of the starting M DoE. Thus, the K worst DoE are identified as those DoE in the starting set that have the smallest possible value of the scalar d_{rr} . It is appreciated that computation of the d_{rr} term of all $2(P+1)$ DoE can be performed cheaply since the matrix inverse $\Psi^{(0)}$ needs to be computed only once. Once the K worst DoE have been identified, the search algorithm of the previous subsection is

run for only these DoE. Thereafter, a check is made to ascertain if the determinant of the information matrix $\mathbf{A}'\mathbf{A}$ is reasonably high. If not, then the next worst DoE (i.e., $K+1^{\text{th}}$ worst DoE) is identified using (3.13) and substituted as before. This sequential process continues until the determinant of the information matrix $\mathbf{A}'\mathbf{A}$ is deemed to be sufficiently large. It is observed from numerous examples that $K = \lceil M/5 \rceil$ is a good starting guess for K and rarely does this value need to be increased further.

3.4.2 Implicit Matrix Inversion

Although the above strategy will reduce the number of searches, and consequently the number of matrix inversions, given that the cost to directly invert the information matrix even once scales in a near-exponential manner with the number of random dimensions (see (3.12)), the overall cost of matrix inversions may still remain prohibitively large for high-dimensional random spaces.

In this dissertation, a new strategy is adopted whereby $\Psi^{(0)}$ (i.e., inverse of the information matrix for the starting set of DoE) is computed once and stored. Thereafter, the substitution of any r^{th} DoE ($\lambda^{(r)}$) ($r < K$) will change the information matrix. The inverse of the new information matrix (i.e., $\Psi^{(r)}$ of (3.8)) will now be expressed as a $P+1$ rank correction to the previous inverse $\Psi^{(r-1)}$ using the Sherman-Morrison-Woodbury formula as [49]

$$\begin{aligned}\Psi^{(r)} &= ((\mathbf{A}'\mathbf{A}) + \mathbf{R}^t(\lambda^{(k)})\mathbf{R}(\lambda^{(k)}) - \mathbf{R}^t(\lambda^{(r)})\mathbf{R}(\lambda^{(r)}))^{-1} \\ &= \Psi^{(r-1)} + w_k \mathbf{V}_k^t \mathbf{V}_k - w_r \mathbf{U}_r^t \mathbf{U}_r\end{aligned}\tag{3.14}$$

where

$$\begin{aligned}
w_k &= \frac{-1}{(1 + \mathbf{R}(\boldsymbol{\lambda}^{(k)})\mathbf{V}_k)}; & \mathbf{V}_k &= \boldsymbol{\Psi}^{(r-1)}\mathbf{R}'(\boldsymbol{\lambda}^{(k)}) \\
w_r &= \frac{1}{(1 - \mathbf{R}(\boldsymbol{\lambda}^{(r)})\mathbf{U}_k)}; & \mathbf{U}_k &= (\boldsymbol{\Psi}^{(r-1)} + w_k\mathbf{V}_k'\mathbf{V}_k)\mathbf{R}'(\boldsymbol{\lambda}^{(r)})
\end{aligned} \tag{3.15}$$

Based on the recursive expressions of (3.14) and (3.15), it is observed that for the substitution of any r^{th} DoE $(\boldsymbol{\lambda}^{(r)})$ ($r < K$) the new inverse $\boldsymbol{\Psi}^{(r)}$ will be updated efficiently using numerically cheap matrix-vector and vector-vector multiplications as opposed to the direct matrix inversions.

In the next section, we discuss the numerical efficiency of the modified search algorithm.

3.5 Numerical Efficiency of the Modified Search Algorithm

It is emphasized that the modified search algorithm described above offers two clear benefits. Firstly, the number of searches will decrease from $M((m+1)^n - M)$ searches to $K((m+1)^n - M)$ where $K = \lceil M/5 \rceil$. This automatically reduces the search cost of (3.10) approximately by a factor of 5 to

$$C_a \approx K((m+1)^n - 2(P+1))C_1 = \left\lceil \frac{2(P+1)}{5} \right\rceil (m+1)^n C_1 \tag{3.16}$$

Secondly, the CPU cost of performing the matrix inversions for the modified search algorithm will also decrease significantly as quantified using the following lemma.

Lemma 2: Utilization of the Sherman-Morrison-Woodbury formula of (3.14) and (3.15) will ensure that the total CPU costs to perform the matrix inversions in the modified search algorithm will scale as $O((P+1)^3) \approx O(n^{3m})$ with respect to the number of random dimensions (n).

Proof: Based on (3.15) it is noted that the main computations required in order to evaluate \mathbf{V}_k is a matrix-vector multiplication of dimensions $P+1$ where $\boldsymbol{\Psi}^{(r-1)}$ is assumed to be known. The cost of

this operation will be $C_3 = k(P+1)^2$ where k is the cost of each floating point operation. Next, to compute the matrix $\mathbf{V}_k^t \mathbf{V}_k$ a vector-vector multiplication of dimensions $P+1$ is required. This will incur an additional CPU cost of $C_4 = k(P+1)^2$. Finally, to compute the denominator of the scalar term w_k , another matrix-vector multiplication of dimensions $P+1$ will be required at the cost $C_3 = k(P+1)^2$. Thus, the overall CPU cost to evaluate the second term in (16) (i.e., $w_k \mathbf{V}_k^t \mathbf{V}_k$) will be

$$C_3 + C_4 + C_3 = 3k(P+1)^2 \quad (3.17)$$

It is observed that computing the third term in (3.14) (i.e., $w_r \mathbf{U}_r^t \mathbf{U}_r$) proceeds exactly in the same way as that of the second term. Hence, the associated cost too will equal to that of (3.17). Adding all the above CPU costs for K substitutions along with the cost of directly inverting the starting information matrix (i.e., computing $\Psi^{(0)}$), the total CPU cost incurred to perform the matrix inversions in the modified search algorithm can be quantified as

$$C_b = C_2 + 6kK(P+1)^2 \quad (3.18)$$

It is observed that for $K = \lceil M/5 \rceil$ both the first and the second terms of (3.18) will scale as $O((P+1)^3) \approx O(n^{3m})$ with respect to the number of random dimensions (n). Thus, it is concluded that the overall costs of performing the matrix inversions for the modified search algorithm will also scale as $O((P+1)^3) \approx O(n^{3m})$. Comparing this result with that of (3.12) reveals a distinct improvement in the CPU cost to the order of $O(n)$ – a major numerical benefit for high-dimensional problems (i.e., for large n).

Finally, it is remarked that the cost of identifying the K worst nodes will require the additional computation of the scalar d_{rr} in (3.13) for the entire $2(P+1)$ starting DoE. This cost can be expressed as

$$C_c = 2(P+1) \frac{C_1}{3} \quad (3.19)$$

since C_1 is defined in (3.11). Comparing (3.16) and (3.19) it is evident that the cost of identifying the K worst DoE is a negligible fraction of the search cost C_a and can be safely ignored. Overall, it is appreciated that the proposed modified search algorithm will be able to significantly reduce both the search cost C_a of (3.10) and the cost of the matrix inversions C_b of (3.12), thereby substantially accelerating the original search algorithm of Section 3.3.2.

3.6 Comparative Analysis of Overall CPU Costs

In this section, the CPU cost of the proposed D-optimal linear regression approach is compared against that of conventional non-intrusive PC approaches.

3.6.1 Proposed Linear Regression Approach

Based on the discussion of Section 3.5, it is appreciated that the CPU cost required for the proposed linear regression approach can be divided into two parts – the cost incurred by the modified search algorithm and the cost incurred to perform the M deterministic SPICE simulations to extract the \mathbf{E} matrix of (3.3). The cost of the modified search algorithm is expressed using (3.16) and (3.18) as

$$C_t \approx K(m+1)^n C_1 + C_2 + 6k K(P+1)^2 \quad (3.20)$$

where typically $K = [M/5]$. As for the SPICE simulation cost, it is assumed that each of the M simulations requires the same CPU cost which is a reasonable assumption since the variation in the number of unknowns in the network equations from one DoE to another will be typically small. Thus, the SPICE simulation cost can be quantified as

$$C_S = 2(P+1)C_0 \quad (3.21)$$

where C_0 is the cost of each deterministic SPICE simulation. Thus, the overall cost of the SPICE simulations scales as $O(2n^m)$ with respect to the number of random dimensions (n).

3.6.2 Stochastic Testing Approach

The proposed linear regression approach has some interesting features compared to the stochastic testing algorithm of [37], [38]. Firstly, the modified search algorithm allows only K substitutions as opposed to the significantly larger $P+1$ substitutions required by the stochastic testing algorithm, although the CPU cost for each substitution is similar. Further, the proposed linear regression approach can directly utilize the SPICE results of the M DoE without the need of any intrusive coding or access to the internals of the SPICE engine, thereby making the proposed approach truly non-intrusive in nature. These benefits are offset by the fact that the stochastic testing algorithm requires only $P+1$ SPICE simulations (i.e., $C_S = (P+1)C_0$) as opposed to the $2(P+1)$ simulations required by the proposed D-optimal linear regression approach.

3.6.3 Stochastic Collocation Approach

Stochastic collocation (SC) has been a very popular non-intrusive PC approach [29], [30], [42], [43]. In this approach, if the non-intrusive multidimensional nodes are selected to be the full tensor product of 1D quadrature nodes, then $M = (m+1)^n$. These nodes can be analytically identified at negligible computational costs (i.e., $C_t = 0$). Thus, the cumulative costs of the entire SC approach is equal to that of the SPICE simulations and is expressed as

$$C_S = (m+1)^n C_0 \quad (3.22)$$

This corresponds to an exponential scaling of the time costs with respect to the number of random dimensions (n), quantified as $O((m+1)^n)$. This means that for even moderate dimensional problems, the massive cost of SPICE simulations in (3.22) will make this approach highly cost intensive compared to the proposed linear regression approach.

In order to mitigate this prohibitive scaling, an intelligent choice of only a sparse subset of the tensor product nodes guided by the Smolyak algorithm has been proposed [29], [30], [42], [51]. Once again, this method allows the fast identification of the sparse nodes (i.e., $C_i = 0$ compared to the proposed linear regression approach). This approach results in a decrease in the number of multidimensional nodes from $M = (m+1)^n$ to approximately $M = (2n)^m/m!$, thereby improving the CPU time costs of the SC algorithm from that of (3.22) to

$$C_s = \frac{(2n)^m}{m!} C_0 \quad (3.23)$$

For this approach, it is observed that the number of deterministic SPICE simulations required scales as $O(2^m n^m)$ which is still 2^{m-1} times more than that required for the proposed linear regression approach (see (3.23)). Thus, for large variation in the random dimensions requiring high degrees of PC expansion (m), the proposed linear regression approach may still be more cost effective than even this sparse collocation approach.

3.6.4 Other Approaches

Among other existing non-intrusive approaches, the pseudo-spectral collocation has been recently reported for full-wave EM problems [26]. However, this approach suffers from the same exponential scaling of the SPICE simulation costs as the classical SC approach. Other methods based on the Stroud low order cubature methods have also recently been explored for packaging problems [23], [31], [33], [35]. This approach can easily locate the multidimensional nodes using

simple analytic formulas and exhibits only a linear scaling of the number of SPICE simulations with number of random dimensions (i.e., $O(n)$). However, this excellent scaling with the number of random dimensions only exists for a second and third degree PC expansion and cannot be extended to higher degree expansions [23].

Finally, it is remarked that a promising non-intrusive PC approach has been proposed in [34]. In this approach the selection of the non-intrusive nodes is determined exactly as proposed in the stochastic testing approach of [37]. As a result, this approach too relies on the costly $P+1$ substitutions as opposed to the relative smaller K substitutions used in the modified search algorithm. On the other hand, this approach requires only $P+1$ SPICE simulations as opposed to the $2(P+1)$ simulations required by the proposed D-optimal linear regression approach.

From the above analysis, it is observed that the proposed linear regression approach offers clear benefits over the state-of-the-art non-intrusive PC approaches and this is validated through multiple lumped and distributed microwave network examples in the next section.

3.7 Numerical Examples

In this section, three examples are presented to compare the accuracy and scalability of the proposed D-optimal linear regression approach against existing intrusive and non-intrusive PC approaches. All relevant PC computations are performed using MATLAB 2013b while the deterministic transient simulations, whether using intrusive or non-intrusive PC approaches, are performed using HSPICE. In particular, the transmission line networks are modeled using the W-element transmission line model provided by HSPICE which can automatically consider frequency dependent per-unit-length parameters. The above simulations are run on a workstation with 8 GB RAM, 500 GB hard disk memory and an Intel i5 processor with 3.4 GHz clock speed.

3.7.1 Example 1: CMOS Low Noise Amplifier (LNA)

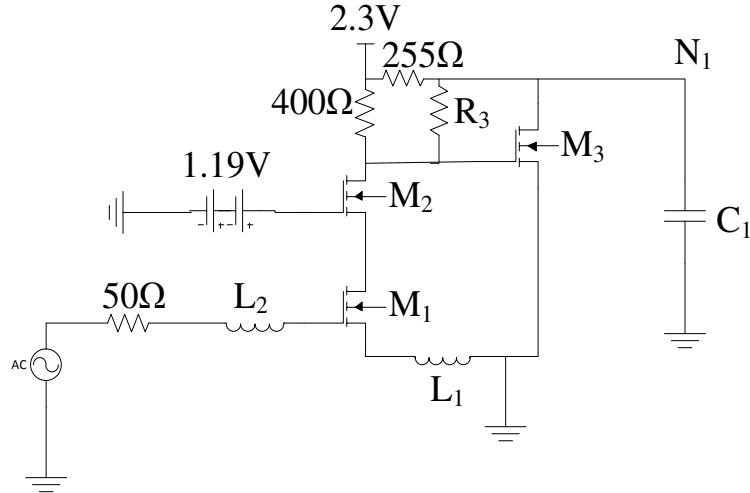


Fig. 3.1: Circuit schematic of the CMOS low-noise amplifier network of Example 1.

The objective of this example is to demonstrate the accuracy of the proposed linear regression approach. For this purpose, the RF low noise amplifier (LNA) network of Fig. 3.1 comprising of three SPICE level-49 CMOS transistor models are considered. The RF input to the network is a sinusoidal wave with amplitude of 1V and a frequency of 1 GHz. The uncertainty in the network is introduced via six normal random variables ($n = 6$) whose characteristics are listed in Table 3.1. A Hermite PC expansion of degree $m = 3$ is required for this example.

In order to evaluate the accuracy of the proposed approach, the mean and standard deviation (σ) of the transient response at the output node N1 of Fig. 3.1 is computed using two methods – the proposed D-optimal linear regression approach described in Section 3.3 and the pseudo-spectral collocation approach based on Gauss-Hermite quadrature techniques. For the proposed approach, only $K = \lceil 2(P+1)/5 \rceil = 33$ substitutions are performed as described in Section 3.4. The comparison of the above results is shown in Fig. 3.2 (a) where the proposed linear regression approach is found to exhibit good agreement with the pseudo-spectral collocation approach.

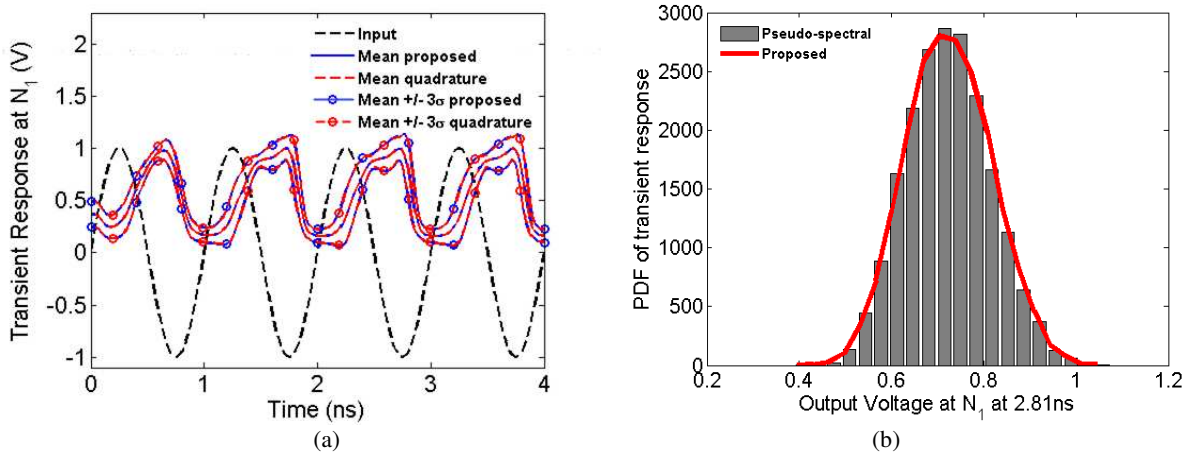


Fig. 3.2: Comparison of mean and higher order statistical moments of the transient response of Example 1 computed using the proposed linear regression approach and pseudo-spectral collocation approach [26]. (a) Mean and statistical corners of the transient response at N_1 . (b) Probability distribution function of transient response at N_1 at the time point of maximum standard deviation ($t = 2.81ns$) using 20,000 samples.

Table 3.1: Characteristics of Random Variables of Example 1 (Fig. 3.1)

Random Variables	Mean	% Standard Deviation (Normal Distribution)
w_1 (width of M_1)	7.5 μm	+/- 10 %
w_2 (width of M_2)	7.5 μm	
w_3 (width of M_3)	7.5 μm	
L_1	13 nH	
L_2	0.9 nH	
R_3	120 Ω	

Next, in order to test the accuracy for higher order statistical moments, the probability distribution function of the transient response at node N_1 evaluated at the time point of maximum standard deviation ($t = 2.81 ns$) is computed using the above two approaches and the results are displayed in Fig. 3.2(b). As expected, the probability distribution results for 20,000 samples exhibit good agreement demonstrating the accuracy of the proposed linear regression approach.

Finally, it is noted that the proposed approach requires 15 seconds for completing the K substitutions and another 13.44 seconds for the $2(P+1) = 84$ SPICE simulations. On the other hand, the pseudo-spectral collocation approach requires 327.68 seconds to perform the necessary 4096 SPICE simulations at the Gauss-Hermite quadrature nodes. This amounts to a speedup of 11.5 provided by the proposed algorithm over the pseudo-spectral collocation approach. This is as expected from the discussion of Section 3.6.

3.7.2 Example 2: Transmission Line Network

The objective of this example is to compare the performance of the proposed linear regression approach with the existing intrusive SG approach for a large distributed network. For this purpose, the multiconductor stripline network driven by nonlinear transmission lines shown in Fig. 3.3(a) is considered. The layout of the stripline network is illustrated in Fig. 3.3(b). The nonlinear transmission lines are represented using cascaded lumped nonlinear RLGC segments as shown in Fig. 3.4 where the nonlinear capacitance $C(V)$ is represented as

$$C(V) = C_a (b + (1-b)e^{-V/a}) \quad (3.24)$$

and V is the potential difference across the capacitor. It is noted that (3.24) is a strongly nonlinear function used for benchmarking the proposed approach. For the network in Fig. 3.3(a), 10 nonlinear RLGC segments are considered. The input to the network is a trapezoidal waveform with rise/fall time $T_r = 10$ ns, pulse width $T_w = 400$ ns and amplitude equal to 5V. The uncertainty in the network is introduced via five random variables ($n = 5$) whose characteristics are listed in Table 3.2. A mixed Legendre-Hermite PC expansion of degree $m = 2$ is required for this example.

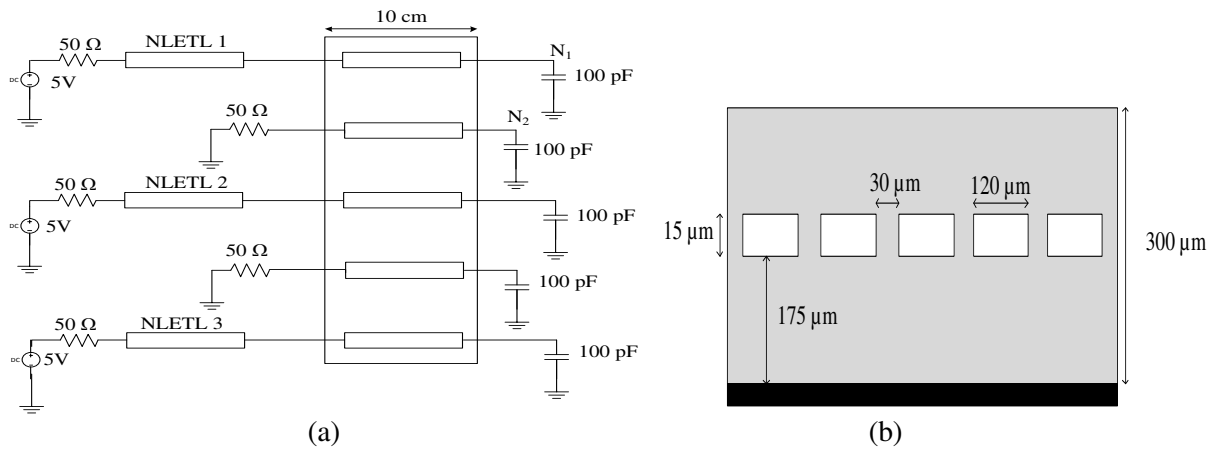


Fig. 3.3: Transmission line network of Example 2. (a) Circuit schematic. (b) Geometry of coupled transmission lines.

Table 3.2: Characteristics of Random Variables of Example 2 (Fig. 3)

Random Variables	Mean	Distribution	% Relative Variation
“a” parameter in NL capacitors of NLETL 1	2.137	Normal	+/- 10 %
“a” parameter in NL capacitors of NLETL 2	2.637		
“a” parameter in NL capacitors of NLETL 3	1.637		
“b” parameter in NL capacitors of NLETL 1	6.037 e-3	Uniform	
“b” parameter in NL capacitors of NLETL 2	9.108 e-3		

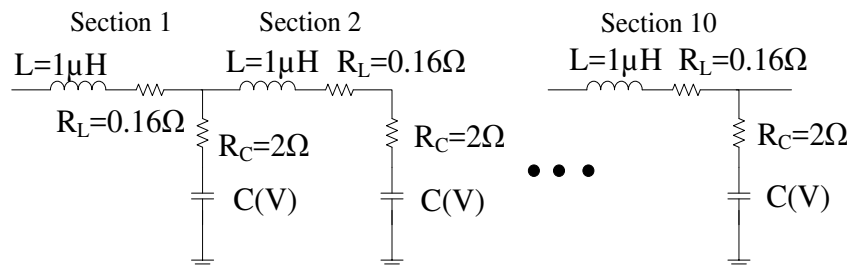


Fig. 3.4: Equivalent lumped RLGC model of nonlinear transmission lines of Fig. 3.

In order to evaluate the accuracy of the proposed approach, the mean and standard deviation (σ) of the transient response at the output nodes N_1 and N_2 of Fig. 3.3(a) is computed two methods – the proposed D-optimal linear regression approach described in Section 3.3 and the SG approach [15]. For the proposed approach, only $K = \lceil 2(P+1)/5 \rceil = 8$ substitutions are performed as described in Section 3.4. The comparison of the above results is shown in Fig. 3.5 where the proposed linear regression approach is found to exhibit good agreement with the SG approach.

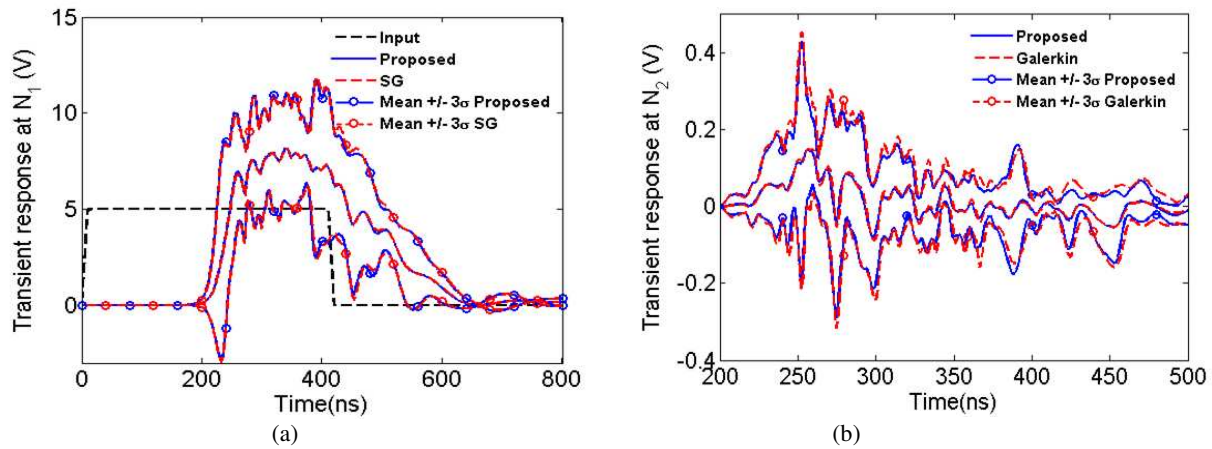


Fig. 3.5: Comparison of mean and higher order statistical moments of the transient response of Example 2 computed using the proposed linear regression approach and the stochastic Galerkin approach [15]. (a) Mean and statistical corners of the transient response at N_1 . (b) Mean and statistical corners of the transient response at N_2 .

To further probe the accuracy of the proposed approach, the PC expansion of the voltage response at node N_1 is computed using the same above two methods where the input sources in Fig. 3.3 are changed to random pulse trains with rise/fall time $T_r = 10$ ns, pulse width $T_w = 400$ ns and amplitude equal to 1V. From the PC expansion the eye diagram is generated as shown in Fig. 3.6(a). The probability distribution function of the eye height is then extracted using both the above methods and compared in Fig. 3.6(b). It is observed from Fig. 3.6(b) that the proposed linear regression approach matches very well the results of the SG approach.

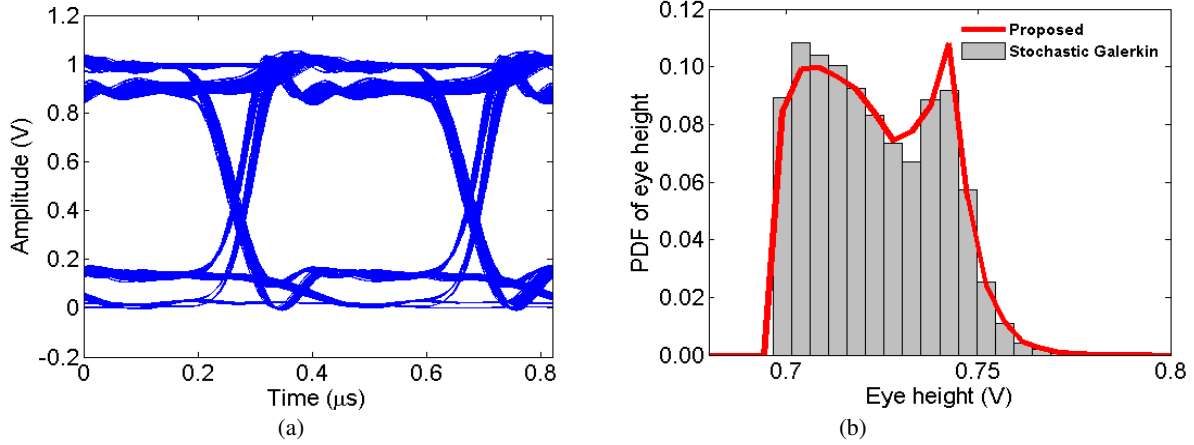


Fig. 3.6: Eye diagram comparison for Example 2 computed using the proposed linear regression approach and the stochastic Galerkin approach [15]. (a) Example of the eye diagram obtained for a DoE at N_1 . (b) Probability distribution function of the eye height.

It is appreciated that the proposed approach requires 1.022 seconds for completing the K substitutions and another 23.94 seconds for the $2(P+1) = 42$ SPICE simulations. On the other hand, the SG approach requires 4722.45 seconds to perform the solitary augmented SPICE simulation. This is because the augmented network is 21 times larger than the original model and includes an additional $(m+1)^n = 243$ companion circuits to model the uncertainty in each nonlinear capacitor [15]. Thus, the proposed approach provides a speedup of roughly 189 over the SG approach. If the size of the network and/or the number of random dimensions is increased, the achieved speedup will be even higher, thereby clearly validating the advantage of the proposed linear regression approach over the intrusive SG approach.

3.7.3 Example 3: BJT Low Noise Amplifier (LNA)

The objective of this example is to compare the computational complexity of the proposed linear regression approach against that of conventional non-intrusive PC approaches as the number of random dimensions increases. For this purpose, the low noise amplifier (LNA) network of Fig. 3.7 is considered [38]. This LNA utilizes an NXP BFG425W wideband BJT,

which is represented as a level-1 (Gummel-Poon) SPICE model. This network is driven by a voltage source with a sinusoidal waveform of frequency 2 GHz and amplitude of 1V. The supply voltage of the network is set to $V_s = 4.5$ V. The uncertainty in the network is introduced via twelve random variables ($n = 12$) whose characteristics are listed in Table 3.3 and a Hermite PC expansion of degree $m = 4$ is considered.

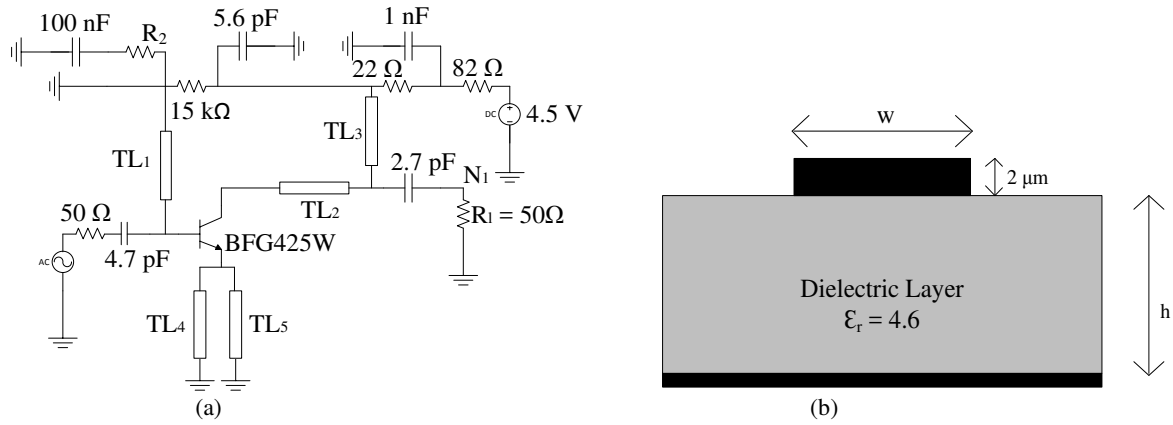


Fig. 3.7: Circuit schematic of the BJT low-noise amplifier network of Example 3. (a) Circuit schematic. (b) Geometry of transmission lines.

Table 3.3: Characteristics of Random Variables of Example 3 (Fig. 3.7)

Random Variables	Mean	% Relative Variation (Normal Distribution)
w_1 (width of TL ₁)	0.2 mm	+/- 25%
w_2 (width of TL ₂)	0.25 mm	
w_3 (width of TL ₃)	0.3 mm	
w_4 (width of TL ₄)	0.7 mm	
w_5 (width of TL ₅)	0.9 mm	
B_f (Current gain of BJT)	145	
C_{js} (Junction Cap. Of BJT)	667.5 fF	
R_1	50 Ω	
h_1 (height of TL ₁)	0.4 mm	
h_2 (height of TL ₂)	0.45 mm	
h_3 (height of TL ₃)	0.5 mm	
h_4 (height of TL ₄)	0.55 mm	
h_5 (height of TL ₅)	0.6 mm	
R_2	100 Ω	

First, the number of random dimensions is set to $n = 8$ represented as the first eight dimensions of Table 3.3. For this case, in order to demonstrate the accuracy of the proposed linear regression approach, the mean and standard deviation (σ) of the transient response and output power at the output node N_1 is computed two methods – the proposed linear regression approach described in Section 3.4 and the Monte Carlo approach. For the proposed approach, only $K = \lceil 2(P+1)/5 \rceil = 198$ substitutions are performed as described in Section 3.4. The comparison of the above results is shown in Fig. 3.8 where the proposed linear regression approach is found to exhibit good agreement with the Monte Carlo approach.

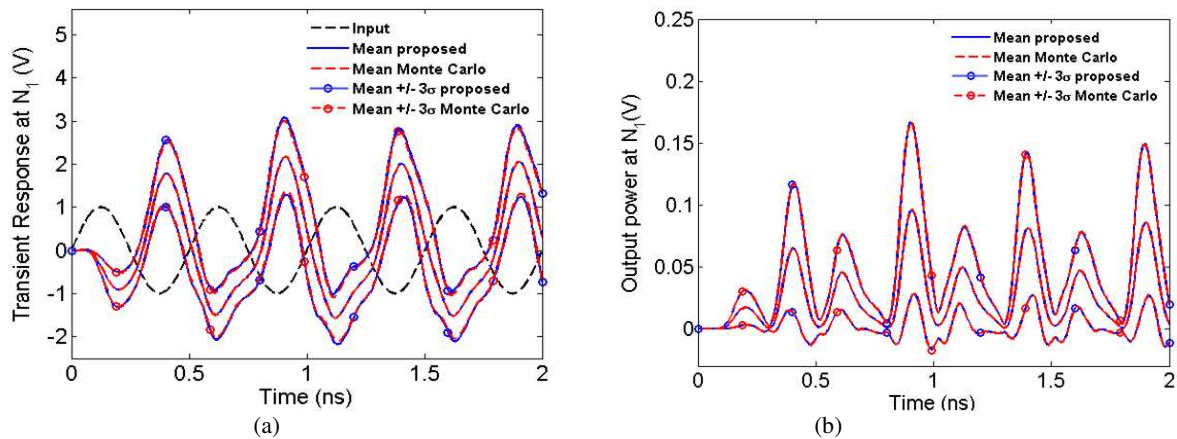


Fig. 3.8: Comparison of mean and higher order statistical moments of the transient response of Example 3 computed using the proposed linear regression approach and the Monte Carlo approach. (a) Mean and statistical corners of the transient response at N_1 . (b) Mean and statistical corners of the output transient power at N_1 .

Next, to demonstrate the efficiency offered by the modified search algorithm over the classical Fedorov search algorithm of [36], the number of random dimensions is progressively increased from 4 to 14. For each test case, the original search algorithm of [36] and the proposed modified search algorithm described in Section 3.4 are implemented. The total time cost for each algorithm is decomposed into two parts – the CPU cost incurred in identifying the regression

nodes (compared in Table 3.4) and the CPU cost incurred in the matrix inversion after every node exchange (compared in Table 3.5).

Table 3.4: Scaling of CPU Time for Identifying D-Optimal Nodes Using Proposed and Classical Search Algorithms

Random Variables	CPU Time for Proposed Algorithm using K Worst Nodes (sec)		CPU Time for Classical Search Algorithm using $2(P+1)$ nodes (sec)		Speedup
	Simulation Cost	Analytic Cost	Simulation Cost	Analytic Cost	
4 (w_1, w_2, w_3, w_4)	0.0005	0.0003	0.0026	0.0014	5
6 ($w_1, w_2, w_3, w_4, w_5, B_f$)	0.0055	0.0077	0.0277	0.0383	
8 ($w_1, w_2, w_3, w_4, w_5, B_f, C_{js}, R_1$)	0.0615	0.1001	0.3074	0.5008	
10 ($w_1, w_2, w_3, w_4, w_5, B_f, C_{js}, R_1, h_1, h_2$)	0.6806	0.8274	3.4034	4.1373	
12 ($w_1, w_2, w_3, w_4, w_5, B_f, C_{js}, R_1, h_1, h_2, h_3, h_4$)	6.3336	4.9714	31.668	24.8570	
14 ($w_1, w_2, w_3, w_4, w_5, B_f, C_{js}, R_1, h_1, h_2, h_3, h_4, h_5, R_2$)	23.6232	23.6219	118.1160	118.1098	

From Table 3.4 it is observed that the speedup achieved using the K worst nodes compared to the full set of $2(P+1)$ regression nodes are consistently 5. This is exactly as expected from (3.16) in Section 3.5. Similarly, from Table 3.5 it is observed that the speedup provided by the Sherman-Morrison-Woodbury method compared to the explicit matrix inversion method closely matches the expected scaling of $O(n^m)$ as illustrated in Fig. 3.9(a). This too is as expected from the comparison of (3.18) with (3.12) in Section III-D.

It is further noted that the simulation CPU cost for both the modified search algorithm and the classical Fedorov search algorithm for Tables 3.4 and 3.5 have been compared with an analytic

Table 3.5: Scaling of CPU Time for Matrix Inverse Computation Using Proposed and Classical Search Algorithms

Random Variables	CPU Time of Proposed Algorithm using Sherman-Morrison-Woodbury Method (sec)		CPU Time for Classical Search Algorithm using Explicit Matrix Inverse (sec)		Speedup
	Simulation Cost	Analytic Cost	Simulation Cost	Analytic Cost	
4 (w_1, w_2, w_3, w_4)	0.0129	0.0029	0.0332	0.0220	2.57
6 ($w_1, w_2, w_3, w_4, w_5, B_f$)	0.2423	0.0805	0.7560	1.7810	3.12
8 ($w_1, w_2, w_3, w_4, w_5, B_f, C_{js}, R_1$)	6.4487	10.5518	94.5450	54.9805	14.66
10 ($w_1, w_2, w_3, w_4, w_5, B_f, C_{js}, R_1, h_1, h_2$)	48.4691	87.2597	1183.1820	919.4419	24.41
12 ($w_1, w_2, w_3, w_4, w_5, B_f, C_{js}, R_1, h_1, h_2, h_3, h_4$)	303.3098	524.4761	14480.6480	10047.8592	47.74
14 ($w_1, w_2, w_3, w_4, w_5, B_f, C_{js}, R_1, h_1, h_2, h_3, h_4, h_5, R_2$)	1201.3000	2492.7336	101776.8240	80292.2630	84.72

estimation of the CPU cost possible using (3.10)-(3.12) and (3.16)-(3.18). The analytic and simulation CPU cost results of Table IV show good agreement. Even for Table V, for higher dimensional problems (i.e., $n > 6$) the analytic CPU costs are within a factor of 1.6 – 2 times the simulation CPU costs for the proposed approach and within a factor of 0.57 – 0.80 times the simulation CPU costs for the proposed approach.

Finally, for the same test cases of Table 3.4 and 3.5, the total PC problem is solved using three methods – the proposed linear regression approach, the original linear regression approach of [36], and the pseudo-spectral collocation approach [26]. The total CPU time incurred by each approach is noted in Table 3.6 and plotted in Fig. 3.9(b). For all methods, the time costs of the corresponding search algorithms have been added with the time cost for the $2(P+1)$ SPICE

simulation costs. It is observed from Table 3.6 that the pseudo-spectral collocation exhibits an exponential scalability with respect to the number of random dimensions [26]. Thus, the pseudo-spectral collocation approach runs out of memory for more than 8 random variables. Similarly, for the linear regression approach of [36], the cost of the original search algorithm quickly becomes very large and also runs out of memory for more than 8 random variables. The CPU costs for $n = 10, 12,$ and 14 for these methods is estimated via extrapolation and added in Fig. 3.9(b) for completeness. As seen from Fig. 3.9(b), the proposed linear regression approach which uses the more efficient modified search algorithm provides far superior scalability of the total CPU costs with respect to the number of random dimensions than the original linear regression approach of [36] or the pseudo-spectral collocation approach [26]. Interestingly, here too the total savings in CPU times increases with the number of random dimensions, thereby validating the benefits of the proposed linear regression approach for high-dimensional problems.

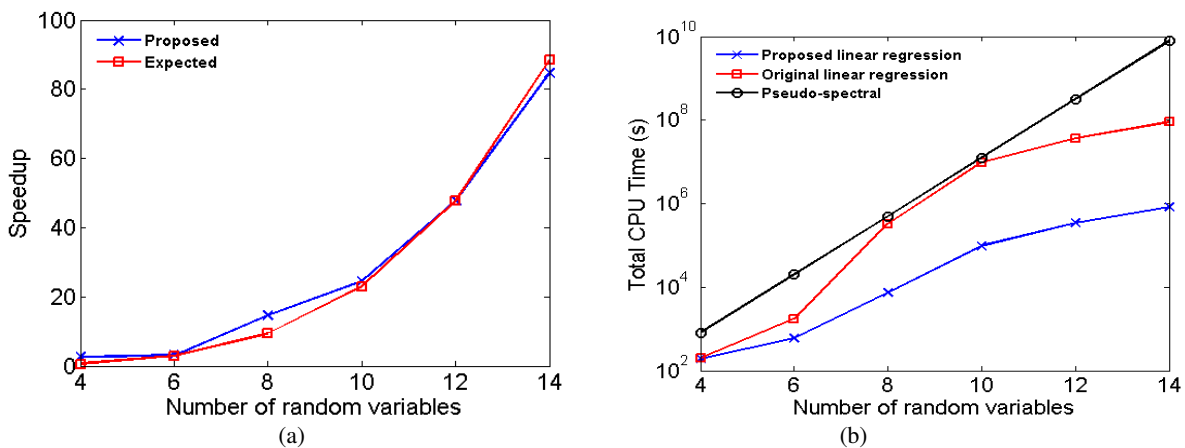


Fig. 3.9: Comparison of CPU time required by proposed linear regression approach with state-of-the-art. (a) Speedup achieved during matrix inverse computation by proposed algorithm compared to expected speedup. (b) Scaling of total CPU time cost of proposed linear regression algorithm compared against the pseudo-spectral approach and the original linear regression approach.

Table 3.6: Scaling of CPU Time Costs Using Proposed, Conventional Linear Regression and Pseudo-Spectral Collocation Approaches

Number of Random Variables	CPU Time (Proposed Approach)		CPU Time (Conventional Linear Regression)		CPU Time (Pseudo Spectral Collocation)
	Proposed Search Algorithm	SPICE Simulations	Original Search Algorithm	SPICE Simulations	SPICE Simulations
4 (w_1, w_2, w_3, w_4)	13.12 s	179.2 s	18.42 s	179.2 s	800 s
6 ($w_1, w_2, w_3, w_4, w_5, B_f$)	62.42 s	537.6 s	1214.99 s	537.6 s	20000 s
8 ($w_1, w_2, w_3, w_4, w_5, B_f, C_{js}, R_1$)	100.68 min	21.12 min	5442.25 min	21.12 min	8333.33 min
10 ($w_1, w_2, w_3, w_4, w_5, B_f, C_{js}, R_1, h_1, h_2$)	26.23 h	0.71 h	Insufficient Memory	0.71 h	Insufficient Memory
12 ($w_1, w_2, w_3, w_4, w_5, B_f, C_{js}, R_1, h_1, h_2, h_3, h_4$)	94.95 h	1.29 h	Insufficient Memory	1.29 h	Insufficient Memory
14 ($w_1, w_2, w_3, w_4, w_5, B_f, C_{js}, R_1, h_1, h_2, h_3, h_4, h_5, R_2$)	229.07 h	2.176 h	Insufficient Memory	2.17 h	Insufficient Memory

CHAPTER 4: DEVELOPMENT OF THE REDUCED DIMENSIONAL POLYNOMIAL CHAOS APPROACH

In the previous chapter, a novel linear regression methodology for evaluating the PC coefficients of microwave/RF circuits in a non-intrusive manner by using the D-optimal criteria to select the DoE nodes was proposed. While this provides significant acceleration in the search algorithm for selecting substitute DoE for high-dimensional problems, the problem size remains unaffected. In other words, the CPU effort to evaluate the PC coefficients of the network still scales badly with the number of random dimensions. In this dissertation, a polynomial chaos (PC) formulation based on the concept of dimension reduction is proposed for the efficient uncertainty analysis of microwave and RF networks. This formulation exploits a high dimensional model representation (HDMR) for quantifying the relative effect of each random dimension on the network response surface. This information acts as problem dependent sensitivity indices guiding the intelligent identification and subsequent pruning of the statistically unimportant random dimensions from the original parametric space. Performing a PC expansion in the resultant low-dimensional random subspace leads to the recovery of a sparser set of coefficients than that obtained from the full-dimensional random space with negligible loss in accuracy. Novel methodologies to reuse the preliminary PC bases and SPICE simulations required to estimate the sensitivity indices are proposed, thereby making the proposed approach more efficient and accurate than standard sparse PC approaches. The validity of the proposed approach is demonstrated using multiple numerical examples.

4.1 Development of Proposed Reduced Dimensional PC Approach

In this section, an explanation of how the HDMR can be utilized to compute the sensitivity indices of the random dimensions is given. These sensitivity indices will be used to guide the dimension reduction scheme. Thereafter, the formulation of a new linear regression approach for evaluating the reduced dimensional PC coefficients will be presented. This linear regression approach will maximize the reuse of SPICE simulations and PC bases. Next, the extension of the proposed method for networks with multiple responses of interest will be described. To conclude, this section will quantify the computational complexity of the proposed method and will contrast its performance with state-of-the-art sparse PC expansions [40], [41], [58], [59].

4.1.1 Evaluating Sensitivity Indices

For ease of understanding, the PC expansion that approximates the uncertainty in the network response $\mathbf{X}(t, \boldsymbol{\lambda})$ described in (2.14) is shown again as

$$\mathbf{X}(t, \boldsymbol{\lambda}) \approx \sum_{k=0}^P \mathbf{X}_k(t) \phi_k(\boldsymbol{\lambda}) \quad (4.1)$$

The HDMR of any output $x(t, \boldsymbol{\lambda})$ of the network of is expressed as a hierarchical sum of component functions as [60]

$$x(t, \boldsymbol{\lambda}) = x_0(t) + \sum_{i=1}^N x_i(t, \lambda_i) + \sum_{1 \leq i, j \leq N} x_{ij}(t, \lambda_i, \lambda_j) + \dots + x_{12\dots N}(t, \lambda_1 \dots \lambda_N) \quad (4.2)$$

where x_0 is the nominal value of $x(t, \boldsymbol{\lambda})$, $x_i(t, \lambda_i)$ represents the contribution of λ_i to $x(t, \boldsymbol{\lambda})$ acting alone, $x_{ij}(t, \lambda_i, \lambda_j)$ represents the pairwise contribution of λ_i and λ_j to $x(t, \boldsymbol{\lambda})$ etc. In this work, only

the zero-th and first order component functions of (4.2) are utilized, mathematically described as [54]

$$\begin{aligned} x_0(t) &= x(t, \boldsymbol{\lambda}^{(0)}) \\ x_i(t, \lambda_i) &= x(t, \boldsymbol{\lambda})\big|_{\boldsymbol{\lambda}^{(0)} \setminus \lambda_i} - x_0(t); \quad 1 \leq i \leq N \end{aligned} \quad (4.3)$$

In equation (4.3), $\boldsymbol{\lambda}^{(0)} = \mathbf{0}$ and the notation $\boldsymbol{\lambda}^{(0)} \setminus \lambda_i$ represents the scenario where all random dimensions except λ_i are set to 0 [54]. The zero-th component function represents the mean while the first order component functions of (6) represent the zero mean contribution of each random dimension to the network response acting alone. These contributions are then described using one dimensional (1D) PC expansions as

$$x_i(t, \lambda_i) \approx \sum_{k=1}^m x_i^{(k)}(t) \phi_k(\lambda_i); \quad 1 \leq i \leq N \quad (4.4)$$

The coefficients of (4.4) satisfy the inner product operation

$$\begin{aligned} x_i^{(k)}(t) &= \langle x_i(t, \lambda_i), \phi_k(\lambda_i) \rangle \\ &= \int_{\Omega} \left(x(t, \boldsymbol{\lambda})\big|_{\boldsymbol{\lambda}^{(0)} \setminus \lambda_i} - x_0(t) \right) \phi_k(\lambda_i) \rho(\lambda_i) d\lambda_i \end{aligned} \quad (4.5)$$

where $\rho(\lambda_i)$ represents the marginal probability density function of random dimension λ_i . The integral in (4.5) is evaluated using Gaussian quadrature rules [61] allowing one to compute the coefficients of (4.4) as

$$x_i^{(k)}(t) \approx \sum_{j=0}^m w_j x_i(t, \lambda_i^{(j)}) \phi_k(\lambda_i^{(j)}) \quad (4.6)$$

where w_j represents the j -th 1D Gaussian quadrature weight corresponding to the j -th quadrature node $\lambda_i^{(j)}$. From (4.5) and (4.6), it can be concluded that only $(m+1)N$ SPICE simulations are required to evaluate the coefficients of (4.6).

Next, by neglecting the higher order component functions of (4.2), the variance of $x(t, \lambda)$ can be approximated as

$$\sigma_x^2 \approx \sigma_1^2 + \sigma_2^2 + \dots + \sigma_N^2 \quad (4.7)$$

where σ_x^2 is the total variance of $x(t, \lambda)$ and σ_i^2 is the variance of the contribution of λ_i acting alone (i.e., variance of $x_i(t, \lambda_i)$). Using (4.6) and (4.7), the variance based sensitivity index of each i^{th} random dimension can be analytically measured as [55], [56]

$$S_i(t) = \frac{\sigma_i^2}{\sigma_x^2} = \frac{\sum_{j=1}^m (x_i^{(j)})^2}{\sum_{i=1}^N \sum_{j=1}^m (x_i^{(j)})^2} \quad (4.8)$$

These sensitivity indices serve as problem dependent statistical information. It is noted that each sensitivity index S_i is a positive dynamic function whose value is bounded between 0 and 1. Moreover, it is observed from (4.7) and (4.8) that the sum of the sensitivity indices is always equal to unity. Thus, the magnitude of S_i at any particular time point directly reveals the relative impact of λ_i on the variance of the network response $x(t, \lambda)$ at that time point. However, these sensitivity indices being time dependent, their values change at every time point. Thus, the indices of (4.8) cannot be directly used to guide the dimension reduction approach for most electrical networks. In this dissertation, to address this problem, the normalized integral of the sensitivity indices of (4.8) will be computed as

$$L_1(S_i(t)) = \frac{1}{T_{\max}} \int_0^{T_{\max}} S_i(t) dt \quad (4.9)$$

where T_{\max} represents the time point of simulation. The integral of (4.9) is efficiently evaluated using the trapezoidal rule. This integral is a scalar quantity that reflects the average relative contribution of each random dimension over the entire time window of simulation. It is used to

rank the random dimensions in decreasing order of their impact on the variance of the network response. All dimensions with the integral of (4.9) falling below a prescribed tolerance ε are considered to be non-impactful and will be removed from the original N -dimensional random space to contract it into a n -dimensional random subspace Ω_n where $n < N$. Thus, the random vector $\lambda \in \mathfrak{R}^N$ will be replaced by a new random vector $\xi \in \mathfrak{R}^n$ where the entries of vector ξ are the most impactful n random variables of λ . From the various numerical examples performed, it has been concluded that the prescribed tolerance of $\varepsilon = 0.01$ works very well for most problems.

It is pointed out that the sensitivity indices of (4.8) are based on the impact of the random dimensions acting alone and does not consider their interactions. Thus, these indices do not accurately capture the total impact of each dimension. However, the sparsity of effects principle claims that the lower order interaction terms are statistically more significant than their higher order counterparts [62]. This means that considering the first order terms of (4.2) can still yield an accurate relative measure of the impact of each dimension if not the accurate total impact. Since at this stage only the relative impact of the random dimensions is required to identify the non-impactful dimensions and not their total impact, the indices of (4.8) will suffice. This particular point will be demonstrated using numerical examples in Section 4.2. It is further noted that in the above approach, no cumbersome iterative hierarchical methods are required to evaluate the sensitivity indices, as opposed to existing works on sparse PC expansions [40], [41]. Moreover, this work is able to address the dynamic nature of the sensitivity indices of (4.9) guiding the dimension reduction scheme. In the next subsection, the methodology to recover the reduced dimensional PC expansion will be described.

4.1.2 Recovering the Reduced Dimensional PC Expansion via Linear Regression

Once the N -dimensional network has been reduced to an n -dimensional problem, a reduced dimensional PC expansion of the network response can be expressed as

$$x(t, \boldsymbol{\lambda}) \approx \sum_{k=0}^Q x_k(t) \psi_k(\boldsymbol{\xi}) \quad (4.10)$$

where $\psi_k(\boldsymbol{\xi})$ is the k -th reduced dimensional basis, $x_k(t)$ is the corresponding coefficient and the number of terms in (4.10) is $Q+1 = (n+m)!/(n!m!)$ where $Q+1 \ll P+1$. Next, in order to intelligently evaluate the coefficients of (4.10), instead of directly adopting the linear regression approach of Section 3.1, first the expansion of (4.10) is separated into the mean, 1D terms, and multidimensional interactions terms as

$$x(t, \boldsymbol{\lambda}) = x_0(t) + \sum_{i=1}^N x_i(t, \lambda_i) + \sum_{k=1}^{Q-m} y_k(t) \phi_k(\boldsymbol{\xi}) \quad (4.11)$$

It is noted that in (4.11), the 1D PC expansions of all the random dimensions have been included. This is because the 1D PC coefficients have already been evaluated anyway in (4.6) and including these terms will enhance the accuracy of the final expansion. The mean is already known from (4.3) while the 1D terms are already known from the 1D PC expansions of (4.4), thereby leaving only the multidimensional terms to be represented as

$$\sum_{k=1}^{Q-m} y_k(t) \phi_k(\boldsymbol{\xi}) = x(t, \boldsymbol{\lambda}) - x_0(t) - \sum_{i=1}^N x_i(t, \lambda_i) \quad (4.12)$$

The coefficients of the multidimensional terms can now be computed via the regression analysis approach described in Section 3.1 in conjunction with (4.12) instead of (4.10). In doing so, the linear overdetermined system of equations of (3.2) can be reformulated as

$$\mathbf{A}\tilde{\mathbf{X}} = \mathbf{E} - \mathbf{E}_0 - \mathbf{E}_1 \quad (4.13)$$

where

$$\mathbf{E} = \begin{bmatrix} x(t, \xi^{(1)}) \\ \vdots \\ x(t, \xi^{(M)}) \end{bmatrix}; \quad \mathbf{E}_0 = \begin{bmatrix} x_0(t) \\ \vdots \\ x_0(t) \end{bmatrix}; \quad \mathbf{E}_1 = \begin{bmatrix} \sum_{i=1}^N x_i(t, \lambda_i^{(1)}) \\ \vdots \\ \sum_{i=1}^N x_i(t, \lambda_i^{(M)}) \end{bmatrix} \quad (4.14)$$

It is noted that the 1D regression node in (4.14) is $\lambda_i^{(k)} = \zeta_i^{(k)}$ if λ_i has been deemed an impactful dimension and $\lambda_i^{(k)} = 0$ otherwise. It is also noted that the number of unknown multidimensional PC coefficients are $Q-mn$ and as a result only $M = 2(Q-mn) (< 2(P+1))$ regression nodes are required to be identified. Next, instead of directly utilizing the D-optimal condition to identify these nodes, in this work the first $(m+1)n$ regression nodes are taken to be the purely 1D m -th degree Gaussian quadrature nodes used in (4.6) to evaluate the PC coefficients of the impactful 1D expansions of (4.4). Since the SPICE solution for these initial nodes are already known, they are not required to be extracted again. Only for the remaining $2(Q-mn)-(m+1)n$ regression nodes, the D-optimal condition can be used (i.e., new SPICE simulations will be required).

It is pointed out that in (4.13)-(4.14), both the 1D PC basis from the expansions of (4.4) and the 1D quadrature nodes required to evaluate the coefficients in (4.6) are reused – in other words, the maximum possible amount of information from the sensitivity analysis procedure is reused. The outcome of this reutilization of information is that only $2(Q-mn)-(m+1)n$ SPICE simulations are required to recover the unknown multidimensional PC coefficients of (4.12) instead of $2Q$. This efficiency due to information reuse is above and beyond that already achieved due to the dimension reduction procedure itself.

4.1.3 Sensitivity Analysis for Multiple Network Responses

The above dimension reduction strategy is based on the assumption that there is only one network response of interest $x(t, \lambda)$. Now consider that for the network there exist K responses of interest. In that case, each random dimension will have a different effect on each response thereby complicating the proposed strategy of Section 4.1.2.

In this work, in order to determine the most impactful random dimensions across all the K responses, first the sensitivity indices of (4.8) for each random dimension is computed for all the K responses and denoted as $S_i^{(k)}$ where $1 \leq k \leq K$. Thereafter, the integrals of (4.9) for the corresponding sensitivity indices are computed as

$$L_i^{(k)} = \frac{1}{T_{\max}} \int_0^{T_{\max}} S_i^{(k)}(t) dt \quad (4.15)$$

Finally, these average quantities are checked against the prescribed tolerance value ε . Any i -th dimension is considered to be non-impactful only if the following criterion is satisfied

$$\max(L_i^{(k)}) < \varepsilon; \quad 1 \leq k \leq K \quad (4.16)$$

In this way, the random vector ξ will contain only those dimensions which are impactful over all the K network responses. It is pointed out that this strategy for multiple network responses of interest does not require any additional SPICE simulations thereby ensuring that the CPU costs of the proposed approach does not depend on the number of responses probed.

4.1.4 Contraction of PC due to Dimension Reduction

This section begins with the following lemma to quantify the contraction in the PC expansion achieved.

Lemma 1: The contraction in the number of PC basis terms of the proposed reduced dimensional approach over full-dimensional PC approaches is approximately as $O((n/N)^m)$.

Proof: Given the negligible computational costs to identify the regression nodes, the overall costs for any non-intrusive PC approach can be reduced to the one required by the SPICE simulations needed to evaluate the PC coefficients. For full-dimensional PC approaches, the number of SPICE simulations can be quantified as

$$P+1 = \frac{(N+m)!}{N!m!} = \frac{\prod_{j=1}^m (N+j)}{\prod_{j=1}^m j} = \frac{N^m}{m!} + O\left(\frac{N^{m-1}}{m!}\right) \quad (4.17)$$

On the other hand, the number of bases in the reduced dimensional PC expansion of (4.10) is only

$$Q+1 = \frac{(n+m)!}{n!m!} = \frac{\prod_{j=1}^m (n+j)}{\prod_{j=1}^m j} = \frac{n^m}{m!} + O\left(\frac{n^{m-1}}{m!}\right) \quad (4.18)$$

Thus, the sparsity of the reduced dimensional PC expansion can be quantified as

$$\eta = \frac{Q+1}{P+1} = \frac{n^m + O(n^{m-1})}{N^m + O(N^{m-1})} \approx \left(\frac{n}{N}\right)^m \quad (4.19)$$

If $n < N$, the reduced dimensional PC expansion will represent a substantial contraction of the original full-blown PC expansion.

Section III A-B clearly demonstrates that the total number of SPICE simulations required in the regression analysis of (4.10) is equal to those required to construct the sensitivity indices

of (4.8) plus those required for the linear regression analysis of (4.12) minus the reused nodes. Together, that makes

$$\begin{aligned} R &= (m+1)N + 2(Q - mn) - (m+1)n \\ &= 2(Q - mn) + (m+1)(N - n) \end{aligned} \quad (4.20)$$

As will be demonstrated in Section 4.2, if $n \ll N$, then the required number of SPICE simulations $R \ll 2(P+1)$ used in traditional linear regression approaches [24], [25], [63].

4.1.5 Comparing Performance of Proposed Approach with Respect to Existing Sparse PC Approaches

The more popular sparse PC approaches are the hierarchical basis reduction techniques of [40], [41]. These techniques also utilize variance based sensitivity indices similar to this work. However, the major distinction of these works from the proposed approach is that they utilize an iterative methodology to determine which of the higher order interactions of (4.2) are to be retained. As a result, these approaches can even ignore the statistically insignificant higher order terms of important dimensions. This is not possible in the proposed approach where all higher order interactions of the n important dimensions are accounted for in (4.10). As a result, the basis reduction techniques of [40], [41] may require fewer basis than the proposed approach. On the other hand, due to the ability of the proposed approach to reuse the $(m+1)n$ Gaussian quadrature nodes of (4.6), both these approach still require nearly the same number of SPICE simulations despite having different number of PC bases.

As a second distinction, because the works of [40], [41] utilize a hierarchical approach to evaluate the relevant higher order interactions of (4.2), the error of the PC expansions representing the lower order interactions gets propagated to the higher levels. For example, the

approximation of (4.4) introduces some nonzero error into the 1D PC expansions. When considering the second order interactions of (4.2), they are expressed as

$$\begin{aligned}
x_{ij}(t, \lambda_i, \lambda_j) &= x(t, \boldsymbol{\lambda}) \Big|_{\lambda^{(0)} \setminus (\lambda_i, \lambda_j)} - x_0(t) - x_i(t, \lambda_i) - x_j(t, \lambda_j) \\
&\approx x(t, \boldsymbol{\lambda}) \Big|_{\lambda^{(0)} \setminus (\lambda_i, \lambda_j)} - x_0(t) - \sum_{k=1}^m x_i^{(k)}(t) \phi_k(\lambda_i) - \sum_{k=1}^m x_j^{(k)}(t) \phi_k(\lambda_j)
\end{aligned} \tag{4.21}$$

where the error due to the 1D PC expansions is included. This in turn introduces error in the PC representation of the 2D interaction term $x_{ij}(t, \lambda_i, \lambda_j)$. Due to the hierarchical nature of HDMR, this error will get propagated to the third order interactions and beyond. In contrast, the proposed approach requires a single step reduction, thus precluding any error propagation beyond that in (4.12) due to the 1D PC expansions. This feature combined with the fact that the works of [40], [41] may ignore the higher order interactions of even the impactful n dimensions, automatically ensures that the proposed approach is relatively more accurate – this despite the fact that the proposed approach and the sparse approaches require very similar number of SPICE simulations. This has been demonstrated using the numerical examples of Section 4.2.

Finally, a new HPCE approach has been recently proposed in [58]-[59]. This work is based on the concept of hyperbolic truncation of PC expansions. These works attempt to prune the number of PC bases by automatically removing the high dimensional interactions among the bases guided by the sparsity of effects principle [62]. However, this approach lacks sophisticated control over the number of pruned basis e.g., such as those based on sensitivity indices of the dimensions. As a result, for high-dimensional problems, the hyperbolic truncation may overestimate/underestimate the number of pruned bases leading to an inaccurate PC expansion. In fact, the proposed approach is both more efficient and more accurate than the HPCE for high-dimensional problems as demonstrated in Section 4.2.

4.2 Numerical Examples

In this section, we present three examples in order to demonstrate the computational benefits of the proposed reduced dimensional PC approach over full-dimensional PC approaches and existing sparse PC approaches. For all examples, the threshold for pruning the number of dimensions using (4.9) is $\varepsilon = 0.01$.

4.2.1 Example 1

In this example, the microstrip MTL network consisting of 10 coupled lines of Fig. 4.1 is considered. The cross-section of the MTL network is shown in Fig. 4.2. The uncertainty in the network is introduced via forty random variables ($N = 40$) with Gaussian distribution as listed in Table 4.1 and a Hermite PC expansion of degree $m = 3$ is considered.

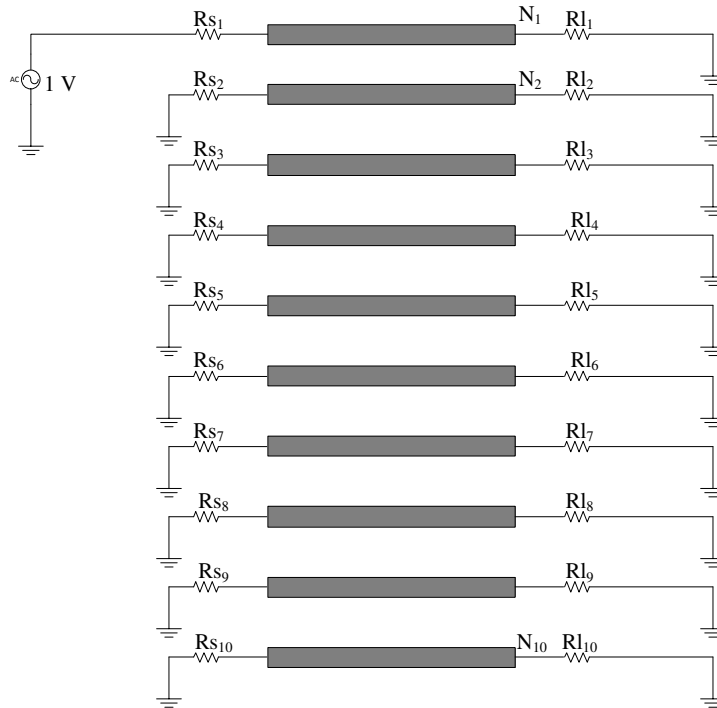


Fig. 4.1: The schematic of the MTL network of Example 1

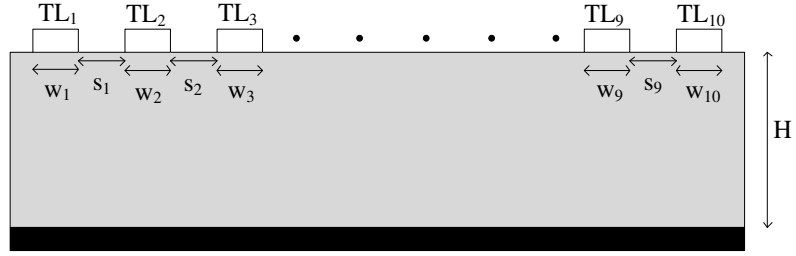


Fig. 4.2: Cross sectional view of the MTL network of Fig. 1.

For the accuracy demonstration of this example, the uncertainty quantification for this example is performed using four methods – the Monte Carlo sampling approach using 25,000 samples, the hierarchical sparse PC approach of [41], the HPCE approach of [59], and the proposed approach. To ensure the fairest comparison, all three PC approaches of above employ the linear regression approach described in Chapter 3. For this example, the response at node N_1 of Fig. 4.1 is considered as the only output of interest. For the proposed approach, the sensitivity indices of the random dimensions with respect to this response are computed using the methodology of Section 4.1. For this example, only $n = 7$ dimensions of Table 4.1 are retained ($RS_1, RI_1, w_1, w_2, s_1, s_2,$ and H).

Table 4.1: Random Variables of Example 1 (Fig 4.1)

Random Variables	Mean Values	% Standard Deviation (Normal Distribution)
RS_{1-10}	50Ω	20%
RI_{1-10}	50Ω	
w_{1-10}	$130 \mu\text{m}$	
s_{1-9}	$100 \mu\text{m}$	
H	$100 \mu\text{m}$	

The standard deviation (σ) of the frequency domain response at N_1 of Fig. 4.1 is computed using all the above methods and the magnitude results are compared in Fig. 4.3(a). It is demonstrated that the proposed approach exhibits good agreement with MC while both the hierarchical sparse PC approach of [41] and the sparse HPCE expansion exhibits distinct errors.

The L_2 error norm for the three PC approaches for the standard deviation result of response at N_1 is listed in Table 4.2 (MC results taken as reference). The results of Table 4.2 show that the proposed approach is roughly 3 times more accurate than the work of [41] and 13 times more accurate than the sparse HPCE expansion of [59]. The reasons behind the poor accuracy of the works of [41] and [59] have already been discussed in Section 4.1.5.

Next, the probability density function (PDF) of the response of N_1 at 20 GHz obtained using the same four approaches as above is evaluated and the results shown in Fig. 4.3(b). The yield of the network is defined to be the probability that the magnitude of the response at N_1 is less than 0.1 at 20 GHz. From the Fig. 4.3(b) it is observed that the proposed approach and MC results provide similar yields of roughly 38%. On the other hand, due to errors in the work of [41], the yield computed using this approaches is 51.8% – significantly different from the MC result.

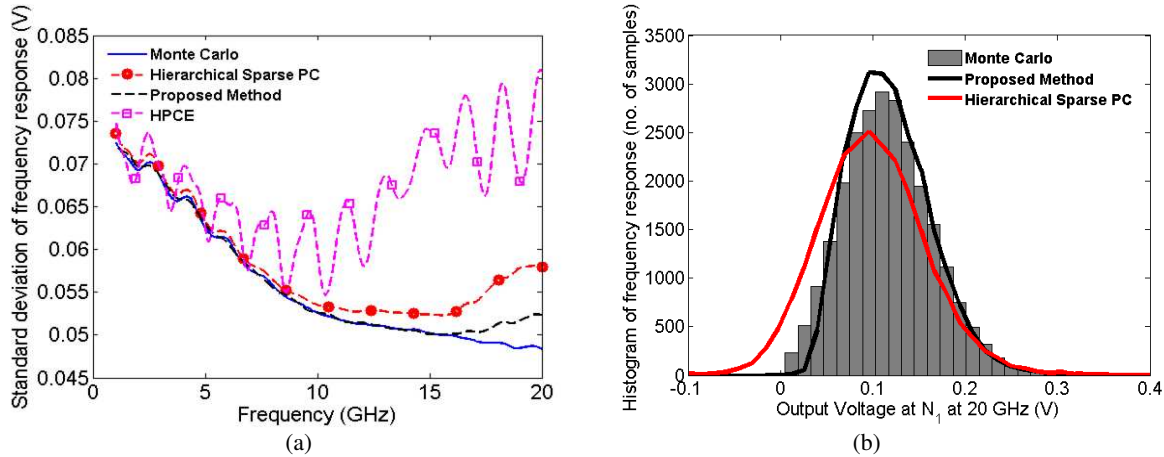


Fig. 4.3: Statistical analysis of Example 1 using proposed approach, the work of [41] and [59], all compared against Monte Carlo approach (25,000 samples). (a) Magnitude of standard deviation of the frequency response at node N_1 . (b) Histogram of the response data from node N_1 at 20 GHz.

Finally, for a comparison of the CPU costs incurred, the total number of SPICE simulations required by all PC approaches considered is recorded in Table 4.2. As expected, all the PC approaches require lesser number of SPICE simulations than the MC approach. The results

Table 4.2: L_2 Error Norm of Standard Deviation for Example 1 (Monte Carlo with 25,000 Samples Taken as Reference)

	L_2 Error Norm	# SPICE Simulations	# Bases	Speedup w.r.t full blown PC (24,682 Simulations)
Hierarchical sparse PC approach [41]	0.1097	333	207	74.12
Proposed approach	0.0356	331	219	74.57
Proposed approach (work of [53])	0.0433	401	219	61.55
HPCE approach [59]	0.4679	901	901	27.39

reported in Table 4.2 show that the proposed approach and the hierarchical sparse PC approach of [41] require almost the same number of SPICE simulations. This is despite the fact that the proposed approach requires 219 PC bases compared to the 207 required by the work of [41] (as expected from the discussion of Section 4.1.5). Thus both these approaches exhibit almost the same speedup over full-blown PC approaches (roughly 74 times faster). In addition, the proposed reuse of information in (4.12) allows the further reduction of 70 SPICE simulations over the preliminary work of [53]. The results of Table 4.2 also demonstrate that the proposed approach is 2.7 times faster than the sparse HPCE approach of [59].

4.2.2 Example 2

In this example, the same MTL network of Fig. 4.1 is considered with the outputs of interest being both nodes N_1 and N_2 . The uncertainty quantification for this example is performed using three methods – the Monte Carlo sampling approach using 35,000 samples, the hierarchical sparse PC approach of [41], and the proposed approach. For probing the new outputs of interest, this example requires $n = 8$ dimensions to be considered (R_{s_1} , R_{l_1} , R_{l_2} , w_1 , w_2 , s_1 , s_2 , and H). Note that the new random dimension R_{l_2} has to be considered as it displays a significant sensitivity on the crosstalk results at node N_2 .

The standard deviation (σ) of the frequency domain response at N_1 , N_2 , and N_{10} of Fig. 4.1 are computed using all the above methods. The magnitude of the standard deviation at N_2 and N_{10} are illustrated in Fig. 4.4 and 4.5 respectively. The L_2 error norm for the PC approaches for the standard deviation result of response at nodes N_1 , N_2 , and N_{10} is computed and listed in Table 4.3 (MC results taken as reference). The results of Table 4.3 show that the proposed approach is roughly 2 times more accurate than the work of [41] for the outputs N_1 and N_2 .

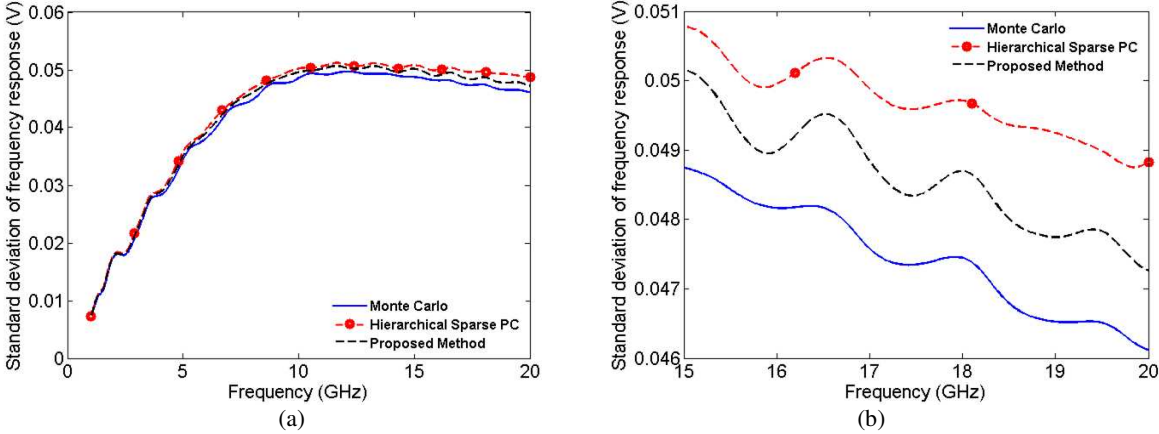


Fig. 4.4: Statistics of Example 2 evaluated using proposed approach and the work of [32], both compared against Monte Carlo approach (25,000 samples). (a) Magnitude of standard deviation of the frequency response at node N_2 . (b) Zooming in on the standard deviation results of node N_2 between 15 and 20 GHz, thereby illustrating the accuracy of the proposed approach.

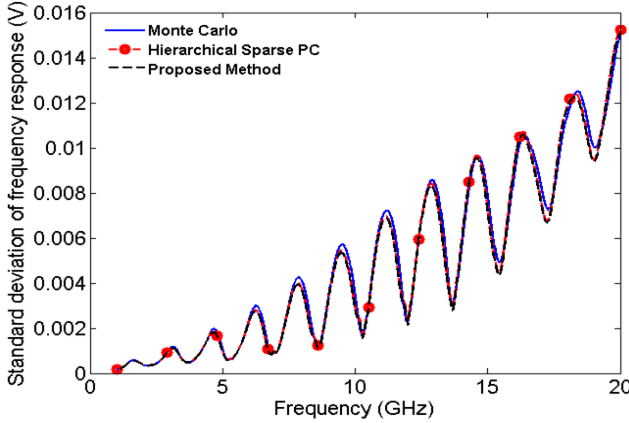


Fig. 4.5: Magnitude of standard deviation of frequency response at node N_{10}

Importantly, the error norm for node N_1 for both approaches has improved from the results of Example 1 (Table 4.2). This is to be expected since a new dimension has been taken into account to ensure good accuracy for the results of node N_2 as well.

For a comparison of the CPU costs, the total SPICE simulations incurred by both the PC methods are recorded in Table 4.3. From the results of Table 4.3 it is observed that the proposed approach is once again virtually just as efficient as the sparse PC approach of [41] (both are roughly 57-60 times faster than the full-blown PC approach). This is despite the fact that the proposed approach requires 261 PC bases compared to the 255 required by the work of [41]. In addition, because the number of reduced dimensions have increased in Example 2 from Example 1, the proposed approach requires 10 less SPICE simulations compared to the preliminary work of [53] (i.e., total reduction of 80 SPICE simulations over [41]).

Table 4.3: L_2 Error Norm of Standard Deviation for Example 2 (Monte Carlo with 25,000 Samples Taken as Reference)

	L_2 Error Norm at N_1	L_2 Error Norm at N_2	L_2 Error Norm at N_{10}	# SPICE Simulations	# Bases	Speedup w.r.t full blown PC (24,682 Simulations)
Hierarchical sparse PC approach [41]	0.0694	0.0520	0.0106	429	255	57.53
Proposed approach	0.0334	0.0295	0.0097	411	261	60.05
Proposed approach [53]	0.0413	0.0311	0.00101	491	261	50.26

4.2.3 Example 3

In this example, the enhanced performance of the proposed reduced dimensional approach over existing sparse PC approaches when considering larger degrees of expansion is illustrated. For this purpose, the 16 conductor stripline MTL network of Fig. 4.6 is considered.

The lengths of the MTL networks are set to 5 cm and their layout and geometric dimensions are shown in Fig. 4.7.

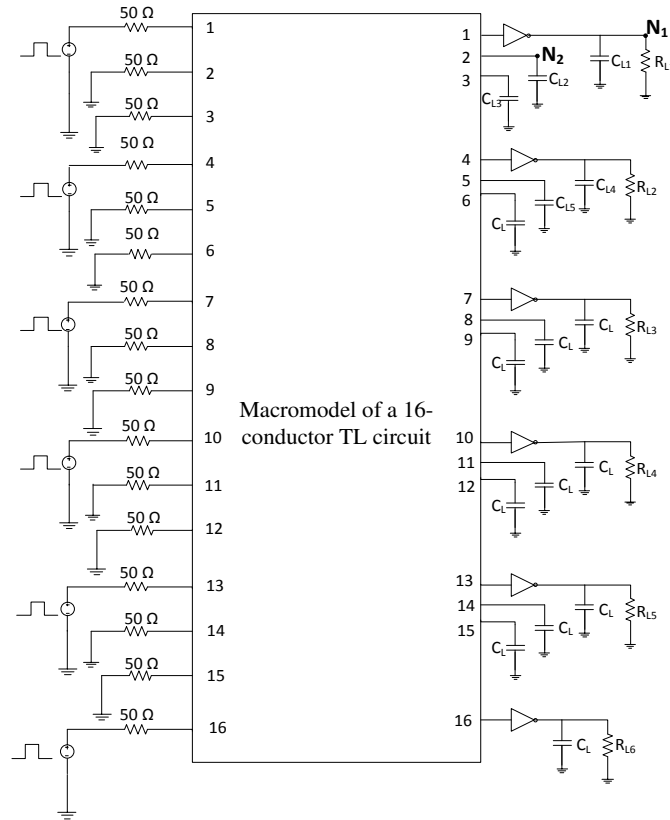


Fig. 4.6: Circuit layout of the MTL network with 16 coupled lines terminated by inverters (Example 3).

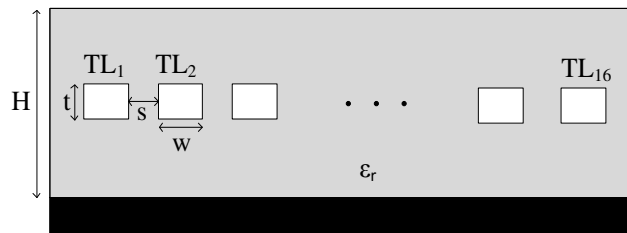


Fig. 4.7: Cross sectional view of the MTL network of Example 3 (Fig. 4.6).

The voltage sources of Fig. 4.6 exhibit trapezoidal waveforms of rise/fall time $T_r = 0.1$ ns, pulse width $T_w = 1$ ns and amplitude of 5V. The uncertainty in the network is introduced via

twenty two random variables ($N = 22$) with uniform distribution as listed in Table 4.4 and a Hermite PC expansion of degree $m = 4$ is required. It is noted that for $N = 22$ and $m = 4$, the number of PC bases $P+1 = 14,950$ – a larger problem than $N = 40$ and $m = 3$ ($P+1 = 12,341$) as considered in Examples 1 and 2.

Table 4.4: Characteristics of Random Variables of Example 3 (Fig. 4.6)

Random Variables	Mean Values	% Standard Deviation (Uniform Distribution)
w (TL width)	150 μm	20%
t (TL height)	30 μm	
H (Dielectric thickness)	450 μm	
s (TL separation)	150 μm	
ϵ_r (Relative permittivity of dielectric)	4.1	
L (TL length)	6 cm	
σ (TL conductance)	5.8e7	
PL (PMOS length)	0.1 μm	10%
PW (PMOS width)	10 μm	
NL (NMOS length)	0.1 μm	
NW (NMOS width)	10 μm	
R_{L1-6}	1.5 k Ω	20%
C_{L1-5}	1 pF	

For the accuracy demonstration, the uncertainty quantification for this example is performed using three methods – the Monte Carlo sampling approach with 35,000 samples, the hierarchical sparse PC approach of [41], and the proposed approach. For this example, the outputs of interest are the nodes N_1 and N_2 of Fig. 4.5. For the proposed approach, only $n = 4$ dimensions of Table 4.4 are retained (w, s, ϵ_r , and L).

The statistical assessment of the response at the nodes N_1 and N_2 in Fig. 4.6 are computed using all the above methods as illustrated in Fig. 4.8 and 4.9. The proposed approach is found to display good agreement with MC while the hierarchical sparse PC approach of [41] exhibit distinct errors for the mean results of node N_2 . The L_2 error norm for the PC approaches relative

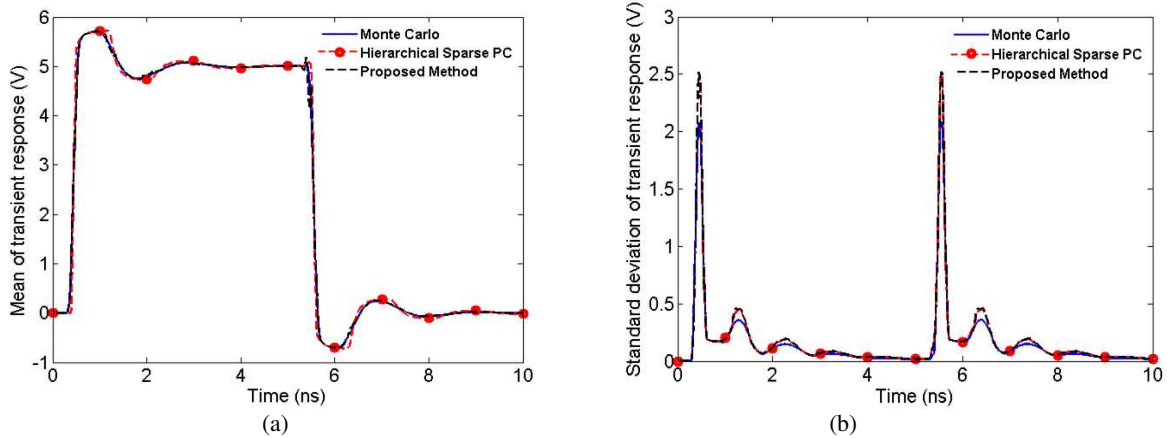


Fig. 4.8: Statistics of Example 3 evaluated using proposed approach and the work of [41], both compared against Monte Carlo approach. (a) Nominal response at node N_1 . (b) Standard deviation of the response at node N_1

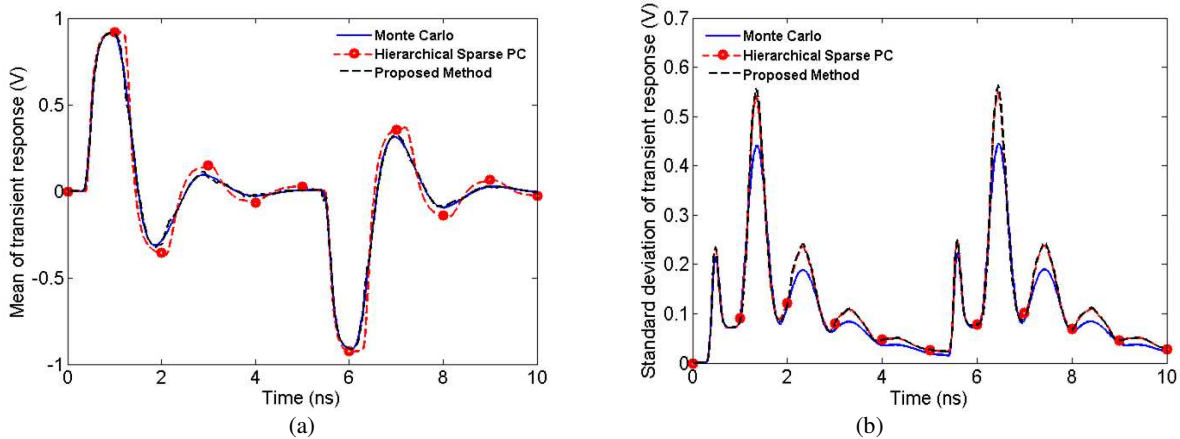


Fig. 4.9: Statistics of Example 3 evaluated using proposed approach and the work of [41], both compared against Monte Carlo approach. (a) Nominal response at node N_2 . (b) Standard deviation of the response at node N_2

to the MC results for the mean and standard deviation results is listed in Table 4.5. The results of Table 4.5 show that the proposed approach is roughly 2.6 and 5.6 times more accurate than the work of [41] when considering the mean of N_1 and N_2 respectively. However, both approaches are similarly accurate when considering the standard deviation results of Table 4.5.

For a comparison of the CPU costs incurred, the total number of SPICE simulations required by both the PC approaches is recorded in Table 4.5. These results show that the proposed approach is once again virtually just as efficient as the sparse PC approach of [41] (both are roughly 150

times faster than the full-blown PC approach). This is despite the fact that the proposed approach requires 142 PC bases compared to the 133 required by the work of [41]. Importantly, even though the number of reduced dimensions in Example 3 is very small ($n = 4$), the work of [41] still requires a substantially large 50 additional SPICE simulations over the proposed approach.

Table 4.5: L_2 Error Norm of Statistical Results for Example 3 (Monte Carlo with 35,000 samples used as reference)

	L_2 Error Norm at N_1		L_2 Error Norm at N_2		# SPICE Simulations	# Bases	Speedup w.r.t full blown PC (29,990 simulations)
	Mean	Standard Deviation	Mean	Standard Deviation			
Hierarchical sparse PC approach [41]	0.0043	0.0017	0.0019	7.53e-4	199	133	150.70
Proposed approach	0.0016	0.0018	3.34e-4	8.41e-4	202	142	148.47
Proposed approach[23]	6.70e-4	4.2e-4	3.23e-4	2.18e-4	251	142	119.48

CHAPTER 5: EXTENDING THE REDUCED DIMENSIONAL POLYNOMIAL CHAOS APPROACH FOR MIXED EPISTEMIC-ALEATORY PROBLEMS

In the previous chapter, a novel reduced dimensional PC approach for performing uncertainty quantification of microwave/RF circuits was presented where the input uncertainty was aleatory in nature. Aleatory uncertainty refers to the kind of uncertainty where the random dimensions are characterized by a known probability density function. It is irreducible in nature. Currently, there is a growing interest in studying the effect of epistemic uncertainty alongside random or aleatory uncertainty. Epistemic uncertainty is that uncertainty arising from the lack of knowledge regarding the value of the network parameters. Due to this lack of knowledge or ignorance, no probability density functions are known regarding these parameters and they are represented as pure interval valued variables [64].

So far, within the context of circuit simulation, the literature has been dominated by purely aleatory [13]-[20] or epistemic problems [76]-[81] with very little attention given to the more general problems where both forms of uncertainty are present (i.e., mixed uncertainty problems). When tackling mixed uncertainty problems, it is noted that all statistical moments of the response are no longer unique. Rather, these moments become functions of the epistemic dimensions. Thus, the main goal of mixed uncertainty quantification (UQ) is to evaluate the maximum and minimum bounds that enclose the possible variability of the response statistical moments [82], [83].

Traditionally, mixed UQ has been performed using the second order probability (SOP) approach [70]. While the SOP approach can be easily applied to circuit simulation, unfortunately this approach requires a nested sampling of the aleatory and epistemic dimensions, leading to

possibly thousands of SPICE simulations of the overall network. In recent engineering research, this computational burden has been alleviated by developing a surrogate model or metamodel of the system response [84]-[86]. A metamodel maps the effects of the input mixed dimensions on the system response using simple closed form functions. This metamodel can then be used to analytically emulate the network response in the SOP framework at negligible computational costs compared to solving the massive original system model.

Of the many metamodeling techniques available, unified polynomial chaos (PC) metamodels are particularly attractive due to their fast convergence to the actual response statistics even in high-dimensional spaces [65], [87]. Unified PC metamodels are so called because they represent epistemic dimensions as aleatory dimensions with uniform PDFs. Thereafter, the overall effect of all the aleatory dimensions on the system response is modeled using a linear combination of orthonormal basis functions as described in Section 2.4. Once the coefficients are determined, the unified PC metamodel can be used in the SOP framework to analytically and cheaply emulate the system response and extract the maximum and minimum bounds of any statistical functions of the response.

Unfortunately, the scalability issue of PC which is described in Section 1.1 is further exacerbated for mixed problems because the number of mixed dimensions is usually much more than that seen in purely aleatory or epistemic problems [87]. Thus, unified PC approaches are often too computationally expensive for high-dimensional mixed problems. Methods to develop sparse and reduced PC metamodels described in Section 2.6 are generally incompatible with mixed problems. This is because these works exploit the statistical information of the response such as the variance, covariance, or probability density function in order to determine how to best reduce the PC metamodel. However, for mixed problems, as explained before, all statistical

information of the response become functions of the epistemic dimensions. This means that the statistical information of the response cannot be uniquely known, thereby making it impossible to use such information to reliably reduce the PC metamodel. This inability to reduce the unified PC metamodels makes tackling mixed uncertainty in microwave networks a computationally intractable challenge.

In this dissertation, the above poor scalability of unified PC metamodels with respect to the number of mixed dimensions is remedied. As a first step of this remedy, a crude model of the response will be derived from a high dimensional model representation (HDMR) of the network [54]. This model will be used to estimate the sensitivity of the response variance with respect to each epistemic and aleatory dimension of the problem. In particular, when estimating the sensitivity of the response variance with respect to each aleatory dimension, the sensitivity indices will be swept over the entire epistemic space. Similarly, when estimating the sensitivity of the response variance with respect to each epistemic dimension, the sensitivity indices will also be swept over the entire epistemic space. This sensitivity sweeping algorithm will provide a clear picture of how the sensitivity indices vary over the entire domain of the multidimensional epistemic space – critical global information that could not be otherwise revealed. This global knowledge of the sensitivity indices is essential to objectively identify those epistemic and aleatory dimensions which exhibit a marginal contribution to the response variance across the entire epistemic space. Once these globally unimportant mixed dimensions have been identified and removed, a more compact unified PC metamodel of the network response can be constructed at far smaller CPU costs than a full-dimension metamodel without much loss in accuracy.

5.1 Overview of Mixed Uncertainty Problems and Unified Polynomial Chaos

Consider a general distributed interconnect network where the mixed parametric uncertainty is represented by N mutually uncorrelated aleatory (random) dimensions $\lambda = [\lambda_1, \lambda_2, \dots, \lambda_N]$ and M independent epistemic dimensions $\xi = [\xi_1, \xi_2, \dots, \xi_M]$. There currently exists two different ways in which mixed uncertainty can be introduced into the network as described below.

5.1.1 Epistemic and Aleatory Uncertainty is Separated

Let e_i represent the i -th epistemic network parameter and a_i the i -th aleatory network parameter. If the parameters e_i and a_i are different, then the epistemic and aleatory uncertainty is said to be separated. In that case, these parameters can be described as

$$e_{\min,i} \leq e_i \leq e_{\max,i}; \quad a_i = a_{i,0}(1 + s_i \lambda_i) \quad (5.1)$$

where $[e_{\min,i}, e_{\max,i}]$ represent the closed interval of values the epistemic parameter e_i can assume, $a_{i,0}$ is the nominal (mean) value of the aleatory parameter a_i and s_i is the corresponding relative standard deviation. In the work of [65], the epistemic parameter is modeled as an aleatory parameter with a uniform PDF using the transformation

$$e_i = \frac{(e_{\max,i} + e_{\min,i})}{2} + \frac{(e_{\max,i} - e_{\min,i})}{2} \xi_i \quad (5.2)$$

where $\xi_i \in [-1,1]$. It is appreciated that based on the transformation of (5.2), the mixed uncertainty problem is converted to a $N+M$ -dimensional purely aleatory problem. The effect of the $N+M$ aleatory dimensions can be propagated from the network parameters to any response $x(t, \lambda, \xi) \in \mathbf{X}(t, \lambda, \xi)$ of using conventional PC techniques [65], [87].

5.1.2 Epistemic and Aleatory Uncertainty is Not Separated

It is possible for both epistemic and aleatory uncertainty to be present in the same network parameter. For example, epistemic uncertainty can arise from the lack of precise knowledge of the nominal value and relative standard deviation of an otherwise aleatory network parameter. In other words, the network parameter can be described as

$$\begin{aligned} a_i &= a_{i,0} (1 + s_i \lambda_i) \\ a_{\min, i} &\leq a_{i,0} \leq a_{\max, i}; \quad s_{\min, i} \leq s_i \leq s_{\max, i} \end{aligned} \quad (5.3)$$

where $[a_{\min, i}, a_{\max, i}]$ and $[s_{\min, i}, s_{\max, i}]$ represent the closed intervals of values the nominal value and relative standard deviation can take. In such a scenario, a similar linear transformation as (5.2) can be used on the nominal and relative standard deviation values as

$$\begin{aligned} a_{i,0} &= \frac{(a_{\min, i} + a_{\max, i})}{2} + \frac{(a_{\max, i} - a_{\min, i})}{2} \mu_i; \\ s_i &= \frac{(s_{\min, i} + s_{\max, i})}{2} + \frac{(s_{\max, i} - s_{\min, i})}{2} \theta_i \end{aligned} \quad (5.4)$$

where $\mu_i \in [-1, 1]$ and $\theta_i \in [-1, 1]$. The new vectors $\boldsymbol{\mu} = [\mu_1, \mu_2, \dots, \mu_N]$ and $\boldsymbol{\theta} = [\theta_1, \theta_2, \dots, \theta_N]$ will together make up the vector of epistemic dimensions $\boldsymbol{\xi}$ as $\boldsymbol{\xi} = [\boldsymbol{\mu} \ \boldsymbol{\theta}]$ and $M = 2N$. Based on the transformation of (4), the mixed uncertainty problem of (1) is now converted into a $3N$ -dimensional aleatory problem. The effect of the $3N$ aleatory dimensions on the network response can be again propagated using classical PC techniques [65], [87].

The above two scenarios demonstrate that irrespective of how mixed uncertainty appears in the problem, it can be transformed into an aleatory problem [35]. Now, the overall aleatory uncertainty can be propagated to any network response $x(t, \boldsymbol{\lambda}, \boldsymbol{\xi}) \in \mathbf{X}(t, \boldsymbol{\lambda}, \boldsymbol{\xi})$ using a PC expansion as

$$x(t, \boldsymbol{\lambda}, \boldsymbol{\xi}) = \sum_{k=0}^P x_k(t) \phi_k(\boldsymbol{\lambda}, \boldsymbol{\xi}) \quad (5.5)$$

where $\phi_k(\boldsymbol{\lambda}, \boldsymbol{\xi})$ is the k -th multivariate polynomial, $x_k(t)$ is the corresponding coefficient, and the number of terms in the expansion of (5.5) is equal to $P+1 = (N+M+d)!/(N+M!)(d!)$, d being the maximum degree of the expansion. The polynomial bases $\phi_k(\boldsymbol{\lambda}, \boldsymbol{\xi})$ are all orthogonal with respect to the joint probability density function $\rho(\boldsymbol{\lambda}, \boldsymbol{\xi})$ of the aleatory dimensions [65]. The expansion of (5.5) is hereafter referred to as a unified PC metamodel [87]. The coefficients of (5.5) can be evaluated using any non-intrusive approach. Once the coefficients are known, the metamodel of (5.5) can be used as a surrogate of the response $x(t, \boldsymbol{\lambda}, \boldsymbol{\xi})$. Using this surrogate representation, it will be possible to analytically and efficiently emulate the response $x(t, \boldsymbol{\lambda}, \boldsymbol{\xi})$ in a SOP framework. As a result, the maximum and minimum bounds of all of the response statistics can be quantified [87].

The main limitation of the unified PC approach is that in order to evaluate the coefficients of (5.5), the number of discrete SPICE simulations of the network of (1) that will be required will scale in a polynomial fashion as $O((N+M)^d)$. Thus, even for moderate values of N and M , such an approach can become computationally intractable. Various methods such as those based on ANOVA [75], [40], [41], [89], active subspaces [88], basis adaptations [91], multi-element PC [32], and probabilistic error criteria [90] have been developed to mitigate the above poor scalability of PC metamodels for purely aleatory problems. However, these methods are not extendable to mixed UQ problems. This is because these works rely on statistical information of the response (e.g., variance, covariance, PDFs) in order to determine how to best reduce the metamodel. Unfortunately, quantifying any statistical information of the response requires the knowledge of the input PDFs. However, for mixed problems, the PDFs of the

epistemic dimensions of ξ are never known. In fact, even though the unified PC approach uses the transformations of (5.2) and (5.4) to convert the epistemic dimensions to uniform aleatory dimensions, this is only for the sake of sampling the multidimensional epistemic space in the SOP framework. In other words, for mixed problems, all response statistics becomes functions of the epistemic dimensions. Thus, the response statistics cannot be uniquely known and hence cannot be used to objectively guide the metamodel reduction process. This inability to reduce the unified PC metamodels means that for microwave networks subject to mixed uncertainty, the CPU cost of constructing the unified metamodel of (5.5) will be massively large. In order to address this limitation, a mixed dimension reduction approach is presented next.

5.2 Development of Proposed Mixed Dimension Reduction Approach

Assume a general interconnect network where uncertainties of both forms described in Sections 5.1.1 and 5.1.2 are present. For this kind of general problem, let the full vector of mixed dimensions be defined as $\boldsymbol{\alpha} = [\boldsymbol{\lambda} \ \boldsymbol{\xi}]$ and the total number of mixed dimensions be $Q = M+N$. The following sections will describe how the sensitivity of the response variance with respect to each epistemic and aleatory dimension of $\boldsymbol{\alpha}$ will be estimated.

5.2.1 Constructing a Crude Representation of the Response

The high dimensional model representation (HDMR) of any response of the network of (1) is defined as [54]

$$x(t, \boldsymbol{\alpha}) = x_0(t) + \sum_{i=1}^Q x_i(t, \alpha_i) + \sum_{1 \leq i, j \leq Q} x_{ij}(t, \alpha_i, \alpha_j) + \dots + x_{12\dots Q}(t, \boldsymbol{\alpha}) \quad (5.6)$$

where x_0 is the value of $x(t, \boldsymbol{\alpha})$ in absence of any uncertainty (zero-th order interaction term), $x_i(t, \alpha_i)$ represents the contribution of each α_i on $x(t, \boldsymbol{\alpha})$ acting alone (first order interaction terms),

$x_{ij}(t, \alpha_i, \alpha_j)$ represents the contribution of each $\{\alpha_i, \alpha_j\}$ pair on $x(t, \mathbf{\alpha})$ acting alone (second order interaction terms) etc. The zero-th order and first order interaction terms of (5.6) are expressed using cut-HDMR [54] as

$$\begin{aligned} x_0(t) &= x(t, \mathbf{\alpha}^{(0)}) \\ x_i(t, \alpha_i) &= x(t, \mathbf{\alpha}) \Big|_{\mathbf{\alpha}^{(0)} \setminus \alpha_i} - x_0(t); \quad 1 \leq i \leq Q \end{aligned} \quad (5.7)$$

where $\mathbf{\alpha}^{(0)} = \mathbf{0}$ and the notation $\mathbf{\alpha}^{(0)} \setminus \alpha_i$ represents the vector where all components of $\mathbf{\alpha}$ except α_i are set to 0.

In the work of [36], it was proposed that the network response be crudely represented as the sum of the zero-th order and first order interaction terms of (5.6). However, this representation is not adequate for mixed uncertainty problems of the type described in Section 5.1.2. To better understand why this is the case, consider the scenario when $\alpha_i = \theta_j$ for some $\{i, j\}$ pair. In this scenario, when quantifying $x_i(t, \alpha_i)$, all component of $\mathbf{\alpha}$ except α_i are set to 0. This means that the aleatory dimension λ_j corresponding to the relative standard deviation θ_j is also set to zero. Replacing $\lambda_j = 0$ in (5.3) automatically leads to $x_i(t, \alpha_i) = 0$ in (5.7). This means that using only the zero-th order and first order interaction terms of (5.6) to approximate the network response cannot account for the effects of the epistemic dimensions of $\mathbf{\theta}$. This is a direct outcome of the fact that in some parameters, both epistemic and aleatory uncertainty exists together as shown in (5.3). In order to circumvent this issue, only those second order interaction terms of (5.6) where $\alpha_i = \lambda_k$ and $\alpha_j = \theta_k$ for the triplet $\{i, j, k\}$ will be added to the approximation of the response. Thus, the response will now be approximated as

$$x(t, \mathbf{\alpha}) \approx x_0(t) + \sum_{\alpha_i = \theta_j} x_i(t, \alpha_i) + \sum_{\alpha_i = \lambda_k; \alpha_j = \theta_k} x_{ij}(t, \alpha_i, \alpha_j) \quad (5.8)$$

It is noted that by adding the few second order interaction terms in (5.8), it will now be possible to both map the effects of the epistemic dimensions of $\boldsymbol{\theta}$ on the response while simultaneously keeping the number of terms required to approximate the response to the bare minimum. Next, the right hand side of (5.8) will be represented using a PC metamodel as

$$x(t, \boldsymbol{\alpha}) \approx \sum_{k=0}^R \hat{x}_k(t) \phi_k(\boldsymbol{\alpha}) \quad (5.9)$$

where the basis functions $\phi_k(\boldsymbol{\alpha})$ have to be either only univariate or bivariate by nature. If the basis functions are univariate, then the variable $\alpha_i \neq \theta_j$. If the basis functions are bivariate, then the pair of variables $\{\alpha_i, \alpha_j\}$ must satisfy the condition $\alpha_i = \lambda_k$ and $\alpha_j = \theta_k$ for the triplet $\{i, j, k\}$. Due to these restrictions, the number of terms and coefficients of (5.9) will be much smaller than that of a full-blown PC metamodel of (5.5) (i.e., $R \ll P+1$). Consequently, the coefficients of (5.9) can be evaluated at relatively small CPU costs using any non-intrusive approach including the linear regression approach [63]. This metamodel of (5.9) will now be leveraged to perform the proposed sensitivity analysis.

5.2.2 Sensitivity Sweeping Algorithm for Aleatory Dimensions

The main challenge of estimating the sensitivity of the response variance with respect to the aleatory dimensions of $\boldsymbol{\alpha}$ is that the response variance itself varies with the values of the epistemic dimensions of $\boldsymbol{\xi}$. As a result, the extracted sensitivity information for any aleatory dimension will not be unique. Rather, this information will vary from one point in the multidimensional epistemic space to another, thereby making it useless as an objective and reliable tool for dimension reduction.

To address this problem, in this work, the sensitivity information corresponding to each aleatory dimension will be swept over the entire epistemic space in order to fully understand and characterize its global properties. For this purpose, a nested sampling algorithm is proposed. As part of this nested sampling algorithm, in the outer loop N_e uniformly distributed samples will be taken from the epistemic space without replacement. Let any k -th general sample be described as $\xi^{(k)} = [\xi_1^{(k)}, \xi_2^{(k)}, \dots, \xi_M^{(k)}]$ where $1 \leq k \leq N_e$. Replacing each sample $\xi^{(k)}$ in the metamodel of (5.9) will render the response as a pure PC metamodel of the aleatory dimensions of λ as shown

$$x(t, \lambda, \xi = \xi^{(k)}) \approx \hat{x}_0(t) + \sum_{i=1}^N \sum_{r=1}^d \hat{x}_i^{(r)}(t) \phi_r(\lambda_i) \quad (5.10)$$

where \hat{x}_0 represents the mean and $\hat{x}_i^{(r)}$ are the r -th PC coefficients capturing the impact of λ_i on the response, all computed at the location $\xi = \xi^{(k)}$. Note that the values of \hat{x}_0 and $\hat{x}_i^{(r)}$ will change for each sample point $\xi^{(k)}$ in the outer loop. Now, in the inner loop, the first order Sobol's sensitivity index of the aleatory dimension λ_1 will be computed as

$$A_{a,1}(t, \xi = \xi^{(k)}) = \frac{V(\lambda_1, \xi^{(k)}, t)}{V_u(\lambda, \xi^{(k)}, t)} = \frac{\sum_{r=1}^d (\hat{x}_1^{(r)}(t))^2}{\sum_{i=1}^N \sum_{r=1}^d (\hat{x}_i^{(r)}(t))^2} \quad (5.11)$$

where $V(\lambda_1, \xi^{(k)}, t)$ is the contribution of the aleatory dimension λ_1 to the response variance and $V_u(\lambda, \xi^{(k)}, t)$ is the overall response variance at the location $\xi = \xi^{(k)}$. Thus, the first order Sobol's sensitivity index of (5.11) is a metric representing the relative impact of the dimension λ_1 on the response variance at the location $\xi = \xi^{(k)}$ [56]. Since this index of (5.11) is time-varying, it is reduced to a scalar quantity by averaging its value over the entire time window of simulation, $[0 - T_{\max}]$, as

$$\hat{A}_{a,1}(\xi = \xi^{(k)}) = \frac{\int_0^{T_{\max}} \sum_{r=1}^d (\hat{x}_1^{(r)}(t))^2 dt}{\int_0^{T_{\max}} \sum_{i=1}^N \sum_{r=1}^d (\hat{x}_i^{(r)}(t))^2 dt} \quad (5.12)$$

The integrals of (5.12) can be evaluated using any numerical integration scheme [93]. This process will now be repeated for all N_e samples of the outer loop, thereby leading to an ensemble of the scalar sensitivity indices of (5.12) distributed across the entire epistemic space. If the sensitivity index of (5.12) is consistently below a prescribed tolerance of ε across all N_e samples then the impact of λ_1 will be considered to be globally marginal. As a result, the dimension λ_1 will be removed from the problem definition by setting $\lambda_1 = 0$. This dimension reduction process needs to be redone for all the N aleatory dimensions. As an outcome of the dimension reduction, the original vector of aleatory dimensions, $\lambda \in \mathfrak{R}^N$, will be reduced to a new vector $\lambda_{red} \in \mathfrak{R}^n$, where $n < N$.

It is noted that by sweeping the sensitivity indices of (5.12) across all N_e sample points, it will be possible to distinguish between those aleatory dimensions that are globally marginal in their impact from those that are locally marginal in their impact at some regions in the epistemic space. Thus, the above algorithm is referred to as a sensitivity sweeping algorithm. As part of this algorithm, N_e response variances and NN_e Sobol's sensitivity indices of (5.11) needs to be quantified. All of these computations does not involve any SPICE simulations and can be done analytically using the metamodel of (5.9) as shown in (5.11). Moreover, all of these computations can be easily performed in parallel as well. Thus, the computational expense of the sensitivity sweeping algorithm is negligible.

5.2.3 Modified Sensitivity Sweeping Algorithm for Epistemic Dimensions

The aforementioned sensitivity sweeping algorithm is now modified for the case of the epistemic dimensions of α . As part of the modified sensitivity sweeping algorithm, it is first pointed out that in Section 5.2.2, the response variance $V_u(\lambda, \xi^{(k)}, t)$ has already been evaluated at all N_e sample points. These variance measures are referred to as unconditional variances. From the knowledge of these N_e instances of the unconditional variances, for each time point the unconditional maximum and minimum bounds of the variance will be determined as

$$\begin{aligned} V_{\min}(t) &= \min(V_u(\lambda, \xi^{(k)}, t), 1 \leq k \leq N_e); \\ V_{\max}(t) &= \max(V_u(\lambda, \xi^{(k)}, t), 1 \leq k \leq N_e) \end{aligned} \quad (5.13)$$

Next, the same nested sampling approach of Section 5.2.2 will be reused in order to reevaluate the variance bounds of (5.13), this time subject to the constraint $\xi_1^{(k)} = \xi_1^{(1)}$ in all the sample points $\xi^{(k)}$. The new variance bounds evaluated will be the conditional maximum and minimum bounds. Mathematically, the conditional bounds can be described as

$$\begin{aligned} V_{\min,1,1}(t) &= \min(V_u(\lambda, \xi^{(k)}, t), \xi_1^{(k)} = \xi_1^{(1)}, 1 \leq k \leq N_e); \\ V_{\max,1,1}(t) &= \max(V_u(x, \xi^{(k)}, t), \xi_1^{(k)} = \xi_1^{(1)}, 1 \leq k \leq N_e) \end{aligned} \quad (5.14)$$

From the knowledge of the above unconditional and conditional bounds, the raw change in the bounds will be measured as

$$E_{e,1}(t) = \frac{(V_{\max}(t) - V_{\max,1,1}(t)) - (V_{\min}(t) - V_{\min,1,1}(t))}{2} \quad (5.15)$$

It is important to note that the above change is time dependent. As a result, the index of (5.15) will be reduced to a scalar quantity by averaging over the entire time window of simulation as

$$\hat{E}_{e,1} = \frac{1}{2T_{\max}} \left(\int_0^{T_{\max}} (V_{\max}(t) - V_{\max,1,1}(t)) dt - \int_0^{T_{\max}} (V_{\min}(t) - V_{\min,1,1}(t)) dt \right) \quad (5.16)$$

As before, the integral of (5.16) can be evaluated using any numerical integration scheme. It is pointed out that the integral of (5.16) measures the change in the variance bounds caused by fixing ζ_1 at the location $\zeta_1^{(1)}$. In other words, this integral reveals the sensitivity of the variance bounds with respect to ζ_1 at the location $\zeta_1 = \zeta_1^{(1)}$. Thus, the integral of (5.17) will hereafter be referred to as the sensitivity index of ζ_1 . Next, the entire above process will be repeated to quantify the sensitivity index of the epistemic dimension ζ_1 at all $\zeta_1 = \zeta_1(k)$, $1 \leq k \leq N_e$ sample points. If the sensitivity index of (5.16) is constantly less than a prescribed tolerance of η across all the sample points, then the impact of ζ_1 will be considered to be globally marginal and this dimension will be removed from the problem definition. This modified sensitivity sweeping algorithm needs to be repeated for all epistemic dimensions of ζ . It is assumed that due to the epistemic dimension reduction, the original vector $\xi \in \mathfrak{R}^M$ will be reduced to a new vector, $\xi_{red} \in \mathfrak{R}^m$ where $m < M$.

It is observed that for the modified sensitivity sweeping algorithm, N_e instances of the variances have to be computed to find out the variance bounds of (4.14). This process has to be then repeated for N_e sample points and M dimensions. In other words, a total of MN_e^2 variances have to be computed. However, as explained in Section 5.2.2, these variance computations can be done analytically using the metamodel of (5.9) and even parallelized to ensure that the modified sensitivity sweeping algorithm incurs negligible CPU costs.

5.2.4 Constructing the Reduced Dimensional PC Expansion

Once the Q -dimensional network has been reduced to a $q = m+n$ dimensional problem ($q < Q$) using the dimension reduction process described in Sections 5.2.2 and 5.2.3, the reduced dimensional PC metamodel of the network response can now be formulated as

$$x(t, \mathbf{a}) \approx \sum_{k=0}^U \tilde{x}_k(t) \psi_k(\mathbf{a}_{red}) \quad (5.17)$$

Where $\psi_k(\mathbf{a}_{red})$ is the k^{th} reduced dimensional basis, $\mathbf{a}_{red} = [\lambda_{red} \ \xi_{red}]$, $\tilde{x}_k(t)$ is the corresponding coefficient, and the number of terms in the expansion of (5.17) is truncated to $U+1 = (n+m+d)!/((n+m)!d!)$. The coefficients of (5.17) will be evaluated using the linear regression scheme suggested in [63]. Based on the complexity analysis performed in [75], the reduction in SPICE simulations to evaluate the coefficients of (5.17) compared to that of (5.5) will be bounded by the factor $(Q/q)^d$ where the factor Q/q is referred to as the dimension reduction factor.

5.3 Numerical Examples

In this section, three examples are presented to demonstrate the accuracy and efficiency of the proposed mixed dimension reduction based PC approach over the unified full-dimensional PC approach. In all of these examples, the sensitivity thresholds for judging if an epistemic or aleatory dimension is unimportant are set to $\eta = 10^{-4}$ and $\varepsilon = 0.01$ respectively.

5.3.1 Example 1

In this example, the 16 conductor stripline MTL network of Fig. 5.1 terminated by inverters consisting of SPICE level 49 CMOS transistors is considered. The response of interest

for this example is the transient voltage at node N_1 of Fig. 5.1. The cross-section layout and geometric dimensions of the transmission lines are shown in Fig. 5.2.

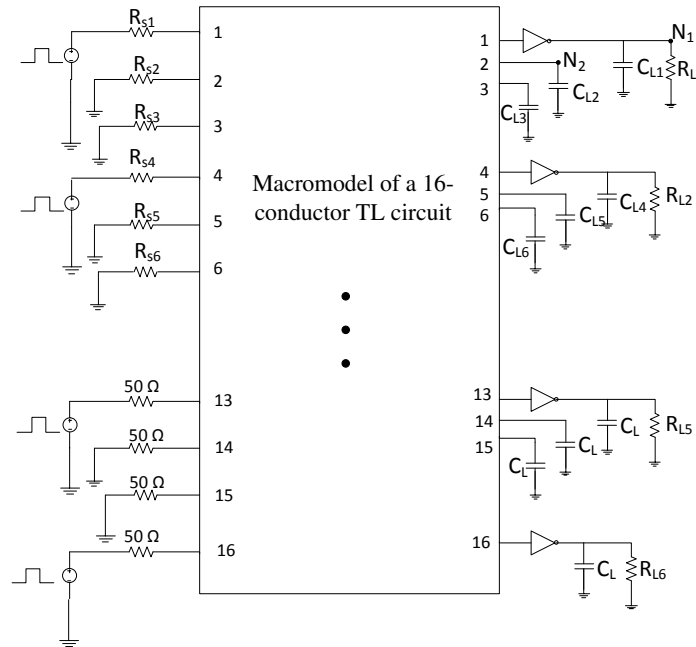


Fig. 5.1: The schematic of the MTL network of Example 1

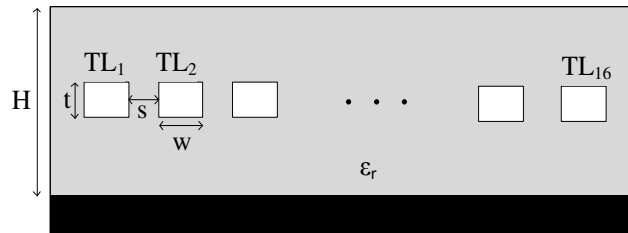


Fig. 5.2: Cross section view of the MTL network of Fig.5. 1.

The voltage sources of Fig. 5.1 exhibit a trapezoidal waveform of rise/fall time $T_r = 0.1$ ns, pulse width $T_w = 5$ ns and amplitude of 5V. The uncertain parameters of this example are listed in Table 5.1. A general scenario where some epistemic and aleatory parameters are separated while others are coupled together is considered.

Table 5.1: Uncertain Parameters of Example 1 (Fig 5.1)

Random Variable	Mean ($a_{i,0}$)	Standard Deviation (s_i)
w	150 μm	10% (Normal Distribution)
s	150 μm	
R_{L1}	1.5 k Ω	
R_{L2}		
R_{L3}		
R_{L4}		
PL (PMOS length)	0.1 μm	
PW (PMOS width)	10 μm	
NL (NMOS length)	0.1 μm	
NW (NMOS width)	10 μm	
R_{s3}	50 Ω	
R_{s4}		
σ (TL conductance)	5.8 e7	
C_{L3}	1 pF	
C_{L4}		
C_{L5}		
C_{L6}		
t	[27.5 – 32.5] μm	
H	[427.5 – 495] μm	
C_{L1}	[0.95 – 1.05] pF	
C_{L2}		
R_{s5}	[47.5 – 52.5] Ω	
R_{s6}		
ϵ_r	[3.89 – 4.30]	
R_{L5}	[1.35 – 1.65] k Ω	
R_{L6}	[1.35 – 1.65] k Ω	
R_{s1}	[1.35 – 1.65] k Ω	
R_{s2}	[1.35 – 1.65] k Ω	
C_{L7}	[0.9 – 1.1] pF	
L (TL length)	6 cm	5% (Uniform Distribution)

In order to demonstrate the accuracy of the proposed approach, the uncertainty quantification for this example is performed using two methods – the conventional unified full-dimensional PC approach [65], [87] and the proposed reduced dimensional PC approach of Section 5.2 where the degree of expansion of both metamodels is set to $d = 3$. In performing the dimension reduction approach of Section 5.2, the number of epistemic samples used in the sensitivity sweeping algorithm is set to $N_e = 20,000$. As a result of the dimension reduction

strategy of Section 5.2, the original $Q = 36$ dimensions of the problem is reduced to $q = 12$ dimensions.

Next, the maximum and minimum bounds of mean plus three times the standard deviation of the transient response at node N_1 is evaluated using the above two methods. These results are compared in Fig. 5.3(a). Furthermore, in order to demonstrate the accuracy of the proposed approach for higher order statistical moments, the bounds of the cumulative density function (CDF) of the transient response at N_1 is evaluated at the time point where the mean is maximum ($t = 1.1$ ns) using the above two methods. These results are compared in Fig. 5.3(b). From Fig. 5.3(a) and Fig. 5.3(b), it can be concluded that the reduced dimensional PC approach shows good agreement with the full dimensional PC approach.

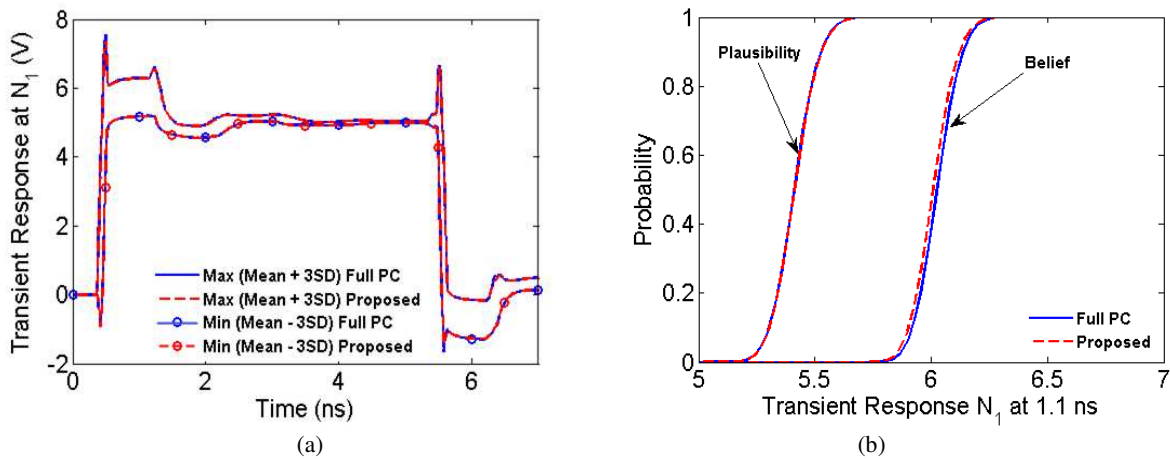


Fig. 5.3: Statistics of the MTL network of Fig. 5.1. (a) Maximum and minimum bounds of the mean plus three times the standard deviation of the transient response at node N_1 . (b) Belief and plausibility functions of the transient response at N_1 ($t = 1.1$ ns).

Finally, for a comparison of the CPU costs incurred, the total number of SPICE simulations required by the full dimensional PC approach is $2(P+1) = 18,278$. For the proposed approach, the total number of SPICE simulations including the simulations required for constructing the metamodel of (10) is $2(R+U) = 218+910 = 1128$. This indicates that the

proposed approach exhibits a speedup of more than 16 times compared to the unified full dimensional PC approach.

5.3.2 Example 2

In this example, the same MTL network of Fig. 5.1 is considered with the responses of interest being the transient voltage at both nodes N_1 and N_2 . The uncertainty in the network is introduced using $Q = 45$ parameters, the characteristics of which are listed in Table 5.2. All the epistemic and aleatory parameters of this example are coupled together.

Table 5.2: Uncertain Parameters of Example 2 (Fig 5.1)

Random Variable	Mean ($a_{i,0}$)	Standard Deviation (s_i)
w	[147.5 – 152.5] μm	[9.5 – 10.5] %
s		
R_{L1}	[1.425 – 1.575] k Ω	
R_{L2}		
R_{L3}		
PL	[0.095 – 0.105] μm	
PW	[9.5 – 10.5] μm	
NL	[0.095 – 0.105] μm	
NW	[9.5 – 10.5] μm	
T	[28.5 – 31.5] μm	
H	[427.5 – 472.5] μm	
C_{L1}	[0.95 – 1.05] pF	
C_{L2}		
C_{L3}		
ϵ_r	[3.895 – 4.305]	

The uncertainty quantification for this example is performed using the same two methods as in Example 1. When performing the dimension reduction approach of Section 5.2, the number of epistemic samples used in the sensitivity sweeping approach is $N_e = 20,000$. As a result of the dimension reduction strategy, the original $Q = 45$ mixed dimensions is reduced to $q = 9$ dimensions. Note that because there are two response quantities of interest, only those dimensions that exhibit marginal global sensitivity for the response variance of both N_1 and N_2 are removed. The maximum and minimum bounds of mean plus three times the standard

deviation of the transient responses at nodes N_1 and N_2 are evaluated using both the above methods and the results are compared in Fig. 5.4(a) and Fig. 5.5(a) respectively. Furthermore, in order to demonstrate the accuracy of the proposed approach for higher order statistical moments, the bounds of the CDF of the transient responses at N_1 and N_2 are evaluated at the time points when the corresponding means are maximum ($t = 1.04$ ns and $t = 1.09$ ns respectively) using the same two methods. These results are compared in Fig. 5.4(b) and 5.5(b) respectively. From Fig. 5.4 and Fig. 5.5, it can be concluded that the reduced dimensional PC approach shows good agreement with the unified full dimensional PC approach.

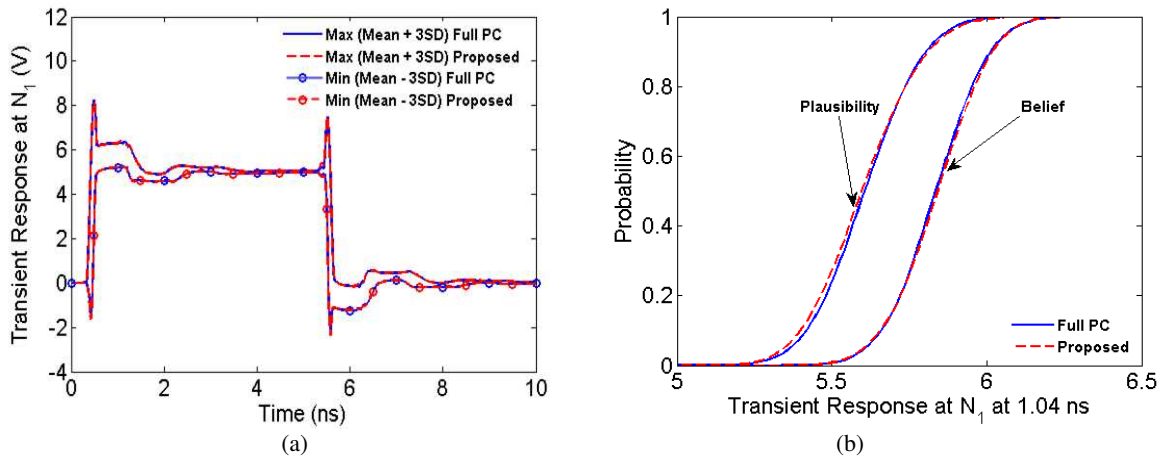


Fig. 5.4: Statistics of the transient response of node N_1 of Fig. 5.1. (a) Maximum and minimum bounds of the mean plus three times the standard deviation of the transient response. (b) Belief and plausibility functions of the transient response ($t = 1.04$ ns).

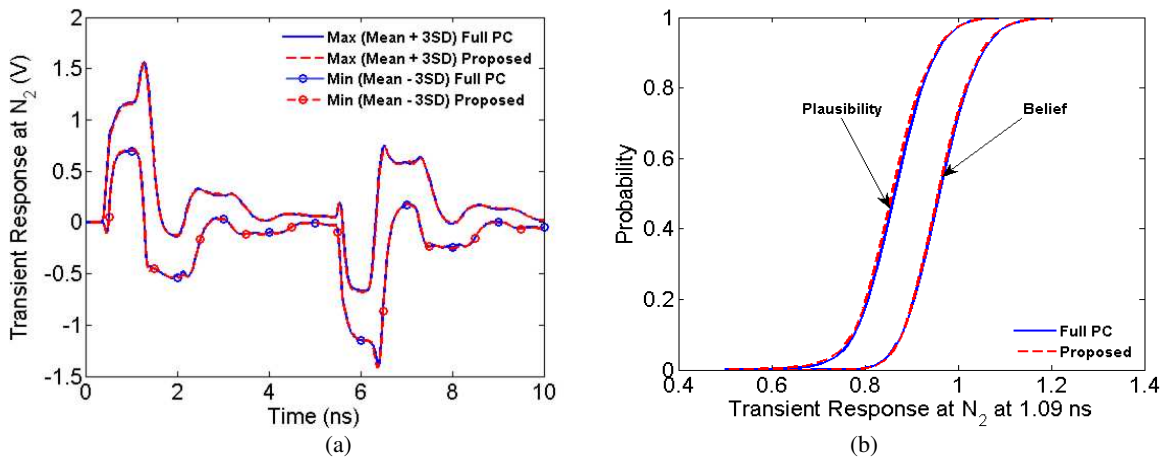


Fig. 5.5: Statistics of the transient response of node N_2 of Fig. 5.1. (a) Maximum and minimum bounds of the mean plus three times the standard deviation of the transient response. (b) Belief and plausibility functions of the transient response ($t = 1.09$ ns).

For a comparison of the CPU costs incurred, the total number of SPICE simulations required by the full dimensional unified PC approach is $2(P+1) = 34,592$. For the proposed approach, the total number of SPICE simulations required including the simulations required to construct the metamodel of (5.9) is $2(R+U) = 272+440 = 712$. This indicates that the proposed approach exhibits a speedup of more than 48 times over the full dimensional PC approach.

5.3.3 Example 3

In this example, the MTL network of Fig. 5.6 terminated by inverters consisting of SPICE level 49 CMOS transistors is considered. The cross-section layout and geometric dimensions of the MTL subnetworks are shown in Fig. 5.7.

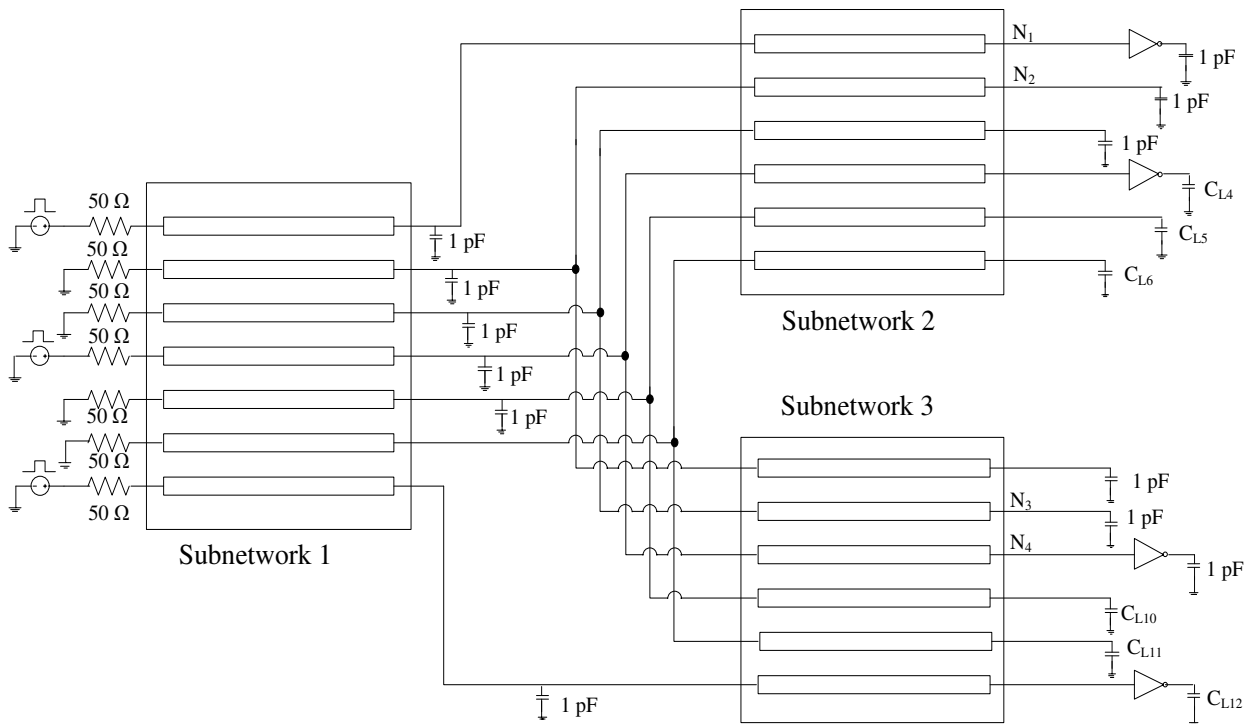


Fig. 5.6: The schematic of the MTL network of Example 3.

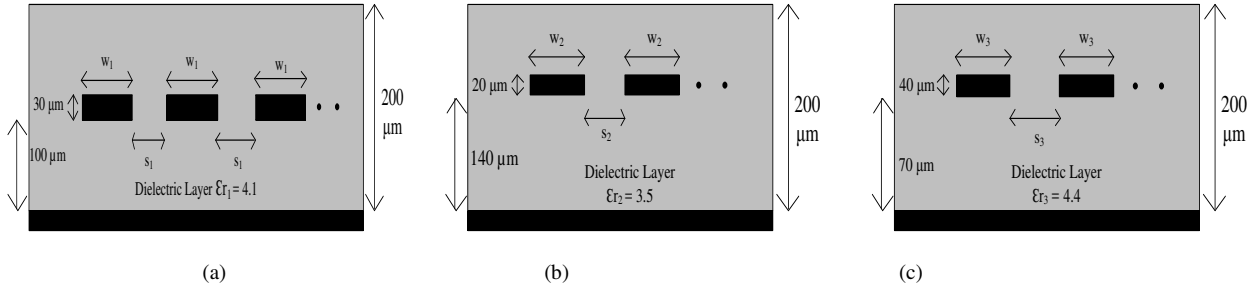


Fig. 5.7: Cross section view of the MTL network of Example 3. (a) Subnetwork 1.
 (b) Subnetwork 2. (c) Subnetwork 3

The lengths of the transmission lines in subnetworks 1, 2 and 3 are set to 5 cm, 10 cm and 15 cm respectively. The voltage sources of Fig. 5.6 exhibit a trapezoidal waveform of rise/fall time $T_r = 0.1$ ns, pulse width $T_w = 5$ ns and amplitude of 5V. The output voltages at the nodes N_1 , N_2 , N_3 and N_4 are considered to be the responses of interest. A total of $Q = 60$ uncertain parameters are considered in this example as listed in Table 5.3. All the epistemic and aleatory parameters of this example are coupled together.

Table 5.3: Uncertain Parameters of Example 2 (Fig 5.1)

Random Variable	Mean ($a_{i,0}$)	Standard Deviation (s_i)
w_1	[142.5 – 157.5] μm	[9.5 – 10.5] %
w_2	[123.5 – 136.5] μm	
w_3	[161.5 – 178.5] μm	
s_1	[95 – 105] μm	
s_2	[142.5 – 157.5] μm	
s_3	[190 – 210] μm	
C_{L4}	[0.95 – 1.05] pF	
C_{L5}		
C_{L6}		
C_{L10}		
C_{L11}		
C_{L12}		
PL_1	[0.095 – 0.105] μm	
PW_1	[9.5 – 10.5] μm	
NL_1	[0.095 – 0.105] μm	
NW_1	[9.5 – 10.5] μm	
PL_3	[0.095 – 0.105] μm	
PW_3	[9.5 – 10.5] μm	
NL_3	[0.095 – 0.105] μm	
NW_3	[9.5 – 10.5] μm	

In order to demonstrate the accuracy of the proposed approach, the uncertainty quantification for this example is performed using the same two methods of Example 1. Even the degree of expansion of both the metamodels are set to $d = 3$. For this example, when performing the dimension reduction approach of Section III, the number of epistemic samples used in the sensitivity sweeping algorithm is $N_e = 10,000$. As a result of the dimension reduction strategy, the original $Q = 60$ mixed dimensions of the example is reduced to $q = 20$ dimensions. As before, only those dimensions that exhibit marginal global sensitivity for the response variance at nodes N_1 - N_4 are removed.

The maximum and minimum bounds of mean plus three times the standard deviation of the transient response at the crosstalk nodes N_2 and N_4 of Fig. 5.6 are evaluated using both the above methods and the results are compared in Fig. 5.8. From Fig. 5.8, it can be concluded that the reduced dimensional PC approach shows good agreement with the full dimensional PC approach.

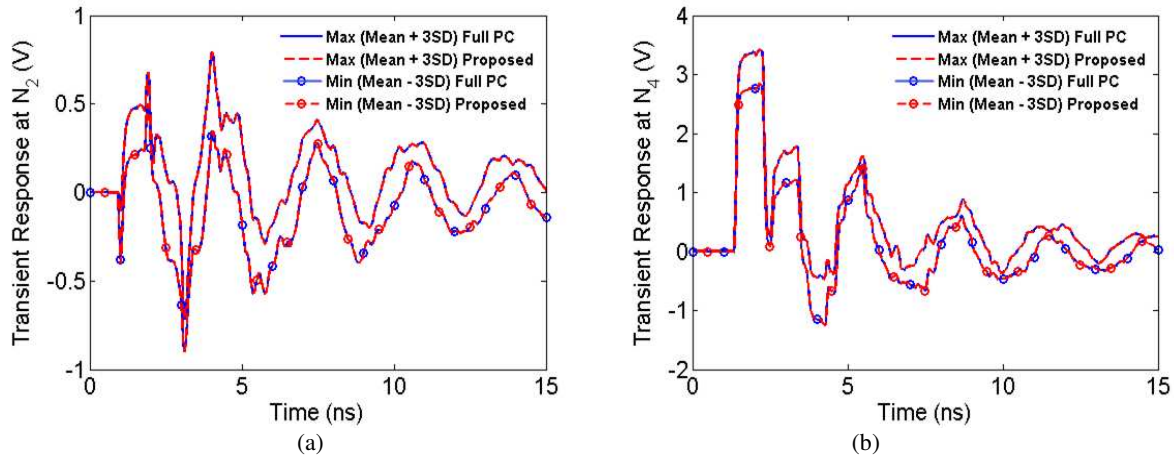


Fig. 5.8: Statistics of transient response of Fig. 5.6. (a) Maximum and minimum bounds of the mean plus three times the standard deviation of the transient response at N_2 . (b) Maximum and minimum bounds of the mean plus three times the standard deviation of the transient response at N_4 .

In this example, the total number of SPICE simulations required by the full dimensional PC approach is $2(P+1) = 79,422$. For the proposed approach, the total number of SPICE simulations required including the simulations required to construct the metamodel of (5.9) is $2(R+U) = 362+3542 = 3904$. This indicates that the proposed approach exhibits a speedup of more than 20 times compared to the unified full dimensional PC approach.

CHAPTER 6: A NOVEL DIMENSION FUSION BASED POLYNOMIAL CHAOS APPROACH FOR MIXED ALEATORY-EPISTEMIC UNCERTAINTY QUANTIFICATION

Traditional uncertainty quantification (UQ) of high-speed interconnects have been performed from the perspective of aleatory uncertainty [4], [12], [41], [57], [68]. As explained in Section 5, aleatory uncertainty refers to the irreducible uncertainty in systems arising from the random variability of model parameters. These parameters are assumed to be well defined using standard probability density functions. Recently, epistemic UQ of engineering problems has garnered significant attention [69], [70]. Epistemic uncertainty refers to that uncertainty arising from the lack of precise knowledge regarding the value of the network parameters. Due to this lack of knowledge, no probability density function can be defined for these parameters. Rather, epistemic dimensions are represented as pure interval valued dimensions [69], [70]. The goal of epistemic UQ is to propagate these intervals through the network model and map their effect on the maximum and minimum bounds of the response.

Recent works have attempted to model epistemic dimensions as uniformly distributed pseudo-random dimensions [64], [65]. In doing so, PC metamodels can be used to propagate mixed epistemic-aleatory uncertainty concurrently. Such mixed metamodels can be probed analytically to find the maximum and minimum bounds of the statistical moments of the network response. However, it is appreciated that mixed problems are characterized by far greater number of dimensions than purely epistemic or aleatory problems. Thus, the poor scalability of PC expansions is even more prominent for mixed problems. This issue is further compounded by the fact that traditional sparse PC methods use statistical measures to decide which PC bases can be removed or retained [41], [57]. However, for mixed problems, the presence of epistemic

uncertainty makes it impossible to define unique statistical moments. Therefore, sparse PC representations are not available for mixed problems.

In this dissertation, a novel dimension fusion approach is proposed to address the above scalability issue of mixed problems. As the name suggests, this approach fuses the epistemic and aleatory dimensions within the same model parameter into a mixed dimension. A key outcome of this fusion process is that the mixed dimension can now encapsulate the epistemic and aleatory effects simultaneously. Thus, they are significantly richer in information content than purely epistemic and aleatory dimensions. Using the mixed dimensions allows the information contained within a large dimensional mixed uncertainty space to be compressed into a low dimensional space without any approximation – in other words, achieve dimension reduction. Unfortunately, this also means that the marginal probability density function describing the mixed dimension may be arbitrary in nature even if the marginal probability density function of the composite epistemic and aleatory dimensions are of standard form. Thus, the Weiner-Askey polynomial bases cannot be used for an optimal PC expansion of the mixed dimensions [44].

In this work, a new methodology is presented that is based on the Cholesky decomposition of a statistical moment matrix of mixed dimensions to elicit a set of optimally orthonormal bases [71]. It is noted that the statistical moments of the mixed dimensions, used to construct the moment matrix, is obtained from the prior knowledge of the statistical moments of the epistemic and aleatory dimensions. Finally, a reduced dimensional PC metamodel is then constructed using these obtained bases. Such a reduced dimensional metamodel is viable over the entire support of the epistemic and aleatory dimensions.

Next, to achieve further reduction in the number of dimensions, the above approach is combined with the sensitivity sweeping approach defined in section 5.2. This approach is used to

find the sensitivity indices for the aleatory and epistemic parts of the mixed dimension. Based on the values of the sensitivity indices, unimportant mixed dimensions can be removed. It is noted that a mixed dimension is considered unimportant and can be removed only if the aleatory parameter and the corresponding epistemic mean and standard deviation can be removed.

6.1 Proposed Dimension Fusion Based PC Approach

6.1.1 Model Parameters with Mixed Uncertainty

Within the context of this dissertation, mixed parameters are defined to be aleatory parameters with embedded epistemic uncertainty in the nominal value and the relative standard deviation of the parameter. Assuming that the nominal value of the general i -th mixed parameter χ_i is bounded within the closed interval $[a_i, b_i]$, then the mixed parameter can be mathematically represented as

$$\chi_i = \left(\frac{b_i + a_i}{2} \right) (1 + \sigma_{mi} \lambda_i) (1 + \sigma_{oi} (1 + \sigma_{si} \gamma_i) \xi_i); \quad 1 \leq i \leq N, \lambda_i \in [-1, 1], \gamma_i \in [-1, 1] \quad (6.1)$$

where the uniformly distributed random dimension λ_i represents the epistemic uncertainty in the mean, the uniformly distributed random dimension γ_i represents the epistemic uncertainty in the standard deviation, the random dimension ξ_i represents the aleatory uncertainty, σ_{mi} , σ_{oi} and σ_{si} represents the relative standard deviation in the epistemic mean, epistemic standard deviation and the aleatory parameter respectively. It is assumed that the total number of mixed parameters are N , in which case the number of epistemic and aleatory dimensions are $2N$ and N each. Let the complete multidimensional epistemic and aleatory uncertainty be described using the vectors $\boldsymbol{\lambda} = [\lambda_1, \lambda_2, \dots, \lambda_N]$, $\boldsymbol{\gamma} = [\gamma_1, \gamma_2, \dots, \gamma_N]$ and $\boldsymbol{\xi} = [\xi_1, \xi_2, \dots, \xi_N]$ with support Ω_e and Ω_a respectively.

For mixed UQ, $\boldsymbol{\lambda}$, $\boldsymbol{\gamma}$ and $\boldsymbol{\xi}$ need to be propagated through the model to the network response. Typically, this can be done by developing a $3N$ -dimensional PC metamodel of the

network response spanning the support of λ , γ and ξ using the Weiner-Askey scheme [64], [65]. However, for high-dimensional problems (i.e., where N is large), such a task may be computationally prohibitive due to the poor scalability of PC expansions with respect to the number of dimensions ($3N$). In fact, the number of discrete model solutions required to construct the PC expansion will scale as $O(3^m N^m)$ where m is the degree of the PC expansion, often in the range $2 < m < 5$ for most problems. To mitigate this bottleneck, a novel dimension fusion approach is described next.

6.1.2 Dimension Fusion

The i -th mixed parameter χ_i can be expressed in terms of a single mixed dimension λ_i as

$$\chi_i = \left(\frac{b_i + a_i}{2} \right) (1 + \sigma_{ii} \eta_i); \quad 1 \leq i \leq N \quad (6.2)$$

Now, it can be assumed that $\sigma_{ii} = \sigma_{0i}$ since the largest value that σ_{ii} can take is σ_{0i} . By comparing (6.2) to (6.1) and using the condition above, it is noted that η_i is a linear combination of the dimensions λ_i , γ_i and ξ_i as

$$\eta_i = \left(\frac{\sigma_{mi}}{\sigma_{0i}} \right) \lambda_i + \xi_i + \sigma_{mi} \lambda_i \xi_i + \sigma_{si} \gamma_i \xi_i + \sigma_{mi} \sigma_{si} \lambda_i \gamma_i \xi_i; \quad 1 \leq i \leq N \quad (6.3)$$

The linear mapping of (6.3) represents the fusion of the aleatory and epistemic dimensions into a mixed dimension. An important feature of the mixed dimension η_i is that it can perfectly encapsulate the entire mixed uncertainty due to λ_i , γ_i and ξ_i . The mixed dimension is always significantly richer in information than the epistemic or aleatory dimensions alone. As an outcome of using information rich dimensions, the mixed uncertainty that originally was contained in the $3N$ -dimensional space spanned by $[\lambda, \gamma, \xi]$ is now compressed into the N -

dimensional space spanned by the vector $\boldsymbol{\eta} = [\eta_1, \eta_2, \dots, \eta_N]$. This compression is free from any numerical inaccuracy. Now, the number of discrete model solutions to construct the PC expansion of the network response will scale only as $O(N^m)$. However, a drawback of the fusion approach is the fact that the probability density function (PDF) of the mixed dimension η_i will no longer conform to the shape of the PDF of either λ_i or γ_i or ξ_i – it will be arbitrary in nature. Thus, a new methodology to construct orthonormal bases for dimensions with arbitrary shaped PDFs needs to be developed.

6.1.3 Orthonormal Basis Construction for Mixed Dimensions

In the work of [71], an innovative method to obtain the orthonormal polynomials, nodes and weights for any arbitrary distribution is described. It is based on the Cholesky decomposition of the Hermitian positive-definite matrix M comprising of $2m+1$ statistical moments of the mixed dimension η_i as

$$M = \begin{bmatrix} \beta_0 & \cdots & \beta_m \\ \vdots & \ddots & \vdots \\ \beta_m & \cdots & \beta_{2m} \end{bmatrix} = \mathbf{R}^T \mathbf{R} \quad (6.4)$$

where β_k is the k -th statistical moment of the mixed dimension η_i represented as a multinomial expansion

$$\begin{aligned} \beta_k &= \int (\eta_i)^k \rho(\eta_i) d\eta_i \\ &= \int \left(\left(\frac{\sigma_{mi}}{\sigma_{0i}} \right) \lambda_i + \xi_i + \sigma_{mi} \lambda_i \xi_i + \sigma_{si} \gamma_i \xi_i + \sigma_{mi} \sigma_{si} \lambda_i \gamma_i \xi_i \right)^k \rho(\lambda_i) \rho(\xi_i) \rho(\gamma_i) d\lambda_i d\xi_i d\gamma_i \end{aligned} \quad (6.5)$$

and \mathbf{R} is the upper triangular matrix. The function $\rho(\cdot)$ is the marginal probability density function. The term in (\cdot) in (6.5) can be expanded using the multinomial theorem. Since the mapping between the mixed, aleatory and epistemic dimensions is linearly predefined in (6.3),

the k -th statistical moment of (6.5) can be explicitly expressed as a linear combination of the first $2k+1$ statistical moments of λ_i , γ_i and ξ_i which are known *a priori* as

$$\begin{aligned} \int \xi_i^k \rho(\xi_i) d\xi_i &= 0; & k \text{ odd} \\ &= \frac{k!}{2^{k/2} \left(\frac{k}{2}\right)!}; & k \text{ even} \end{aligned} \quad (6.6)$$

and

$$\begin{aligned} \int \lambda_i^k \rho(\lambda_i) d\lambda_i &= \int \gamma_i^k \rho(\gamma_i) = 0; & k \text{ odd} \\ &= \frac{1}{(k+1)}; & k \text{ even} \end{aligned} \quad (6.7)$$

Now the three term recurrence relation for the j -th degree polynomial basis ψ_j is represented as

$$\lambda_i \psi_{j-1}(\lambda_i) = c_{j-1} \psi_{j-2}(\lambda_i) + d_j \psi_{j-1}(\lambda_i) + c_j \psi_j(\lambda_i) \quad (6.8)$$

and

$$c_j = \frac{r_{j+1,j+1}}{r_{j,j}}; \quad d_j = \frac{r_{j,j+1}}{r_{j,j}} - \frac{r_{j-1,j}}{r_{j-1,j-1}} \quad (6.9)$$

where $r_{i,j}$ is the element belonging to the i -th row and j -th column of the upper triangular matrix **R**. Once the polynomial coefficients of the arbitrary distribution are obtained, the corresponding nodes and weights can be computed using the Golub-Welsh algorithm [61]. The univariate orthonormal bases of (6.6) now can be used to construct a PC metamodel of the network response, say $x(t, \boldsymbol{\lambda}, \boldsymbol{\gamma}, \boldsymbol{\xi})$, as

$$x(t, \boldsymbol{\lambda}, \boldsymbol{\gamma}, \boldsymbol{\xi}) = \sum_{k=0}^P p_k(t) \psi_k(\boldsymbol{\eta}); \quad P+1 = \frac{(N+m)!}{N!m!} \quad (6.10)$$

where p_k is the k -th unknown coefficient and $\psi_k(\boldsymbol{\eta})$ is the corresponding multidimensional basis formed from the product of the unidimensional bases of (6.6). These coefficients can now be obtained using a nonintrusive linear regression based approach [57].

6.2 Dimension Reduction Using Sensitivity Sweeping Approach for Mixed Parameters

In section 6.1, the dimension fusion approach to propagate $3N$ parameters as N mixed parameters was explained, thereby reducing the computational cost for developing the PC expansion of the network response by a factor of 3^m . In this section, an approach to achieve further reduction in computation cost by identifying and excluding unimportant mixed dimensions is explained. This is similar to the approach in section 5.2 and is explained again in this chapter for the sake of clarity. First, an approximate model of the response is derived from a high dimensional model representation (HDMR) of the network [54] using only the zeroth and first order interaction terms.

$$x(t, \boldsymbol{\eta}) \approx x_0(t) + \sum_{i=1}^N x_i(t, \eta_i) \quad (6.11)$$

where x_0 is the value of $x(t, \boldsymbol{\eta})$ in absence of any uncertainty (zero-th order interaction term), $x_i(t, \eta_i)$ represents the contribution of each η_i on $x(t, \boldsymbol{\eta})$ acting alone (first order interaction terms). The zero-th order and first order interaction terms of (6.11) are expressed using cut-HDMR [54] as

$$\begin{aligned} x_0(t) &= x(t, \boldsymbol{\eta}^{(0)}) \\ x_i(t, \eta_i) &= x(t, \boldsymbol{\eta}) \Big|_{\boldsymbol{\eta}^{(0)} \setminus \eta_i} - x_0(t); \quad 1 \leq i \leq N \end{aligned} \quad (6.12)$$

where $\boldsymbol{\eta}^{(0)} = \mathbf{0}$ and the notation $\boldsymbol{\eta}^{(0)} \setminus \eta_i$ represents the vector where all components of $\boldsymbol{\eta}$ except η_i are set to 0. The LHS of 6.12 is evaluated using 1D PC expansions as explained in chapter 4

using equation (4.4) and the 1D coefficients are evaluated using equation (4.5) and (4.6). As explained in chapter 4, $(m+1)N+1$ simulations are required to evaluate this approximate model.

This model is now used to estimate the sensitivity of the response variance with respect to the epistemic and aleatory parts of each mixed dimension. While doing so, the sensitivities need to be swept over the entire epistemic space. This will provide a clear picture of how the sensitivity indices vary over the entire domain of the multidimensional epistemic space.

6.2.1 Sensitivity Sweeping for Aleatory Part of the Mixed Parameters

The main challenge of estimating the sensitivity of the response variance with respect to the aleatory part of the mixed dimensions of $\boldsymbol{\eta}$ is that the response variance varies with the values of the epistemic parts of the mixed dimensions. As a result, the extracted sensitivity information for any aleatory parts of the mixed dimension will not be unique and will vary across the entire epistemic space.

To address this problem, in this work, the sensitivity information corresponding to the aleatory part of each mixed dimension will be swept over the entire epistemic space in order to fully understand and characterize its global properties. For this purpose, a nested sampling algorithm is proposed where in the outer loop N_e uniformly distributed samples will be taken from the epistemic space without replacement. Let any k -th general sample be described as $[\boldsymbol{\lambda}^{(k)}, \boldsymbol{\gamma}^{(k)}] = [\lambda_1^{(k)}, \lambda_2^{(k)}, \dots, \lambda_N^{(k)}, \gamma_1^{(k)}, \gamma_2^{(k)}, \dots, \gamma_N^{(k)}]$ where $1 \leq k \leq N_e$. Replacing each sample $[\boldsymbol{\lambda}^{(k)}, \boldsymbol{\gamma}^{(k)}]$ in the mapping of (6.3) will render $\eta^{(k)}$ purely as a function of the aleatory parameter $\xi^{(k)}$. Now, in the inner loop, N_a aleatory samples are taken without replacement. The 1D PC expansion of (4.10) is evaluated for all the N_a samples as

$$x^{(l)}(t, \lambda = \lambda^{(k)}, \gamma = \gamma^{(k)}, \xi) \approx \hat{x}_0(t) + \sum_{i=1}^N \sum_{r=1}^d \hat{x}_i^{(r)}(t) \phi_r(\xi_i); \quad 1 \leq l \leq N_a \quad (6.13)$$

The total variance of all N_a samples is computed using (2.2) as

$$V_u(t, \lambda^{(k)}, \gamma^{(k)}, \xi) = \frac{1}{N_a} \sum_{i=1}^{N_a} \left(x^{(i)}(t, \lambda^{(k)}, \gamma^{(k)}, \xi^{(i)}) - \mu_X^{(k)} \right)^2; \quad (6.14)$$

$$\mu_X^{(k)} = \frac{1}{N_a} \sum_{i=1}^{N_a} \left(x^{(i)}(t, \lambda^{(k)}, \gamma^{(k)}, \xi^{(i)}) \right)$$

Repeating this process for each of the N_e epistemic samples results in an ensemble of variances called unconditional variances. From the knowledge of these N_e instances of the unconditional variances, for each time point the unconditional maximum and minimum bounds of the variance will be determined as

$$V_{\min}(t) = \min(V_u(\lambda^{(k)}, \gamma^{(k)}, \xi, t), 1 \leq k \leq N_e); \quad (6.15)$$

$$V_{\max}(t) = \max(V_u(\lambda^{(k)}, \gamma^{(k)}, \xi, t), 1 \leq k \leq N_e)$$

Next, the same nested sampling approach as above is reused to reevaluate the variance bounds of (6.15), this time subject to the constraint $\xi_j^{(k)} = 0$ for $1 \leq j \leq N$ in all the sample points $\xi^{(k)}$. The new variance bounds evaluated will be the conditional maximum and minimum bounds. Mathematically, the conditional bounds can be described as

$$V_{\min,a,j}(t) = \min(V_u(\lambda^{(k)}, \gamma^{(k)}, \xi, t), \xi_j^{(k)} = 0, 1 \leq k \leq N_e, 1 \leq j \leq N); \quad (6.16)$$

$$V_{\max,a,j}(t) = \max(V_u(\lambda^{(k)}, \gamma^{(k)}, \xi, t), \xi_j^{(k)} = 0, 1 \leq k \leq N_e, 1 \leq j \leq N);$$

From the knowledge of the above unconditional and conditional bounds, the raw change in the bounds will be measured as

$$E_{a,j}(t) = \frac{(V_{\max}(t) - V_{\max,a,j}(t)) - (V_{\min}(t) - V_{\min,a,j}(t))}{2}; \quad 1 \leq j \leq N \quad (6.17)$$

It is important to note that the above change is time dependent. As a result, the index of (6.17) will be reduced to a scalar quantity by averaging over the entire time window of simulation as

$$\hat{E}_{a,j} = \frac{1}{2T_{\max}} \left(\int_0^{T_{\max}} (V_{\max}(t) - V_{\max,a,j}(t)) dt - \int_0^{T_{\max}} (V_{\min}(t) - V_{\min,a,j}(t)) dt \right); \quad 1 \leq j \leq N \quad (6.18)$$

Any numerical integration method can be used to evaluate the integral in (6.18). The integral of (6.18) measures the change or sensitivity in the variance bounds for every aleatory parameter ξ_j , $1 \leq j \leq N$ by switching off ξ_j at every point in the epistemic space. Thus, the integral of (6.18) will hereafter be referred to as the sensitivity index of ξ_j . If the sensitivity index of (6.18) is constantly less than a prescribed tolerance of δ across all the points in the epistemic space, then the impact of ξ_j will be considered to be globally marginal.

6.2.2 Sensitivity Sweeping for Epistemic Part of Mixed Parameters

The sensitivity sweeping algorithm mentioned in section 6.2.1 is now modified for the case of the epistemic parts of the mixed dimensions of $\boldsymbol{\eta}$. The unconditional response variances $V_u(t, \boldsymbol{\lambda}^{(k)}, \boldsymbol{\gamma}^{(k)}, \boldsymbol{\xi})$ have already been evaluated at all N_e sample points. These variance measures are referred to as unconditional variances. Now, to compute the variance bounds for the epistemic parts of the mixed parameters, the same nested sampling approach as listed in section 6.2.1 is adopted where in the outer loop, the same N_e uniformly distributed samples are taken from the epistemic space without replacement. The k -th sample is described as $[\boldsymbol{\lambda}^{(k)}, \boldsymbol{\gamma}^{(k)}] = [\lambda_1^{(k)}, \lambda_2^{(k)}, \dots, \lambda_N^{(k)}, \gamma_1^{(k)}, \gamma_2^{(k)}, \dots, \gamma_{N'}^{(k)}]$ where $1 \leq k \leq N_e$. The constraint introduced now is $[\lambda_j^{(k)}, \gamma_j^{(k)}] = 0$ for $1 \leq j \leq 2N$ in all the sample points $[\boldsymbol{\lambda}^{(k)}, \boldsymbol{\gamma}^{(k)}]$. The same N_a aleatory samples as in section 6.2.1 are considered in the inner loop and the new variances are computed using the

1D PC expansions as shown in (6.13) and (6.14). The conditional variance bounds are now evaluated as

$$\begin{aligned} V_{\min,j}(t) &= \min(V_u(\boldsymbol{\lambda}^{(k)}, \boldsymbol{\gamma}^{(k)}, \boldsymbol{\xi}, t), \lambda_j^{(k)} = 0, \gamma_j^{(k)} = 0, 1 \leq k \leq N_e, 1 \leq j \leq 2N); \\ V_{\max,j}(t) &= \max(V_u(\boldsymbol{\lambda}^{(k)}, \boldsymbol{\gamma}^{(k)}, \boldsymbol{\xi}, t), \lambda_j^{(k)} = 0, \gamma_j^{(k)} = 0, 1 \leq k \leq N_e, 1 \leq j \leq 2N); \end{aligned} \quad (6.19)$$

The sensitivity indices for the epistemic parts of the mixed parameters are evaluated using

$$\hat{E}_{e,j} = \frac{1}{2T_{\max}} \left(\int_0^{T_{\max}} (V_{\max}(t) - V_{\max,e,j}(t)) dt - \int_0^{T_{\max}} (V_{\min}(t) - V_{\min,e,j}(t)) dt \right); \quad 1 \leq j \leq 2N \quad (6.20)$$

It is noted that a mixed parameter η_j can be removed from the parametric space only if each of its aleatory and epistemic parts fall below the prescribed tolerance of δ .

It is assumed that due to the aleatory and epistemic dimension reduction, the original vector $\boldsymbol{\eta} \in \mathfrak{R}^N$ will be reduced to a new vector, $\boldsymbol{\eta}_{red} \in \mathfrak{R}^n$ where $n < N$. In this sensitivity sweeping algorithm, N_e instances of the variances have to be computed to find out the variance bounds of (6.20). This process has to be then repeated for N_e sample points and $3N$ dimensions. In other words, a total of $3NN_e^2$ variances have to be computed. The 1D PC metamodel of (6.13) is used to compute the variances and the computations can be performed with negligible CPU cost.

6.2.3 Constructing the Reduced Dimensional PC Expansion

Once the N -dimensional network has been reduced to an n dimensional problem ($n < N$) using the dimension reduction process described in Section 6.2, the reduced dimensional PC metamodel of the network response can now be formulated as

$$x(t, \boldsymbol{\eta}) \approx \sum_{k=0}^U \tilde{x}_k(t) \psi_k(\boldsymbol{\eta}_{red}) \quad (6.21)$$

where $\psi_k(\boldsymbol{\eta}_{red})$ is the k^{th} reduced dimensional basis, $\tilde{x}_k(t)$ is the corresponding coefficient, and the number of terms in the expansion of (6.21) is truncated to $U+1 = (n+m)!/(n!m!)$. The coefficients of (6.21) will be evaluated using the linear regression scheme suggested in Chapter 3.

6.2.4 Evaluating max/min bounds of statistical moments

For mixed problems, it is not possible to define unique statistical moments of a model response because they are functions of the epistemic dimensions. In other words, considering any model subject to mixed uncertainty, the arbitrary i -th statistical moment of the network response can be expressed as a parametric function of the epistemic dimensions using MC sampling as

$$S_i(t, \boldsymbol{\lambda}, \boldsymbol{\gamma}) = \int_{\Omega_a} x^i(t, \boldsymbol{\lambda}, \boldsymbol{\gamma}, \boldsymbol{\xi}) \eta(\boldsymbol{\xi}) d\boldsymbol{\xi} \approx \frac{1}{N_a} \sum_{l=1}^{N_a} x^i(t, \boldsymbol{\lambda}, \boldsymbol{\gamma}, \boldsymbol{\xi}^{(l)}) \quad (6.22)$$

The maximum and minimum bounds of the family of statistical moments are computed via a second order probability approach, also referred to as the nested MC sampling approach [70]. This approach involves drawing a large number of MC samples of the epistemic dimensions $[\boldsymbol{\lambda}, \boldsymbol{\gamma}] = [\boldsymbol{\lambda}^{(n)}, \boldsymbol{\gamma}^{(n)}]; 1 \leq n \leq N_e$ in the outer loop. For each sample, in the inner loop, the discrete statistical moment $S_i(t, [\boldsymbol{\lambda}, \boldsymbol{\gamma}] = [\boldsymbol{\lambda}^{(n)}, \boldsymbol{\gamma}^{(n)}])$ can be evaluated, again using a set of MC samples as shown in (6.9) provided the network responses at the sample points $[\boldsymbol{\lambda}^{(n)}, \boldsymbol{\gamma}^{(n)}, \boldsymbol{\xi}^{(l)}]$ is known. In this way, an ensemble of realizations of the statistical moment $S_i(t, [\boldsymbol{\lambda}, \boldsymbol{\gamma}] = [\boldsymbol{\lambda}^{(n)}, \boldsymbol{\gamma}^{(n)}])$ is obtained. Provided sufficient MC samples are taken, the maximum and minimum bounds of this ensemble represent the maximum and minimum bounds of the statistical moments [70].

In this work, the dimension fusion strategy is used to model the impact of both aleatory and epistemic uncertainty on CNT interconnects. The solution of the CNT model at each $N_a N_e$ MC sample is found analytically using an efficient two step method. At the first step, the sample

point $\boldsymbol{\eta}^{(n)} = [\boldsymbol{\lambda}^{(n)} \boldsymbol{\gamma}^{(n)} \boldsymbol{\omega}^{(l)}]$ is obtained using the linear mapping of (6.3). Thereafter, the model solution at $\boldsymbol{\eta} = \boldsymbol{\eta}^{(n)}$ is obtained analytically from the dimension fused PC expansion of (6.8). It is noted that the only CNT model solutions required are those needed to construct the PC metamodel of (6.8) and not $N_a N_e$. Importantly, by using the novel dimension fusion strategy, the number of CNT model solutions required scales as $O(N^m)$ as opposed to the $O(3^m N^m)$ scalability of full-blown PC.

6.3 Numerical Examples

In this section, three examples are presented to demonstrate the accuracy and efficiency of the proposed mixed dimension reduction based PC approach over the unified full-dimensional PC approach. In all of these examples, the relative sensitivity thresholds for judging if an epistemic or aleatory dimension is unimportant are set to $\delta = 0.01$ respectively.

6.3.1 Example 1

In this example, the 3-conductor multiwalled CNT network of Fig. 6.1 is considered. The network is represented using the lumped model proposed in [72] where the tunneling conductivity is taken into account. A total of $N = 20$ mixed dimensions are used in this example, the characteristics for which are listed in Table 6.1. All the dimensions have epistemic uncertainty embedded in their mean values. Conductors 1 and 3 are excited by a voltage source with a saturated ramp waveform of rise/fall time $T_r = 0.1$ ps and an amplitude of 1 V. Two approaches are used to quantify uncertainty for the network at the outputs of conductors 1 and 2 of Fig. 6.1 – the proposed dimension fusion approach combined with dimension reduction described in Section 6.1 and 6.2 and the full-blown PC expansion of the $2N$ dimensions. Both metamodels are utilized within the nested MC framework to evaluate the maximum and

minimum bounds of the response statistical moments. A maximum degree of $m = 3$ is used for the PC expansions of both the methods and is found to be sufficient to handle the variation in the mixed parameter.

In performing the dimension reduction approach of Section 6.2, the number of epistemic samples used in the outer loop of the sensitivity sweeping algorithm is set to $N_e = 5,000$ and the number of aleatory samples used in the inner loop is $N_a = 10,000$. As a result of the dimension reduction strategy of Section 5.2, the original $N = 40$ dimensions of the problem is reduced to $n = 5$ mixed dimensions.

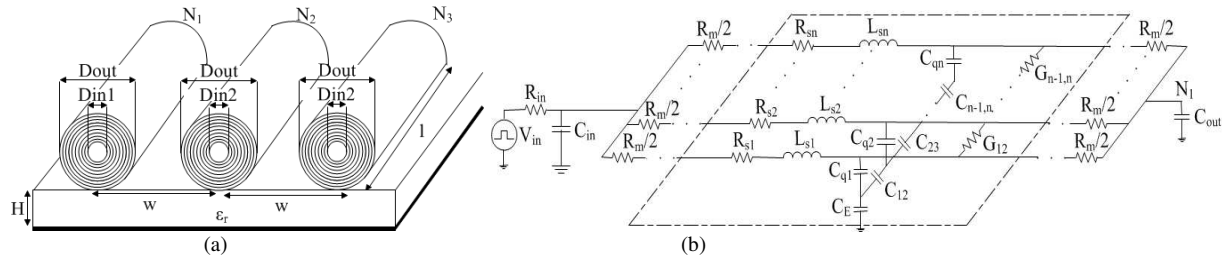


Fig. 6.1: Schematic of the MWCNT interconnect network. (a) Profile view. (b) Equivalent RLGC lumped circuit for a single conductor of the network [72].

Table 6.1: Uncertainty Characteristics of CNT Network of Fig. 6.1

Random Variable	Mean	Aleatory Uncertainty (Normal Distribution)
$D_{in}[1:3]$ (Inner diameter of CNT)	2.17 – 2.39 nm	10%
d (Inter-shell distance)	0.32 – 0.36 nm	
$\sigma[1:3]$ (Tunneling conductivity)	9.5 – 10.5	
H (Height of dielectric)	47.5 – 52.5 nm	
ϵ_r (dielectric constant)	1.9 – 2.1	
$R_m[1:3]$ (Contact Resistance)	0.95 – 1.05 k Ω	
$C_{in}[1:3]$	133 – 147 pf	
$C_{out}[1:3]$	46.6 – 51.5 pf	
w (Spacing between conductors)	20.9 – 23.1 nm	
l (Conductor length)	47.5 – 52.5 μm	

For the full-blown PC approach, 24,682 SPICE simulations of the CNT model are required to construct the PC metamodel whereas for the proposed dimension fusion approach, only 133 simulations are required (including the simulations required for dimension reduction). This indicates that the proposed dimension fusion approach exhibits a speedup of 92 times over

the full-blown PC approach. To establish the accuracy of the dimension fusion approach, the maximum and minimum bounds of the statistics defined to be the mean plus thrice the standard deviation of the response at nodes N_1 and N_2 are compared for both approaches and the results are shown in Figs. 6.2(a) and 6.3(a). Both methods use a total of 10,000 x 20,000 MC samples where the samples for both approaches are different. Next, to validate the accuracy of the proposed approach for higher order statistics, the family of cumulative density functions (CDFs) is computed for the transient response at N_1 and N_2 at the time point when the max mean plot assumes 90% of the maximum value ($t = 111.2$ ps and 35.2 ps). The maximum and minimum bounds (i.e., the plausibility and belief) are evaluated using the two approaches and the results are shown in Figs. 6.2(b) and 6.3(b). It is evident that the proposed approach shows very good agreement with the full-blown PC approach while being computationally much more efficient.

6.3.2 Example 2

In this example, the same network of Fig. 6.1 is considered. The same $N = 20$ mixed dimensions are considered the characteristics for which are listed in Table 6.2. In this example, all the dimensions have epistemic uncertainty embedded in their mean and standard deviation. Two approaches are used to quantify uncertainty for the network at the outputs of conductors 1 and 2 of Fig. 6.1 – the proposed dimension fusion approach combined with dimension reduction described in Section 6.1 and 6.2 and the full-blown PC expansion of the $3N$ dimensions.

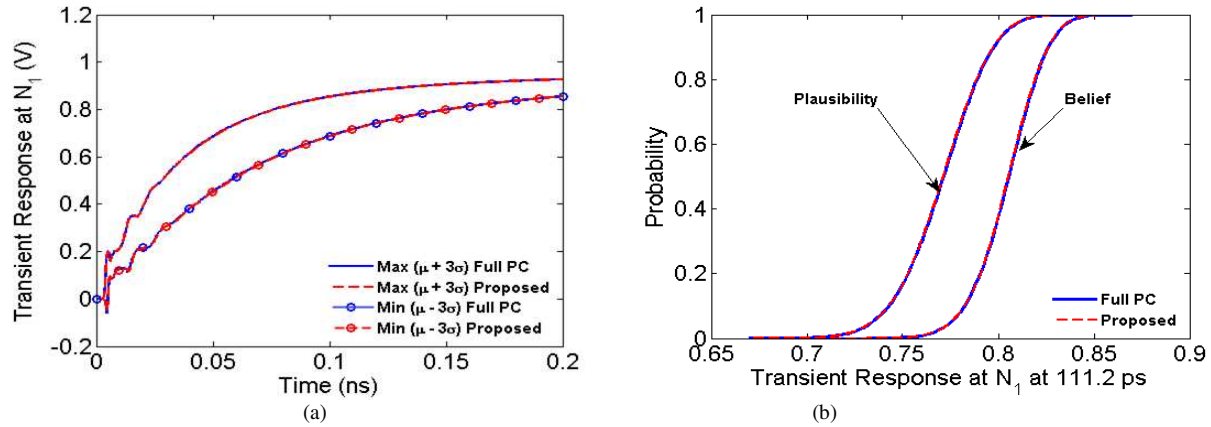


Fig. 6.2: Statistics of the CNT network of Fig 6.1. (a) Maximum/minimum bounds of mean ± 3 SD for the transient response at node N_1 . (b) Maximum and minimum bounds of the CDF for the transient response at node N_1 at time point where max mean is 90% of its max value.

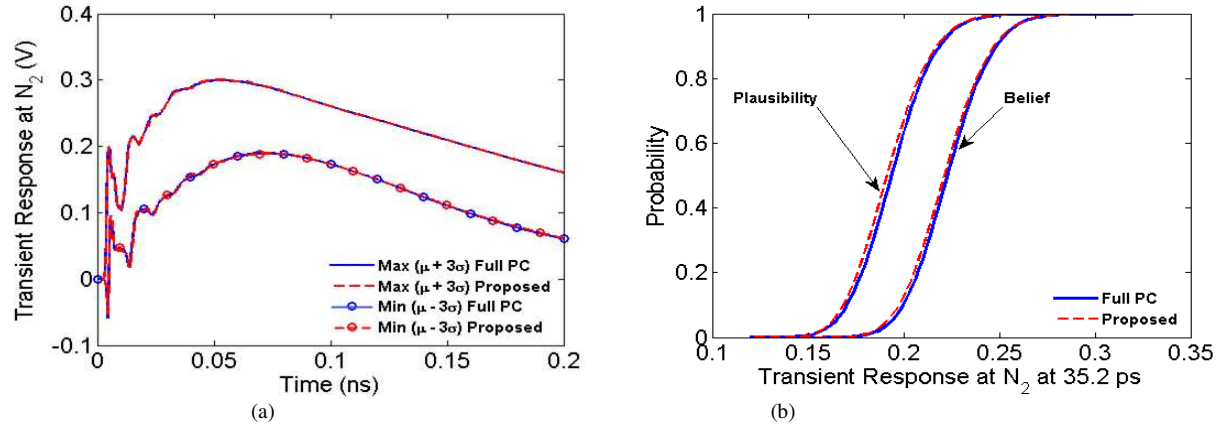


Fig. 6.3: Statistics of the CNT network of Fig 6.1. (a) Maximum/minimum bounds of mean ± 3 SD for the transient response at node N_2 . (b) Maximum and minimum bounds of the CDF for the transient response at node N_2 at time point where max mean is 90% of its max value.

Table 6.2: Uncertainty Characteristics of CNT Network of Fig. 6.1

Random Variable	Mean	SD
$D_{in}[1:3]$ (Inner diameter of CNT)	2.17 – 2.39 nm	[9.5 – 11.5]%
d (Inter-shell distance)	0.32 – 0.36 nm	
$\sigma[1:3]$ (Tunneling conductivity)	9.5 – 10.5	
H (Height of dielectric)	47.5 – 52.5 nm	
ϵ_r (dielectric constant)	1.9 – 2.1	
$R_m[1:3]$ (Contact Resistance)	0.95 – 1.05 k Ω	
$C_{in}[1:3]$	133 – 147 pf	
$C_{out}[1:3]$	46.6 – 51.5 pf	
w (Spacing between conductors)	20.9 – 23.1 nm	
l (Conductor length)	47.5 – 52.5 μm	

As a result of the dimension reduction strategy of Section 5.2, the original $N = 60$ dimensions of the problem is reduced to $n = 7$ mixed dimensions. For the full-blown PC approach, 79,422 SPICE simulations of the CNT model are required to construct the PC metamodel whereas for the proposed dimension fusion approach, only 321 simulations are required (including the simulations required for dimension reduction). This indicates that the proposed dimension fusion approach exhibits a speedup of 247 times over the full-blown PC approach. To establish the accuracy of the dimension fusion approach, the maximum and minimum bounds of the statistics defined to be the mean plus thrice the standard deviation of the response at nodes N_1 and N_2 are compared for both approaches and the results are shown in Fig. 6.4(a) and Fig. 6.5(a).

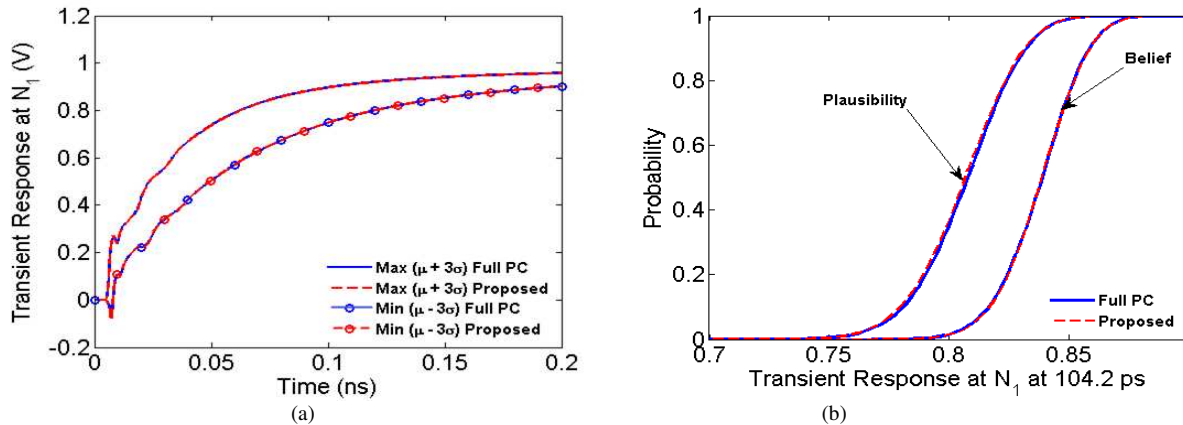


Fig. 6.4: Statistics of the CNT network of Fig 6.1. (a) Maximum/minimum bounds of mean ± 3 SD for the transient response at node N_1 . (b) Maximum and minimum bounds of the CDF for the transient response at node N_1 at time point where max mean is 90% of its max value.

Both methods use a total of 10,000 x 20,000 MC samples where the samples for both approaches are different. Next, to validate the accuracy of the proposed approach for higher order statistics, the family of cumulative density functions (CDFs) is computed for the transient response at N_1 and N_2 at the time point when the max mean plot assumes 90% of the maximum value ($t = 111.2$ ps and 35.2 ps). The maximum and minimum bounds (i.e., the plausibility and belief) are evaluated using the two approaches and the results are shown in Figs. 6.4(b) and

6.5(b). It is evident that the proposed approach shows very good agreement with the full-blown PC approach while being computationally much more efficient.

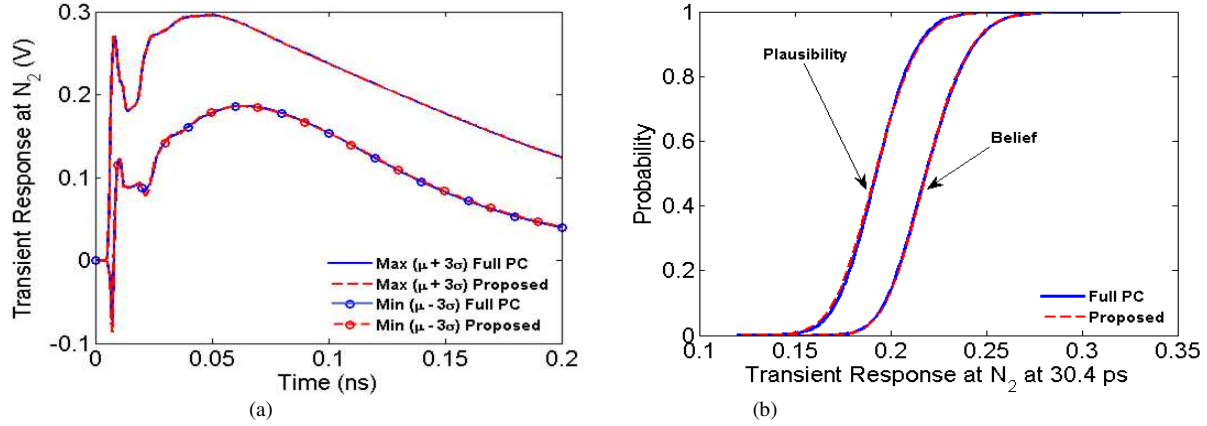


Fig. 6.5: Statistics of the CNT network of Fig 6.1. (a) Maximum/minimum bounds of mean ± 3 SD for the transient response at node N_2 . (b) Maximum and minimum bounds of the CDF for the transient response at node N_2 at time point where max mean is 90% of its max value.

6.3.2 Example 3

In this example, the 5 conductor network of Fig. 6.6 is considered. The equivalent RLGC lumped circuit model for this example is the same as that in Fig. 6.1(b).

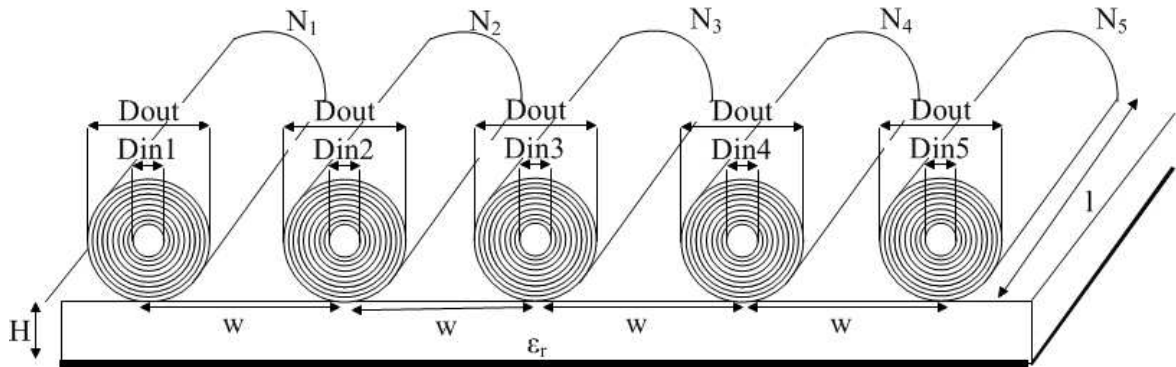


Fig. 6.6: Profile view of the schematic of the MWCNT interconnect network.

For this example also $N=20$ mixed dimensions are considered the characteristics for which are listed in Table 6.3. All the dimensions have epistemic uncertainty embedded in their mean and standard deviation. Conductors 1 and 4 are excited by a voltage source with a saturated ramp waveform of rise/fall time $T_r = 0.1$ ps and an amplitude of 1 V.

Table 6.3: Uncertainty Characteristics of CNT Network of Fig. 6.6

Random Variable	Mean	SD
$D_m[1:5]$ (Inner diameter of CNT)	2.17 – 2.39 nm	[9.5 – 11.5]%
d (Inter-shell distance)	0.32 – 0.36 nm	
$\sigma[1:5]$ (Tunneling conductivity)	9.5 – 10.5	
H (Height of dielectric)	47.5 – 52.5 nm	
ϵ_r (dielectric constant)	1.9 – 2.1	
$R_m[1:5]$ (Contact Resistance)	0.95 – 1.05 k Ω	
w (Spacing between conductors)	20.9 – 23.1 nm	[4.75 – 5.75]%
l (Conductor length)	47.5 – 52.5 μm	

Two approaches are used to quantify uncertainty for the network at the outputs of conductors 3 and 4 of Fig. 6.6 – the proposed dimension fusion approach combined with dimension reduction described in Section 6.1 and 6.2 and the full-blown PC expansion of the 2N dimensions. Both metamodels are utilized within the nested MC framework to evaluate the maximum and minimum bounds of the response statistical moments. A maximum degree of $m = 3$ is used for the PC expansions of both the methods and is found to be sufficient to handle the variation in the mixed parameter. In performing the dimension reduction approach of Section 6.2, the number of epistemic samples used in the outer loop of the sensitivity sweeping algorithm is set to $N_e = 5,000$ and the number of aleatory samples used in the inner loop is $N_a = 10,000$. As a result of the dimension reduction strategy of Section 5.2, the original $N = 60$ dimensions of the problem is reduced to $n = 6$ mixed dimensions. For the full-blown PC approach, 79,422 SPICE simulations of the CNT model are required to construct the PC metamodel whereas for the proposed dimension fusion approach, only 249 simulations are required (including the simulations required for dimension reduction). This indicates that the proposed dimension fusion approach exhibits a speedup of 319 times over the full-blown PC approach. To establish the accuracy of the dimension fusion approach, the maximum and minimum bounds of the statistics defined to be the mean plus thrice the standard deviation of the response at nodes N_3 and N_4 are compared for both approaches and the results are shown in Figs. 6.7(a) and 6.8(a). Both methods

use a total of 10,000 x 20,000 MC samples. Next, to validate the accuracy of the proposed approach for higher order statistics, the family of cumulative density functions (CDFs) is computed for the transient response at N_3 and N_4 at the time point when the mean plot assumes 90% of the maximum value ($t = 32.4$ ps and 125 ps). The maximum and minimum bounds (i.e., the plausibility and belief) are evaluated using the two approaches and the results are shown in Figs. 6.7(b) and 6.8(b). It is evident that the proposed approach shows very good agreement with the full-blown PC approach while being computationally much more efficient.

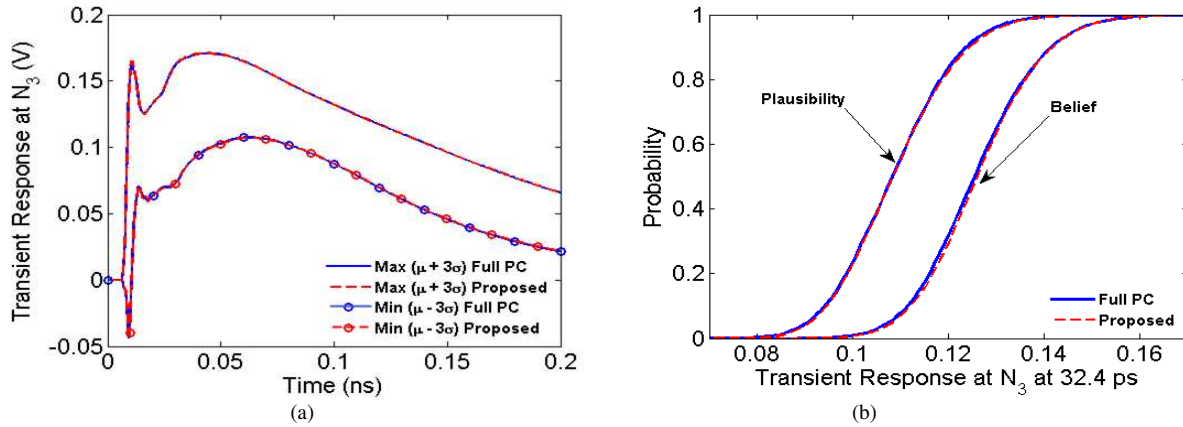


Fig. 6.7: Statistics of the CNT network of Fig 6.6. (a) Maximum/minimum bounds of mean \pm 3 SD for the transient response at node N_3 . (b) Maximum and minimum bounds of the CDF for the transient response at node N_3 at time point where mean is 90% of its max value.

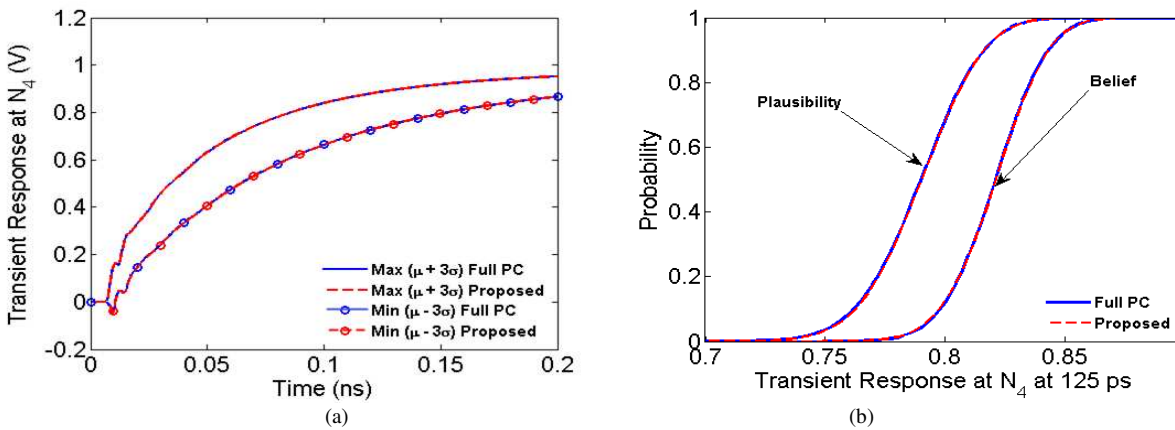


Fig. 6.8: Statistics of the CNT network of Fig 6.6. (a) Maximum/minimum bounds of mean \pm 3 SD for the transient response at node N_3 . (b) Maximum and minimum bounds of the CDF for the transient response at node N_3 at time point where max mean is 90% of its max value.

CHAPTER 7: CONCLUSION

In this dissertation, the need for development of circuit tools/solvers to model the forward propagation of device level uncertainty to the system response was discussed. The benefits of using the generalized Polynomial Chaos (gPC) theory as a robust uncertainty quantification technique for the statistical analysis of high speed microwave/RF networks were highlighted. The gPC technique represents the uncertainty in the network response as an expansion of predefined orthonormal polynomials and their unknown coefficients. These coefficients can be obtained using either intrusive or non-intrusive approaches. This dissertation focuses on non-intrusive approaches to evaluate the unknown coefficients. Non-intrusive approaches are popular because of their ability to reuse existing deterministic SPICE solvers and their parallelizability. A new linear regression methodology for the fast and non-intrusive analysis of high speed circuits was presented. This approach uses the D-optimal DoE to accurately evaluate the PC coefficients of the network responses. Novel techniques to further accelerate the search algorithms to identify the DoE from large multi-dimensional random spaces were presented.

One of the main bottlenecks of the PC approach is that the CPU cost to evaluate the unknown coefficients scales in a polynomial fashion with respect to the number of random input dimensions. To mitigate this effort, various techniques to develop a sparser alternative to the conventional full-blown PC expansion were presented. The first approach uses a HDMR formulation to study the effect of each random dimension on the network output. This sensitivity information guides the truncation of the original number of dimensions to a smaller set of dimensions. Constructing a PC metamodel in this low dimensional space leads to the recovery of a sparser set of coefficients than that obtained for the original number of dimensions with

negligible loss in accuracy. Further, a novel approach to reuse the PC bases and SPICE simulation results from the sensitivity indices estimation back in the nonintrusive recovery of the reduced dimensional PC coefficients were discussed to further expedite the proposed approach. This reduced dimensional PC approach was further extended to model the impact of both aleatory (random) and epistemic (ignorance based) uncertainty on the performance of distributed transmission line networks. A parameterized analysis of variance (ANOVA) strategy to identify which aleatory random dimensions have minimal impact on the response surface of the network was developed thereby enabling the construction of a highly compact PC. This PC representation serves as a metamodel capturing the impact of the purely epistemic, purely aleatory, and mixed epistemic-aleatory effects.

Mixed problems are characterized by far greater number of random dimensions than purely aleatory or epistemic problems, thereby further exacerbating the poor scalability of PC techniques. A novel dimension fusion approach that fuses the epistemic and aleatory dimensions within the same model parameter into a mixed dimension was developed to address the above scalability issue of mixed problems.

REFERENCES

- [1] G.S. Fishman, *Monte Carlo: Concepts, Algorithms, and Applications*. New York, NY: Springer-Verlag, 1996
- [2] Q. Zhang, J. J. Liou, J. McMacken, J. Thomson, and P. Layman, "Development of robust interconnect model based on design of experiments and multiobjective optimization," *IEEE Trans. Electron Devices*, vol. 48, no. 9, pp. 1885–1981, Sept. 2001
- [3] Y. Massoud and A. Nieuwoudt, "Modeling and design challenges and solutions for carbon-nanotube based interconnect in future high performance integrated circuits," *ACM J. Emerg. Technol. Comput. Syst.*, vol. 2, no. 3, pp. 155–196, July 2006
- [4] A. Nieuwoudt and Y. Massoud, "On the impact of process variations for carbon nanotube bundles for VLSI interconnect," *IEEE Trans. Electron. Devices*, vol. 54, no. 3, pp. 446–455, March 2007
- [5] A. Nieuwoudt and Y. Massoud, "On the optimal design, performance, and reliability of future carbon nanotube-based interconnect solutions," *IEEE Trans. Electron. Devices*, vol. 55, no. 8, pp. 2097–2110, Aug. 2008
- [6] J. F. Swidzinski and K. Chang, "Nonlinear statistical modeling and yield estimation technique for use in Monte Carlo simulations [microwave devices and ICs]," *IEEE Trans. Microw. Theory Techn.*, vol. 48, no. 12, pp. 2316–2324, Dec. 2000
- [7] P. Manfredi, I. S. Stievano, and F. G. Canavero, "Time and frequency-domain evaluation of stochastic parameters on signal lines," *Advanced Electromagnetics*, vol. 1, no. 3, pp. 85–93, Dec 2012

- [8] S. Vrudhula, J. M. Wang, and P. Ghanta, "Hermite polynomial based interconnect analysis in the presence of process variations," *IEEE Trans. Computer Aided Design*, vol. 25, no. 10, pp. 2001–2011, Oct. 2006
- [9] I. S. Stievano, P. Manfredi, and F. G. Canavero, "Stochastic analysis of multiconductor cables and interconnects," *IEEE Trans. Electromagn. Compatibility*, vol. 53, no. 2, pp. 501–507, May 2011
- [10] I. S. Stievano, P. Manfredi, and F. G. Canavero, "Parameters variability effects on multiconductor interconnects via Hermite polynomial chaos," *IEEE Trans. Comp., Packag. and Manuf. Technol.*, vol. 1, no. 8, pp. 1234–1239, Aug. 2011
- [11] D. Vande Ginste, D. De Zutter, D. Deschrijver, T. Dhaene, P. Manfredi, and F. Canavero, "Stochastic modeling-based variability analysis of on-chip interconnects," *IEEE Trans. Comp., Packag. and Manuf. Technol.*, vol. 3, no. 7, pp. 1182–1192, Jul. 2012
- [12] I. S. Stievano, P. Manfredi, and F. G. Canavero, "Carbon nanotube interconnects: process variation via polynomial chaos," *IEEE Trans. Electromagn. Compatibility*, vol. 54, no. 1, pp. 140–148, Feb. 2012
- [13] A. Biondi, D. Vande Ginste, D. De Zutter, P. Manfredi, and F. Canavero, "Variability analysis of interconnects terminated by general nonlinear loads," *IEEE Trans. Comp., Packag. and Manuf. Technol.*, vol. 2, no. 7, pp. 1244–1251, Jul. 2013
- [14] P. Manfredi, D. Vande Ginste, D. De Zutter, and F. Canavero, "Uncertainty assessment in lossy and dispersive lines in SPICE-type environments," *IEEE Trans. Comp., Packag. and Manuf. Technol.*, vol. 2, no. 7, pp. 1252–1258, Jul. 2013

- [15] P. Manfredi, D. Vande Ginste, D. De Zutter, and F. Canavero, "Stochastic modeling of nonlinear circuits via SPICE-compatible spectral equivalents," *IEEE Trans. Circuits Syst.*, vol. 61, no. 7, pp. 2057–2065, Jul. 2014
- [16] M. R. Rufuie, E. Gad, M. Nakhla, and R. Achar, "Generalized Hermite polynomial chaos for variability analysis of macromodels embedded in nonlinear circuits," *IEEE Trans. Comp., Packag. and Manuf. Technol.*, vol. 4, no. 4, pp. 673–684, April 2014
- [17] T.-A. Pham, E. Gad, M. S. Nakhla, and R. Achar, "Decoupled polynomial chaos and its applications to statistical analysis of high-speed interconnects," *IEEE Trans. Comp., Packag. and Manuf. Technol.*, vol. 4, no. 10, pp. 1634–1647, Oct. 2014
- [18] D. Spina, F. Ferranti, G. Antonini, T. Dhaene, and L. Knockaert, "Efficient variability analysis of electromagnetic systems via polynomial-chaos and model order reduction," *IEEE Trans. Comp., Packag. and Manuf. Technol.*, vol. 4, no. 6, pp. 1038–1051, June 2014
- [19] D. Spina, F. Ferranti, T. Dhaene, L. Knockaert, G. Antonini, and D. Vande Ginste, "Variability analysis of multiport systems via polynomial-chaos expansion," *IEEE Trans. Microwave Theory Techn.*, vol. 60, no. 8, pp. 2329–2338, Aug. 2012
- [20] A. Rong and A. C. Cangellaris, "Transient analysis of distributed electromagnetic systems exhibiting stochastic variability in material parameters," in *Proc. XXXth General Assembly and Scientific Symp.*, Aug. 2011, pp. 1-4
- [21] Md. A. H. Talukder, M. Kabir, S. Roy, and R. Khazaka, "Efficient generation of macromodels via the Loewner matrix approach for the stochastic analysis of high-speed passive distributed networks," in *Proc. IEEE 18th Workshop on Signal and Power Integrity*, May 2014, pp. 1-4

- [22] Md. A. H. Talukder, M. Kabir, S. Roy, and R. Khazaka, "Efficient stochastic transient analysis of high-speed passive distributed networks using Loewner matrix macromodels," in *Proc. IEEE Intl. Conf. Signal and Power Integrity*, August 2014, pp. 1-4
- [23] A. K. Prasad, and S. Roy, "Multidimensional variability analysis of complex power distribution networks via scalable stochastic collocation approach," *IEEE Trans. Comp., Packag. and Manuf. Technol.*, vol. 5, no. 11, pp. 1656-1668, Nov. 2015
- [24] D. Spina, F. Ferranti, G. Antonini, T. Dhaene, and L. Knockaert, "Non-intrusive polynomial chaos-based stochastic macromodeling of multiport systems," in *Proc. IEEE 18th Workshop on Signal and Power Integrity*, May 2014, pp. 1-4
- [25] D. Spina, D. De Jonghe, D. Deschrijver, G. Gielen, L. Knockaert, and T. Dhaene, "Stochastic macromodeling of nonlinear systems via polynomial-chaos expansion and transfer function trajectories," *IEEE Trans. Microwave Theory Techn.*, vol. 62, no. 7, pp. 1454–1460, July 2014
- [26] M. Ahadi, M. Kabir, E. Chobanyan, A. Smull, Md. A. H. Talukder, S. Roy, R. Khazaka, and B. M. Notaros, "Non-intrusive pseudo spectral approach for stochastic macromodeling of EM systems using deterministic full-wave solvers," in *Proc. 23rd IEEE Conf. Electric. Perform. Electron. Packag.*, October 2014, pp. 235-238
- [27] A. Rong and A. C. Cangellaris, "Interconnect transient simulation in the presence of layout and routing uncertainty," in *Proc. 20th IEEE Conf. Electric. Perform. Electron. Packag.*, October 2011, pp. 157-160
- [28] J. S. Ochoa and A. C. Cangellaris, "Analysis of the impact of interconnect routing variability on signal degradation," in *Proc. 21st IEEE Conf. Electric. Perform. Electron. Packag.*, October 2012, pp. 315-318

- [29] P. Sumant, H. Wu, A. Cangellaris, and N. Aluru, "Reduced-order models of finite element approximations of electromagnetic devices exhibiting statistical variability," *IEEE Trans. Antennas Propag.*, vol. 60, no. 1, pp. 301–309, Jan. 2012
- [30] X. Chen, J. S. Ochoa, J. E. Schutt-Aine, and A. C. Cangellaris, "Optimal relaxation of I/O electrical requirements under packaging uncertainty by stochastic methods," in *Proc. 64th Electronic Comp. Tech. Conf.*, May 2014, pp. 717–722
- [31] A. C. Yucel, H. Bagci, J. S. Hesthaven, and E. Michielssen, "A fast Stroud-based collocation for statistically characterizing EMI/EMC phenomena on complex platforms", *IEEE Trans. Electromagn. Compatibility*, vol. 51, no. 2, pp. 301-311, May 2009
- [32] A. C. Yucel, H. Bagci, and E. Michielssen, "An adaptive multi-element probabilistic collocation method for statistical EMC/EMI characterization," *IEEE Trans. Electromagn. Compatibility*, vol. 55, no. 6, pp. 1154–1168, Dec. 2013
- [33] M. Ahadi, M. Vempa, and S. Roy, "Efficient multidimensional statistical modeling of high speed interconnects in SPICE via stochastic collocation using Stroud cubature," in *Proc. IEEE Symp. Electromagn. Compatibility and Signal Integrity*, March 2015, pp. 300-305
- [34] P. Manfredi, D. Vande Ginste, D. De Zutter, and F. Canavero, "Generalized decoupled polynomial chaos for nonlinear circuits with many random parameters," *IEEE Microwave and Wireless Components Letters*, vol. 25, no. 8, pp. 505–507, Aug. 2015
- [35] M. Ahadi, M. Kabir, S. Roy, and R. Khazaka, "Fast multidimensional statistical analysis of microwave networks via Stroud cubature approach," in *Proc. IEEE International Conf. on Numerical Electromagn., Multiphysics Modeling and Optimiz.*, August 2015, pp. 1-3
- [36] A. K. Prasad, M. Ahadi, B. S. Thakur, and S. Roy, "Accurate polynomial chaos expansion for variability analysis using optimal design of experiments," in *Proc. IEEE*

International Conf. on Numerical Electromagn., Multiphysics Modeling and Optimiz.,
August 2015, pp. 1-4

- [37] Z. Zhang, T. A. El-Moselhy, I. M. Elfadel, and L. Daniel, "Stochastic testing method of transistor level uncertainty quantification based on generalized polynomial chaos," *IEEE Trans. Computer Aided Design*, vol. 32, no. 10, pp. 1533-1545, Oct. 2013
- [38] P. Manfredi and F. Canavero, "Efficient statistical simulation of microwave devices via stochastic testing-based circuit equivalents of nonlinear components," *IEEE Trans. Microw. Theory Techn.*, vol. 63, no. 5, pp. 1502-1511, May 2015
- [39] Z. Zhang, T. A. El-Moselhy, I. M. Elfadel, and L. Daniel, "Calculation of generalized polynomial-chaos basis functions and Gauss quadrature rules in hierarchical uncertainty quantification," *IEEE Trans. Computer Aided Design*, vol. 33, no. 5, pp. 728-740, May 2014
- [40] Z. Zhang, X. Yang, I. V. Oseledets, G. E. Karniadakis, and L. Daniel, "Enabling high-dimensional hierarchical uncertainty quantification by ANOVA and tensor-train decomposition," *IEEE Trans. Computer Aided Design*, vol. 34, no. 1, pp. 63-76, Jan. 2015
- [41] A. C. Yucel, H. Bagci, and E. Michielssen, "An ME-PC enhanced HDMR method for efficient statistical analysis of multiconductor transmission line networks," *IEEE Trans. Comp., Packag. and Manuf. Technol.*, vol. 5, no. 5, pp. 685-696, May 2015
- [42] D. Xiu, *Numerical Methods for Stochastic Computations: A Spectral Method Approach*. New Jersey: Princeton University Press, 2010
- [43] M. S. Eldred, "Recent advance in non-intrusive polynomial-chaos and stochastic collocation methods for uncertainty analysis and design," in *Proc. 50th AIAA/ASME/ASCE/AHS/ASC Structures, Structural Dynamics, and Materials Conf.*, May 2010, pp. 1-37

- [44] D. Xiu and G. E. Karniadakis, "The Wiener-Askey polynomial chaos for stochastic differential equations," *SIAM Journal Sci. Comput.*, vol. 24, no. 2, pp. 619–644, July 2002
- [45] M. Ahadi and S. Roy, "Sparse linear regression (SPLINER) approach for efficient multidimensional uncertainty quantification of High-speed circuits," accepted for publication in *IEEE Trans. Computer Aided Design*, 2016
- [46] N.-K. Nguyen and A. J. Miller, "A review of some exchange algorithms for constructing discrete D-optimal designs," *Comput. Statistics and Data Analysis*, vol. 14, pp. 489-498, 1992
- [47] A. J. Miller and N.-K. Nguyen, "A Fedorov exchange algorithm for D-optimal design," *J. Royal Stat. Society*, vol. 43, no. 4, pp. 669-677, 1994
- [48] V. V. Fedorov, *Theory of Optimal Experiments*, New York, NY: Academic Press, 1972
- [49] R. D. Cook and C. J. Nachtsheim, "A comparison of algorithms for constructing exact D-optimal designs," *Technometrics*, vol. 22, no. 3, pp. 315-324, Aug. 1980.
- [50] W. H. Press, S. A. Teukolsky, W. T. Vetterling, B. P. Flannery, *Numerical Recipes: The Art of Scientific Computing (3rd ed.)*, New York: Cambridge University Press, 2007
- [51] S. Smolyak, "Quadrature and interpolation formulas for tensor products of certain classes of functions," *Soviet Math. Dokl.*, vol. 4, pp. 240–243, 1963
- [52] N. S. Kuek, A. C. Liew, E. Shamiloglu, and J. Rossi, "Circuit modeling of nonlinear lumped element transmission lines including hybrid lines," *IEEE Trans. Plasma Science*, vol. 40, no. 10, pp. 2523–2534, Oct. 2012
- [53] A. K. Prasad and S. Roy, "Global sensitivity based dimension reduction for fast variability analysis of nonlinear circuits," in *Proc. 24th IEEE Conf. Electric. Perform. Electron. Packag.*, October 2015, pp. 97-100.

- [54] H. Rabitz and O. F. Alis, "General formulation of high-dimensional model representations," *Journal of Math. Chem.*, vol. 50, no. 2-3, pp. 197-233, 1999
- [55] A. Saltelli, S. Tarantola, F. Campolongo, and M. Ratto, *Sensitivity Analysis in Practice: A Guide to Assessing Scientific Models*. Sussex, England: J Wiley, 2004
- [56] E. H. Sandoval, F. Anstett-Collin, and M. Basset, "Sensitivity study of dynamic systems using polynomial chaos," *Reliability Eng. and Sys. Safety*, vol. 104, pp. 15-26, Aug. 2012
- [57] A. K. Prasad, D. Zhou, and S. Roy, "Reduced dimension polynomial chaos approach for efficient uncertainty analysis of multi-walled carbon nanotube interconnects," in Proc. IEEE MTT-S 64th International Microwave Symposium, May 2016, pp. 1-3
- [58] I. Kapse and S. Roy, "Anisotropic formulation of hyperbolic polynomial chaos expansion for high-dimensional variability analysis of nonlinear circuits," in *Proc. 25th IEEE Conference on Electrical Performance of Electronic Packaging*, Oct. 2016, pp. 123-125
- [59] M. Ahadi, A. K. Prasad, and S. Roy, "Hyperbolic polynomial chaos expansion (HPCE) and its application to statistical analysis of nonlinear circuits," in *Proc. IEEE 20th Workshop on Signal and Power Integrity*, May 2016, pp. 1-4
- [60] J. S. Ochoa and A. C. Cangellaris, "Random space dimensionality reduction for expedient yield estimation of passive microwave systems," *IEEE Trans. Microw. Theory Techn.*, vol. 61, no. 12, pp. 4313-4321, Dec. 2013
- [61] G. H. Golub and J. H. Welsch, "Calculation of Gauss quadrature rules," *Math. Comp.*, vol. 23, pp. 221-230, 1969
- [62] D. C. Montgomery, *Design and Analysis of Experiment. 8th ed.* John Wiley, NY, 2012

- [63] A. K. Prasad, M. Ahadi, and S. Roy, "Multidimensional uncertainty quantification of microwave/RF networks using linear regression and optimal design of experiments," *IEEE Trans. Microwave Theory Techn.*, vol. 64, no.8, pp. 2433-2446, Aug. 2016
- [64] X. Chen, E.-J. Park, and D. Xiu, "A flexible numerical approach for quantification of epistemic uncertainty," *J. Comput. Physics*, vol. 240, no.12, pp. 211–224, May 2013
- [65] A. Monti, F. Ponci, and F. Valtorta, "Extending polynomial chaos to include interval analysis," *IEEE Trans. Instrumentation and Measurement*, vol. 59, no. 1, pp. 48–55, Jan. 2010
- [66] D. Xiu, "Fast numerical methods for stochastic computatios: a review," *Comm. In Comput. Phys.* vol. 5, no. 2-4, pp. 242-272, Feb. 2009
- [67] M. S. Eldred, L. P. Swiler, G. Tang, "Mixed aleatory-epistemic uncertainty quantification with stochastic expansions and optimization-based interval estimation," *Reliability Engineering and System Safety*, vol. 96, no. 9, pp. 1092–1113, Sept. 2011
- [68] M. R. Rufuie, E. Gad, M. Nakhla R. Achar, "Fast variability analysis of general nonlinear circuits using decoupled polynomial chaos," *IEEE Trans. Comp., Packag. and Manuf. Technol.*, vol. 12, no. 5, pp. 1860–1871, Dec. 2015
- [69] S. Ferson and L. R. Ginzburg, "Different methods are needed to propagate ignorance and variability," *Reliability Engineering and System Safety*, vol. 54, no. 2-3, pp. 133–144, Nov.-Dec. 1996
- [70] I. R. Goodman and H. T. Nguyen, "Probability updating using second order probabilities and conditional event algebra," *Information Sciences*, vol. 121, no. 3-4, pp. 295–347, Dec. 1999
- [71] R. Ahlfeld, B. Belkouchi, and F. Montomoli, "SAMBA: Sparse approximation of moment based arbitrary polynomial chaos," *Journal of Computational Physics*, vol. 320, pp. 1–16, Sept. 2016

- [72] M. Tang and J. Mao, "Modeling and fast simulation of multiwalled carbon nanotube interconnects", *IEEE Trans. Electromagnetic Compatibility*, vol 57, no. 2, pp 232-240, April 2015
- [73] I. Kapse, A. K. Prasad, and S. Roy, "Generalized anisotropic polynomial chaos approach for expedited statistical analysis of non-linear radio- frequency (RF) circuits", in *Proc. IEEE 20th Workshop on Signal and Power Integrity*, May 2016, pp. 1-3
- [74] Y. Tao, B. Nouri, M. S. Nakhla, M. A. Farhan, and R. Achar, "Variability analysis via parameterized model order reduction and numerical of Laplace transform," *IEEE Trans. Comp., Packag. and Manuf. Technol.*, vol. 7, no. 5, pp. 678–686, May 2017
- [75] A. K. Prasad and S. Roy, "Accurate reduced dimensional polynomial chaos for efficient uncertainty quantification of microwave/RF networks," *IEEE Trans. Microwave Theory Tech.*, vol. 65, no.10, pp. 3697-3708, Oct. 2017
- [76] N. Femia and G. Spagnuolo, "Genetic optimization of interval arithmetic based worst case circuit tolerance analysis," *IEEE Trans. Circuits Syst. I, Fundam. Theory Appl.*, vol. 46, no. 12, pp. 1441–1456, Dec. 1999
- [77] N. Femia and G. Spagnuolo, "True worst-case circuit tolerance analysis using genetic algorithms and affine arithmetic," *IEEE Trans. Circuits Syst. I, Fundam. Theory Appl.*, vol. 47, no. 9, pp. 1285–1296, Sep. 2000.
- [78] J. D. Ma and R. A. Rutenbar, "Fast interval-valued statistical modeling of interconnect and effective capacitance," *IEEE Trans. Comput.-Aided Des. Integr. Circuits Syst.*, vol. 25, no. 4, pp. 710–724, Apr. 2006

- [79] J. D. Ma and R. A. Rutenbar, "Interval-valued reduced-order statistical interconnect modeling," *IEEE Trans. Comput.-Aided Des. Integr. Circuits Syst.*, vol. 26, no. 9, pp. 1602–1613, Sep. 2007
- [80] T. Ding, R. Trinchero, P. Manfredi, I. S. Stievano, and F. G. Canavero, "How affine arithmetic helps beat uncertainties in electrical systems," *IEEE Circuits Syst. Mag.*, vol. 15, no. 4, pp. 70–79, Nov. 2015
- [81] R. Trinchero, P. Manfredi, T. Ding, and I. S. Stievano, "Combined parametric and worst case circuit analysis using Taylor models," *IEEE Trans. Circuits Syst. I: Regular Papers*, vol. 63, no. 7, pp. 1067–1078, July 2016
- [82] A. D. Kiureghiana, O. Ditlevsen, "Aleatory or epistemic? Does it matter?," *Structural Safety*, vol. 31, no. 2, pp. 105–112, March 2009
- [83] F. O. Hoffman and J. S. Hammonds, "Propagation of uncertainty in risk assessments: The need to distinguish between uncertainty due to lack of knowledge and uncertainty due to variability," *Risk Analysis*, vol. 14, no. 5, pp. 707–712, Oct. 1994
- [84] J. Wu, Z. Luo, H. Li, and N. Zhang, "A new hybrid uncertainty optimization method for structures using orthogonal series expansion," *Applied Mathematical Modeling*, vol. 45, pp. 474-490, May 2017
- [85] J. Wu, Z. Luo, N. Zhang, and Y. Zhang, "A new interval uncertain optimization method for structures using Chebyshev surrogate models," *Computers and Structures*, vol. 146, pp. 185-196, Jan. 2015
- [86] S. Yin, D. Yu, H. Yin, and B. Zai, "Interval and random analysis for structure–acoustic systems with large uncertain-but-bounded parameters," *Computer Methods in Applied Mechanics and Engineering*, vol. 305, June 2016, pp. 910-935

- [87] A. K. Prasad, and S. Roy, “Mixed aleatory-epistemic uncertainty quantification using reduced dimensional polynomial chaos and parametric ANOVA,” accepted for oral presentation in IEEE 26th Conference on Electrical Performance of Electronic Packages, October 2017
- [88] P. G. Constantine, E. Dow, and Q. Wang, “Active subspace methods in theory and practice: applications to kriging surfaces,” SIAM J. Scientific Comput., vol. 36, no. 4, pp. A1500-A1524, 2014
- [89] K. Tang, P. M. Congedo, and R. Abgrail, “Adaptive surrogate modeling by ANOVA and sparse polynomial dimensional decomposition for global sensitivity analysis in fluid simulation,” J. Comput. Physics, vol. 314, pp. 557–589, June 2016
- [90] G. Blatman and B. Sudret, “An adaptive algorithm to build up sparse polynomial chaos expansions for stochastic finite element analysis,” Prob. Engineering Mechanics, vol. 25, no. 2, pp. 183-197, April 2010
- [91] R. Tipireddy and R.G. Ghanem, “Basis adaptation in homogeneous chaos spaces,” J. Comput. Physics, vol. 259, no. 2, pp. 304–317, Feb. 2014
- [92] J. Vlach and K. Singhal, *Computer Methods for Circuit Analysis and Design*. New York, NY: Van Nostrand Reinhold, 1983

APPENDIX A: LIST OF PUBLICATIONS

Journal Papers:

- [1] A. K. Prasad and S. Roy, "Multidimensional variability analysis of complex power distribution networks via scalable stochastic collocation approach," *IEEE Trans. Comp., Packag. and Manuf. Technol.*, vol. 5, no. 11, pp. 1656-1668, Nov. 2015
- [2] A. K. Prasad, M. Ahadi, and S. Roy, "Multidimensional uncertainty quantification of microwave/RF networks using linear regression and optimal design of experiments," *IEEE Trans. Microwave Theory Techn.*, vol. 64, no.8, pp. 2433-2446, Aug. 2016
- [3] A. K. Prasad and S. Roy, "Accurate reduced dimensional polynomial chaos for efficient uncertainty quantification of microwave/RF networks," *IEEE Trans. Microwave Theory Tech.*, vol. 65, no.10, pp. 3697-3708, Oct. 2017

Conference Papers:

- [1] A. K. Prasad, M. Ahadi, and S. Roy, "Polynomial chaos based variability analysis of power distribution networks using a 3D topology of multiconductor transmission lines", in *Proc. 23rd IEEE Conference on Electrical Performance of Electronic Packaging*, Oct. 2014, pp. 21-24
- [2] A. K. Prasad, M. Ahadi, B. S. Thakur, and S. Roy, "Accurate polynomial chaos expansion for variability analysis using optimal design of experiments," in *Proc. IEEE Int. Conf. Numer. Electromagn., Multiphys. Modeling. Optim*, Aug. 2015, pp. 1-4
- [3] A. K. Prasad and S. Roy, "Global sensitivity based dimension reduction for fast variability analysis of nonlinear circuits," in *Proc. 24th IEEE Conference on Electrical Performance of Electronic Packaging*, Oct. 2015, pp. 97-99

- [4] A. K. Prasad, D. Zhou, and S. Roy, "Reduced dimension polynomial chaos approach for efficient uncertainty analysis of multi-walled carbon nanotube interconnects," in *Proc. IEEE MTT-S 64th International Microwave Symposium*, May 2016, pp. 1-3
- [5] I. Kapse, A. K. Prasad, and S. Roy, "Generalized anisotropic polynomial chaos approach for expedited statistical analysis of non-linear radio- frequency (RF) circuits", in *Proc. IEEE 20th Workshop on Signal and Power Integrity*, May 2016, pp. 1-3
- [6] M. Ahadi, A. K. Prasad, and S. Roy, "Hyperbolic polynomial chaos expansion (HPCE) and its application to statistical analysis of nonlinear circuits," in *Proc. IEEE 20th Workshop on Signal and Power Integrity*, May 2016, pp. 1-4
- [7] X. Gao, Y. Wang, N. Spotts, N. Xie, S. Roy, and A. K. Prasad, "Fast uncertainty quantification in engine nacelle inlet design using a reduced dimensional polynomial chaos approach", *AIAA Propulsion and Energy*, July 25-27, 2016, Salt Lake City, Utah
- [8] X. Gao, J. Weinmeister, N. Xie, S. Roy, and A. K. Prasad, "Combining a reduced polynomial chaos expansion approach with universal kriging", in *8th AIAA Theoretical Fluid Mechanics Conference*, June 5-9, 2017, Denver, Colorado
- [9] I. Kapse, A. K. Prasad and S. Roy, "Analyzing Impact of Epistemic Uncertainty in High-Speed Circuit Simulation Using Fuzzy Variables and Global Polynomial Chaos Surrogates", in *Proc. IEEE Int. Conf. Numer. Electromagn., Multiphys. Modeling. Optim*, May. 2017, pp. 320-322
- [10] A. K. Prasad and S. Roy, "A novel dimension fusion based polynomial chaos approach for mixed aleatory-epistemic uncertainty quantification of carbon nanotube interconnects", in *Proc. IEEE Symp. Electromagn. Compatibility and Signal Integrity*, Aug 2017, pp. 108-111

- [11] A. K. Prasad and S. Roy, "Mixed Epistemic-Aleatory Uncertainty Quantification using Reduced Dimensional Polynomial Chaos and Parametric ANOVA (PANOVA)" in *24th IEEE Conference on Electrical Performance of Electronic Packaging*, Oct. 2017
- [12] Weinmeister, J., Xie, N., **Gao, X.**, Prasad, A., and Roy, S., "Analysis of a Polynomial Chaos-Kriging Metamodel for Uncertainty Quantification in Aerospace Applications", in *2018 AIAA/ASCE/AHS/ASC Structures, Structural Dynamics, and Materials Conference*, January 8-12, 2018, Kissimmee, Florida
- [13] A.K. Prasad and S. Roy, "Multi-Fidelity Approach for Polynomial Chaos based Statistical Analysis of Microwave Networks", accepted for presentation in *Applied Computational Electromagnetic Society Conference*, Denver, March 2018